

Prairie View A&M University

Digital Commons @PVAMU

All Theses

12-2023

Enhancing Short Circuit Fault Detection In Three-Phase Power Systems: A Wavelet-Based Approach

Maysoun Alshrouf

Follow this and additional works at: <https://digitalcommons.pvamu.edu/pvamu-theses>

ENHANCING SHORT CIRCUIT FAULT DETECTION IN THREE-PHASE POWER
SYSTEMS: A WAVELET-BASED APPROACH

A Thesis

by

MAYSOUN ALSHROUF

Submitted to the Office of Graduate Studies of
Prairie View A&M University
in Partial fulfillment of the requirement for the degree of

MASTER IN ELECTRICAL ENGINEERING

December 2023

Major Subject: Engineering

ENHANCING SHORT CIRCUIT FAULT DETECTION IN THREE-PHASE POWER
SYSTEMS: A WAVELET-BASED APPROACH

A Thesis

By

MAYSOUN ALSHROUF

Submitted to the Office of Graduate Studies of
Prairie View A&M University
in Partial fulfillment of the requirement for the degree of
MASTER IN ELECTRICAL ENGINEERING

Approved as to style and content by:

Dr. Cajetan Akujuobi
Chair of Committee

Dr. Samir Abood
Committee Member

Dr. Richard Wilkins
Committee Member

Dr. Justin Foreman
Committee Member

Dr. Pamela Obiomon
Dean of College

Dr. Tyrone Tanner
Dean of Graduate Studies

December 2023

Major Subject: Engineering

ABSTRACT

ENHANCING SHORT CIRCUIT FAULT DETECTION IN THREE-PHASE POWER SYSTEMS: A WAVELET-BASED APPROACH

(December 2023)

Maysoun Alshrouf, B.S., Al-Ahliyya Amman

University; M.S., Keller Graduate School

of Management – Devry University

Chair of Advisory Committee:

Dr. Cajetan Akujuobi

This work aimed to improve fault detection accuracy in three-phase power systems, addressing a critical need for reliable and uninterrupted electrical power supply. Existing approaches often fluctuate in accuracy. The study explored the gaps in current literature, emphasizing the need for precise fault detection strategies. The technique to enhance fault detection is an innovative methodology combining MATLAB simulation with Wavelet analysis. This study explored the application of Wavelet transforms, including Daubechies 4, Haar, Symlet 5, and Discrete Approximation Meyer, to the current signals in a three-phase power system. By extracting and comparing the current signal's detailed coefficients against predefined threshold values for fault detection and identifying optimal Wavelets using Wavelet coefficients' energy analysis, this study provided a comprehensive solution to the complex problem of fault detection in power systems.

The study utilized both qualitative and quantitative methodologies to gather and analyze data. By combining expert insights with numerical data, the study aimed to gain a comprehensive understanding of the fault detection process. The integration of qualitative and quantitative approaches allowed for a more holistic exploration of the subject, providing valuable insights into the complexity of fault detection

The findings highlight the significance of adaptability in choosing the most suitable Wavelet for specific fault scenarios. The study revealed no universal "optimal" Wavelet for all fault types, emphasizing the need for tailored approaches. Applying Wavelet analysis combined with a threshold approach and energy-based analysis enhances the reliability and stability of power systems. This study addressed existing gaps and introduced innovative methodologies, thereby contributing to the advancement of power systems fault detection.

In summary, the study presents significant insights into the realm of electrical engineering and power systems fault detection. With the potential to enhance power system reliability, the findings contribute valuable knowledge to the field. Moreover, the study aims to deepen the overall understanding of fault detection processes, offering further advancements in this crucial aspect of electrical engineering.

Index terms—Detailed coefficients, fault detection, fault types, short circuit fault, Wavelet transforms.

DEDICATION

To My Beloved Family,

This work is dedicated to you, my source of strength, endless fountain of love, and unwavering supporters. Your encouragement, sacrifices, and faith in my abilities have driven my journey. You have stood by my side through every challenge and triumph, and I am profoundly grateful for you. Your love and unwavering support have been my constant inspiration, and this accomplishment is as much yours as it is mine. Thank you for guiding me on this path of knowledge and growth.

With all my love,

Maysoun Alshrouf

ACKNOWLEDGMENTS

I sincerely thank Dr. Cajetan Akujuobi for his unwavering support and exceptional patience, which have been indispensable in my academic journey. His mentorship has been crucial to my study, contributing significantly to my academic growth. I take great pride in being part of his academic endeavors, and his critical thinking and analytical insights have enriched my problem-solving skills, for which I am genuinely thankful.

I also thank Dr. Samir Abood for his exceptional support and guidance throughout my study. His expertise and patience were invaluable in providing insightful feedback, significantly contributing to the refinement of my research. Dr. Abood's kindness and accessibility were instrumental in navigating the complexities of my study, and I genuinely appreciate that.

A special acknowledgment goes to Dr. Richard Wilkins for his kindness, knowledge, and guidance, making the enrollment process at PVAMU a seamless and enjoyable experience. His willingness to assist and availability influenced my decision to choose Prairie View A&M University over other universities.

I express my sincere gratitude to Dr. Justin Foreman for his invaluable support and guidance during my thesis presentation process. His expertise and insightful input have greatly enhanced the quality of my presentation, and I appreciate his time and encouragement.

I also sincerely thank Dr. Annamalai Annamalai for his kindness, knowledge, and understanding. His generosity in reviewing my questions and concerns, clarifications, and offering insightful advice has enhanced my understanding of the subject. I am truly thankful for his guidance.

I would like to express my special thanks to Dr. Suxia Cui for her outstanding efforts in coordinating the arrangements for the thesis defense with various personnel and departments. Her invaluable time, rich input, and encouragement have greatly contributed to the success of this process.

I want to express my gratitude to all the dedicated teachers and the members of the Electrical Engineering Department who imparted their knowledge during my study, with special acknowledgment to Dr. Siew Koay and Dr. Abburi Kumar for their dedication and valuable insights and rich knowledge shared during classes.

A heartfelt thank you extends to the wonderful Prairie View A&M University and all its members. Their collective efforts and interconnected roles have played a pivotal role in making this academic journey a truly enriching experience. I appreciate the entire university community for their teamwork and contributions that have contributed to my growth and learning.

TABLE OF CONTENTS

	Page
ABSTRACT.....	iii
DEDICATION.....	v
ACKNOWLEDGMENTS	vi
LIST OF FIGURES	xii
LIST OF TABLES.....	xix
LIST OF ABBREVIATIONS.....	xx
LIST OF SYMBOLS	xxii
CHAPTER	
1. INTRODUCTION	1
1.1 Background of the Study.....	5
1.2 Problem Statement	8
1.3 Purpose, Scope, and Significance of the Study.....	9
1.4 Study Questions.....	11
1.5 Significance.....	13
1.6 Expected Contributions	14
1.7 Definition of Terms	15
1.8 Organization of the Remainder of the.....	19
1.9 SUMMARY	21
2. LITERATURE REVIEW	22
2.1 Three-Phase Power System Short Fault Detection and Classification Techniques	22
2.2 Power Systems Fault Detection Wavelet-Based Techniques.....	24
2.2.1 Wavelet-Based High-Impedance Fault Detection in Power Systems	25
2.2.2 Wavelet-Based Various Fault Types Detection in Power Systems.....	27
2.3 The Significance of the Proposed Study in Comparison with the Literature.....	30
2.3 SUMMARY	32
3. WAVELETS	34

3.1 Signal Processing Techniques for Power System Analysis: a Comparative of Wavelet Transform and Fourier Transform	34
3.1.1 Wavelet Time-Frequency Resolutions	38
3.2 How Wavelet Transforms Work	41
3.2.1 Wavelet Decomposition Tree	45
3.3 Two Essential Conditions for Wavelet Design	47
3.3 Wavelet Families	48
3.4 Wavelet Transforms Two Primary Categories	51
3.4.1. Continuous Wavelet Transform (CWT)	51
3.4.2 Discrete Wavelet Transforms (DWT)	53
3.5 Wavelet Properties	54
3.6 Summary	55
4. POWER SYSTEM FAULT	56
4.1 Introduction	56
4.2 Power System Faults	58
4.3 Fault Concept	59
4.4 Types of Faults	63
4.4.1 Symmetrical Faults	64
4.4.2 Unsymmetrical Faults	65
4.5 Symmetrical Fault Analysis	69
4.5.1 Simplified Models of Synchronous Machines for Transient Analysis	70
4.5.2 Transient Phenomena	74
4.5.3 Three-Phase Short Circuit – Unloaded Synchronous Machine	78
4.5.4 Effect of Load Current	84
4.6 Unsymmetrical Faults Analysis	86
4.7 Symmetrical Components	86
4.7.1 Effect of Symmetrical Components on Impedance	90
4.7.2 Phase Shift Δ/Y Connection Δ/Y	91
4.7.3 Sequence Network of Unloaded Generator	92
4.8 Analysis of Unsymmetrical Faults Using the Method of Symmetrical Component	97
4.8.1 Single Line-to-Ground Fault	98
4.8.2 Line-to-Line Fault	101
4.8.3 Double Line-to-Ground Fault	102
4.9 Fault Classification	105
4.9.1 Assumptions and Simplifications	105
4.9.2 Fault Voltage-Amps	106
4.10 Summary	107
5. METHODOLOGY	110
5.1 Study Design	110

5.2 Instruments/Measures.....	111
5.3 Academic (Scholarly) Support	112
5.4 Data Collection.....	112
5.5 Data Analysis	113
5.7 Fault Detection Methodology: Comparative Flowchart Analysis.....	114
5.7 SUMMARY	118
6. RESULTS	117
6.1 Introduction	117
6.2 Brief Description of How the Methodology Approach Applied to Data Analysis	121
6.3 System Design and Simulation	119
6.4 Algorithm	120
6.4.1 Threshold Concept.....	121
6.4.2 Fault Detection	123
6.4.3 Fault Classifications	124
6.4.4 Selection of Wavelet Transform Families	125
6.4.5 Understanding Wavelet Characteristics	130
6.5 MATLAB Simulation and Commands to Extract Signals Detailed Coefficients.	131
6.5.1 Wavelet Decomposition and Maximum Detailed Coefficients Process for db4	132
6.5.2 Wavelet Decomposition and Maximum Detailed Coefficients Process for Haar	147
6.5.3 Wavelet Decomposition and Maximum Detailed Coefficients Process for sym5	161
6.5.4 Wavelet Decomposition and Maximum Detailed Coefficients Process for DAM	175
6.6 Presentation of Data and Results of the Analysis	190
6.7 Wavelet Coefficients Energy	197
6.7.1 What is Wavelet Coefficients Energy	197
6.7.2 Selecting the Optimal Wavelet Function for Power System Fault Detection	202
6.8 Investigating the Factors Leading to Optimal Wavelet Selection.....	209
6.9 Summary	209
7. DISCUSSION, CONCLUSIONS AND FUTURE WORK	215
7.1 Introduction	212
7.2 Summary of the Results	212
7.3 Discussion of the Results	213
7.4 Limitations	215
7.5 Conclusions	216
7.6 Future Work	217
7.7 Summary	218

REFERENCES	218
CURRICULUM VITAE.....	227

LIST OF FIGURES

FIGURE	Page
3.1 Visual overview for the time and frequency resolutions of diverse transformations. The dimensions and orientations of the blocks symbolize the corresponding resolution sizes [16]	36
3.2 Wavelet time-frequency resolutions	38
3.3 Wavelet Decomposition Tree	44
4.1 Various types of faults that occur within a three-phase power	62
4.2 Common types of faults	66
4.3 The equivalent circuit for the sub-transient period	69
4.4 The equivalent circuit for the transient period	70
4.5 The equivalent circuit for the steady-state period	71
4.6 Simple series circuit with constant R and L	72
4.7 Current waveform (a) with no DC offset ($\alpha = 0, \pi, 2\pi, \dots$). (b) with maximum DC off set ($\alpha = \pi/2, 3\pi/2, 5\pi/2, \dots$)	74
4.8 Steady-state and transient current terms combine to form the resultant current	75
4.9 The Fault current in one phase shows the sub-transient, transient, and steady-state currents	76
4.10 The sub-transient, transient, and steady-state fault currents	77
4.11 One phase diagram showing the sub-transient, transient, and steady-state currents. (a) Circuit diagram. (b) Phasor diagram	82
4.12 Three sets of balanced phasors are the symmetrical components of three unbalanced phasors.	84
4.13 Three phase unbalanced system phasor diagrams	85
4.14 The transformer has a (Y- Δ) connection	88
4.15 The phasor diagram	88

4.16 Circuit diagram of an unloaded generator grounded.	89
4.17 The path for phase current of positive sequence in the generator and the corresponding sequence networks.	91
4.18 The path for phase Current of the negative Sequence in the generator and the Corresponding Sequence Networks.	92
4.19 The path for phase current of zero sequence in the generator and the corresponding sequence networks.	94
4.20 Circuit diagram at fault point (F).	95
4.21 General three-phase bus.	96
4.22 Interconnected sequence networks for SLG fault.	97
4.23 General three-phase bus.	99
4.24 Interconnected sequence networks.	100
4.25 General three-phase bus.	101
4.26 Interconnected sequence networks.	105
5.1 The flowchart for conventional short circuit fault detection.	112
5.2 The study methodology flowchart for short circuit fault detection.	114
6.1 Power system simulation using MATLAB/Simulink.	120
6.2 Daubechies scaling function ϕ [19].	125
6.3 Daubechies Wavelet function ψ [19].	126
6.4 Haar scaling function ϕ [19].	126
6.5 Haar Wavelet function ψ [19].	127
6.6 Symlet scaling function ϕ [19].	128
6.7 Symlet Wavelet function ψ [19].	128
6.8 Meyer scaling function ϕ [19].	129

6.9 Meyer Wavelet function ψ [19]	129
6.10 Simulink no fault currents.....	133
6.11 Algorithm no fault currents.....	134
6.12 No-fault currents approximation coefficients db4	134
6.13 No-fault currents detailed coefficients db4.....	135
6.14 Simulink single-line-to-ground fault B-G Currents	136
6.15 Single-line-to-ground fault B-G(Phase A and ground currents).....	136
6.16 Algorithm single-line-to-ground fault B-G.....	137
6.17 Single-line-to-ground fault B-G currents approximation coefficients db4.....	137
6.18 Single-line-to-ground fault B-G currents detailed coefficients db4	138
6.19 Simulink double-line fault A-B currents.....	139
6.20 Algorithm double-line fault A-B currents db4.....	139
6.21 Double-line fault A-B currents approximation coefficients db4	140
6.22 Double-line Fault A-B currents detailed coefficients db4	140
6.23 Simulinkdouble-line-to-ground AB-G fault currents.....	141
6.24 Algorithm double-line-to-ground fault AB-G currents.....	141
6.25 Double-line-to-ground fault AB-G currents approximation coefficients db4	142
6.26 Double-line-to-ground fault AB-G currents detailed coefficients db4.....	142
6.27 Simulink three-phase fault ABC currents.....	143
6.28 Algorithm three-phase fault ABC currents.....	143
6.29 Three-phase fault ABC currents approximation coefficients db4	144
6.30 Three-phase fault ABC detailed coefficients db4.....	144
6.31 Simulink three-phase-to-ground fault ABC-G currents db4.....	145

6.32	Algorithm three-phase to ground fault ABC-G currents db4	145
6.33	Three-phase-to-ground fault ABC-G currents approximation coefficients db4	146
6.34	Three-phase-to-ground fault ABC-G currents detailed coefficients db4.....	146
6.35	Simulink no fault three-phase Currents	148
6.36	Algorithm no fault three-phase currents	148
6.37	No fault three-phase currents approximation coefficients Haar	149
6.38	No fault three-phase currents detailed coefficients Haar	149
6.39	Simulink single-line-to-ground B-G fault currents.....	150
6.40	Algorithm single-line-to-ground B-G fault currents.....	151
6.41	Single-line-to-ground B-G fault currents approximation coefficients Haar	151
6.42	Single-line-to-ground B-G fault currents detailed coefficients Haar.....	152
6.43	Simulink double-line-to-ground AB-G fault currents.....	153
6.44	Algorithm double-line-to-ground AB-G fault currents.....	153
6.45	Double-line-to-ground AB-G fault currents approximation coefficients Haar.....	154
6.46	Double-line-to-ground AB-G fault currents detailed coefficients Haar	154
6.47	Simulink double line A-B fault currents	155
6.48	Algorithm double line A-B fault currents	155
6.49	Double line A-B fault currents approximation coefficients Haar	156
6.50	Double line A-B fault currents detailed coefficients Haar.....	156
6.51	Simulink three-phase ABC fault currents	157
6.52	Algorithm three-phase ABC fault currents	157
6.53	Three-phase ABC fault currents approximation coefficients Haar.....	158
6.54	Three-phase ABC fault currents approximation coefficients Haar.....	158

6.55 Simulink three-phase to ground ABC-G fault currents Haar.....	159
6.56 Algorithm three-phase to ground ABC-G fault currents Haar.....	159
6.57 Three-phase-ground ABC-G fault currents approximation coefficients Haar.....	160
6.58 Three-phase-to-ground ABC-G fault currents detailed coefficients, Haar.....	160
6.59 Simulink no-fault three-phase currents.....	162
6.60 Algorithm no-fault three-phase currents.....	162
6.61 No-fault three-phase currents approximation coefficients sym5.....	163
6.62 No-fault three-phase currents approximation coefficients sym5.....	163
6.62 Simulink single-line-to- ground B-G fault currents sym5.....	164
6.63 Algorithm single-line-to- ground B-G fault sym5.....	165
6.64 Single-line-to-ground BG fault currents approximation coefficients sym5.....	165
6.65 Single-line-to-ground B-G fault currents detailed coefficients sym5.....	166
6.66 Simulink double-line-to-ground AB-G fault currents sym5.....	166
6.67 Algorithm double-line-to- ground AB-G fault currents sym5.....	167
6.68 Double-line-to-ground AB-G fault currents approximation coefficients sym5.....	167
6.69 Double-line-to-ground AB-G fault currents detailed coefficients sym5.....	168
6.70 Simulink double-line B-C fault currents sym5	169
6.71 Algorithm double-line B-C fault currents sym5.....	169
6.72 Double—C fault currents approximation coefficients sym5.....	170
6.73 Double-line B-C fault currents detailed coefficients sym5.....	170
6.74 Simulink three-phase ABC fault currents sym5.....	171
6.75 Algorithm three-phase ABC fault currents sym5.....	171
6.76 Three-phase ABC fault currents approximation coefficients sym5.....	172

6.77 Three-phase ABC fault currents detailed coefficients sym5	172
6.78 Simulink three-phase to ground ABC-G fault currentssym5.....	173
6.79 Algorithm three-phase to ground ABC-G fault currents sym5.....	173
6.80 Three-phase-to-ground ABC-G currents approximation coefficients sym5.....	174
6.81 Three-phase-to-ground ABC-G fault currents detailed coefficients sym5.....	174
6.82 Simulink no-fault three-phase currents	176
6.83 Algorithm no-fault three-phase currents	176
6.84 No-fault currents approximation coefficients DAM.....	177
6.85 No-fault currents detailed coefficients DAM.	177
6.86 Simulink single-line-to-ground B-G fault currents DAM	178
6.87 Algorithm single-line-to-ground B-G fault currents DAM	179
6.88 Single-line-to-ground B-G fault currents approximation coefficients DAM	179
6.89 Single-line-to-ground B-G fault currents detailed coefficients DAM	180
6.90 Simulink double-line-to-ground AB-G fault currents DAM	181
6.91 Algorithm double-line-to-ground AB-G fault currents DAM	181
6.92 Double-line-to-ground AB-G currents approximation coefficientsDAM	182
6.93 Double-line-to-ground AB-G fault currents detailed coefficients DAM.....	182
6.94 Simulink double-line B-C fault currents DAM	183
6.95 Algorithm double-line-B-C fault currents DAM	183
6.96 Double-line B-C fault currents approximation coefficients DAM	184
6.97 Double-line B-C fault currents detailed coefficients DAM.....	184
6.98 Simulink three-Phase ABC fault currents DAM	185
6.99 Algorithm three-phase ABC fault currents DAM.....	185

6.100 Three-phase ABC fault currents approximation coefficients DAM.....	186
6.101 Three-phase ABC fault currents detailed coefficients DAM.....	186
6.102 Simulink three-phase to ground ABC-G fault currentsDAM.....	187
6.103 Algorithm three-phase to ground ABC-G fault currents DAM.....	187
6.104 Three-phase-to-ground ABC-G currents approximation coefficients DAM.....	188
6.105 Three-phase-ground ABC-G fault currents detailed coefficients DAM.....	188

LIST Of TABLES

TABLE	Page
4.1 Typical values of multiplying factor for circuit breakers of different speeds.....	84
6.1 Maximum values of detailed coefficients using db4 Wavelet	193
6.2 Maximum value of detailed coefficients using Haar Wavelet.....	197
6.3 Maximum value of detailed coefficients using DAM Wavelet	195
6.4 Maximum value of detailed coefficients using sym5 Wavelet.....	196
6.5 Wavelet coefficients energy for db4 Wavelet.....	201
6.6 Wavelet coefficients energy for Haar Wavelet.....	202
6.7 Wavelet coefficients energy for DAM Wavelet	203
6.8 Wavelet coefficients energy for smy5 Wavelet	204
6.9 Optimal Wavelets based on Wavelet coefficient energy analysis	206

LIST OF ABBREVIATIONS

Abbreviations	Description
AC	Alternating Current
AB	Phase A to Phase B Fault
ABC	Three-Phase (Phase A, Phase B, Phase C) Fault
ABC-G	Three Phase (Phase A, Phase B, Phase C)-to-Ground Fault
AB-G	Double Line (Phase A and Phase B)-to-Ground Fault
AG	Phase A to Ground Fault
ANN	Artificial Neural Network
BC	Phase B to Phase C Fault
BC-G	Double Line (Phase B and Phase C)- to- Ground Fault
BG	Phase B to Ground Current Fault
CA	Approximation Coefficients
CD	Detailed Coefficients
CG	Single Line (Phase C)-to-Ground Fault
db4	Daubechies 4 Wavelet
DAM	Discrete Approximation Meyer Wavelet
DC	Direct Current
DLG	Double-Line-to-Ground Fault
DSP	Digital Signal Processing
DWT	Discrete Wavelet Transform
CWT	Continuous Wavelet Transform
FT	Fourier Transform

Abbreviations	Description
FFT	Fast Fourier Transform
MRA	Multiresolution Analysis
r.m.s	Root Mean Square
SLG	Single-Line-to-Ground Fault
LL	Line-to-Line Fault
LG	Line-to-Ground Fault
LLG	Double-Line-to-Ground Fault
LLL	Three-Phase Fault
LLLG	Three-Phase-to-Ground Fault
sym5	Symlet 5
Td	Threshold
WT	Wavelet Transform

LIST OF SYMBOLS

Symbol	Description
$f(t)$	Input Signal or Function
'a'	Scale Parameter
' τ '	Translation Parameter
$\psi(t)$	Mother Wavelet
$\psi^*(t)$	Complex Conjugate of the Wavelet Function
N	Total Number of Samples in Input Signal
Z	Impedance
R	Real Part of the Signal
jX	Imaginary Part of the Signal
V_L	Nominal Line Voltage
I_F	Fault Current
X_d	Direct Axis Reactance
X_q	Quadrature Axis Reactance
X_f	Reactance of Field Circuit
τ_d''	Direct Axis Short Circuit Sub-Transient Time Constant
X_{kd}	Reactance of damper circuit
τ_{do}'	Direct Axis Open-Circuit Transient Time Constant

1. INTRODUCTION

The development of AC systems began in the United States in 1885. The key figures in the early AC transmission systems were George Westinghouse and Nikola Tesla, a brilliant inventor and engineer. In 1885, Westinghouse purchased the American patents for an AC transmission system developed by Lucien Gaulard and John Dixon Gibbs, who were from France. This acquisition allowed Westinghouse to advance AC technology in the United States. Westinghouse also collaborated closely with Tesla, who significantly contributed to the development and promotion of AC technology.

William Stanley, an early associate of George Westinghouse, played a pivotal role in developing AC systems. In his Great Barrington, Massachusetts laboratory, Stanley conducted experiments and tests related to AC technology. He is known for his work on transformers and other AC components.

The first AC transmission line in the United States was operated in 1890. It was designed to carry electric energy generated by water power from Willamette Falls to Portland, Oregon. This 13-mile transmission line was a significant milestone in developing long-distance electrical power distribution using AC. This period marked the transition from direct current (DC) to AC as the preferred method for long-distance electrical transmission. AC's ability to be easily transformed to different voltage levels and its efficiency over longer distances made it a more practical choice for transmitting electricity over large areas.

This thesis follows the style of the *Institute of Electrical and Electronics Engineers*.

The contributions of Nicola Tesla, George Westinghouse, and William Stanley and the adoption of AC technology for practical applications like the transmission of electricity over long distances played a crucial role in shaping the modern electrical power distribution system in the United States and worldwide. Initially, the early transmission lines were single-phase, and the primary application was for lighting. This period was the earliest stage of electrical distribution systems. On May 16, 1888, Nikola Tesla presented a paper titled "A New System of Alternating Current Motors and Transformers," in which he introduced the concept of two-phase induction and synchronous motors. This concept was a significant advancement as it laid the foundation for more efficient and versatile AC motors, which could be used for broader applications beyond lighting. The advantages of polyphase motors, including increased efficiency and versatility, became evident soon after Tesla's work. Polyphase motors allowed for a broader range of industrial and commercial applications.

The World's Columbian Exposition in Chicago in 1893 was a pivotal moment in the history of electrical engineering. It featured the first major public demonstration of a two-phase AC distribution system, which George Westinghouse and Nikola Tesla developed. This demonstration highlighted the superiority of polyphase AC systems and helped convince the public and industry of their advantages over DC systems.

The advantages of polyphase motors, including enhanced efficiency and versatility, became evident, leading to a shift in the adoption of AC systems, particularly three-phase AC, which gradually replaced DC systems. A pivotal aspect in the success of AC systems was the capability to employ transformers, allowing for the efficient stepping up of voltage during long-distance transmission and subsequent stepping down for local distribution.

This transformative capability addressed challenges in power distribution, contributing significantly to the widespread acceptance and implementation of AC systems over DC alternatives.

By January 1894, multiple polyphase-generating plants were in the United States. Three-phase AC systems became the dominant choice for power generation and transmission because of their efficiency and ability to handle various loads. Overall, the development and widespread adoption of polyphase AC systems and the use of transformers for voltage transformation revolutionized the electricity industry and played a crucial role in the electrification of the United States and other parts of the world. These innovations laid the foundation for the modern electrical power systems we rely on today.

The consistent and predictable growth rate in installed generating capacity and energy production observed from the 1920s to the 1970s or 1980s gave way to a more complex and fluctuating pattern due to economic, technological, environmental, and market factors. The energy industry has continued to evolve, with ongoing changes in the mix of energy sources, generation technologies, and efforts to address environmental concerns and improve energy efficiency. In the later decades of the 20th and 21st centuries, the energy landscape became more complex and diversified, with a growing focus on sustainability and reducing greenhouse gas emissions. This growth led to more diverse energy portfolios, including adopting renewable energy sources like wind, solar, and hydroelectric power.

The transition from consistent and exponential growth in installed capacity and energy production to more erratic and unpredictable growth patterns reflects the evolving energy needs, technologies, and policies of the times. In the early days of AC power

transmission; there was a rapid increase in operating voltage levels. This increase in voltage was driven by the need to transmit electrical power efficiently over longer distances. Higher voltages reduced energy losses during transmission.

Initially, electric power systems in the United States operated as isolated, localized systems. These systems often started as small, remote networks and gradually expanded to larger geographic areas. Individual companies usually use them independently [1].

As electricity demand grew and the need for larger blocks of power and increased reliability became evident, the idea of interconnecting neighboring power systems gained traction. Interconnection allowed for several advantages [2]:

i. Economic Efficiency: interconnected systems could share resources and reduce the need for redundant generation capacity, especially for peak loads. This system was more cost-effective than each system maintaining its excess capacity.

ii. Reliability: interconnected systems could support one another during high demand or equipment failures, enhancing overall system reliability.

iii. Optimal Power Sources: interconnection enabled companies to access the most economical power sources, including hydropower, coal-fired plants, and other resources. This flexibility improved cost-efficiency.

iv. Load Balancing: by exchanging power between systems, companies could better manage sudden jumps in load, ensuring a more stable power supply.

Over time, the practice of interconnection between neighboring power systems became more common and sophisticated. Companies increasingly relied on interconnected grids to meet their electricity needs. This trend continued, developing larger regional and national grids for efficient power distribution and exchange.

1.1 Background of the Study

Power systems play a crucial role in the modern world, and it is essential to ensure power system stability. Detecting and identifying faults in these systems is highly critical. Faults in power systems can result from various factors, including equipment failures, environmental variables, and operational errors. Their occurrence can lead to power outages and disruptions, making the timely identification of these faults vital [1]. This study used Wavelet analysis to detect short-circuits faults in three-phase power systems.

This study holds great importance due to the challenges faced by current fault detection methods, especially their accuracy with noise and disturbances. Having reliable fault detection is crucial for a consistent and steady electricity supply. While previous studies have provided valuable ideas and methods, there is still a need for new approaches and a more detailed examination of Wavelet analysis in this field.

Today, the United States has a highly interconnected and complex electrical grid, allowing for the efficient and reliable transmission and distribution of electrical power across vast geographic regions. Interconnection and coordination between different utility companies and areas have become standard practices in the electricity industry, contributing to a robust and resilient power infrastructure [3].

Interconnecting power systems offers many benefits, such as improved reliability, efficient resource utilization, and access to diverse power sources. However, it also introduces technical challenges that require careful planning, engineering, and ongoing maintenance to ensure the safe and reliable operation of the interconnected grid.

Interconnecting power systems can increase the flow current during a short circuit event. This raise necessitates circuit breaker installation capable of interrupting larger

currents. These circuit breakers are critical for isolating and protecting grid sections during fault conditions to prevent widespread outages.

Short circuits or disturbances in one part of an interconnected system can propagate to other interlinked systems. Protective devices such as relays and circuit breakers are crucial to prevent such cascading failures. These devices can detect abnormal conditions and isolate faulty sections promptly, minimizing the impact of faults.

Interconnected systems must maintain the same nominal frequency (e.g., 60 Hz in the United States) to ensure stable and synchronized operation. If the frequency of one system deviates significantly from that of others, it can lead to issues such as equipment damage and power imbalances. Synchronous generators must also remain in phase and synchronized to maintain grid stability.

Effective planning and engineering studies are essential for power system operation, improvement, and expansion. These studies include load studies to understand demand patterns, fault calculations to assess system behavior during faults, and the design of protection systems to mitigate surges and short circuits. Additionally, stability studies are crucial to ensure the grid remains stable under various operating conditions. As power grids become more complex and interconnected, ensuring their resilience involves developing strategies and technologies to withstand and recover from multiple disturbances, including natural disasters, cyber-attacks, and equipment failures.

With technological advancements, power grids are undergoing modernization efforts, including integrating smart grid technologies, which provide real-time data and control capabilities to enhance grid reliability, efficiency, and flexibility.

Faults in power systems, such as short circuits or equipment failures, can be destructive and disruptive. Preventing damage to transmission lines and equipment and minimizing interruptions in power generation are critical goals in power system engineering. Engineers and researchers continuously work on improving fault detection methods, designing protective devices, and developing schemes to isolate faults and maintain system reliability [1].

Power systems have become increasingly complex due to higher demand, integration of renewable energy sources, and the need for smart grid technologies. This complexity requires advanced and adaptable fault detection methods and protection schemes.

Wavelet analysis is a mathematical technique that can be used for signal processing, including the analysis of electrical waveforms. Wavelet analysis has seen significant development, primarily driven by mathematicians and scientists like Yves Meyer. Alfred Haar first introduced the name “Wavelet” in 1909. However, Jean Morlet proposed the modern theoretical form of Wavelet analysis. Stephane Mallat developed the main algorithm for Wavelet analysis in 1988. Since then, many studies have contributed to the understanding and applications of Wavelets in various fields, including signal processing, image compression, and applications in power system analysis [4, 5].

Wavelet analysis offers a powerful tool for analyzing and processing signals, making it helpful in detecting and characterizing various types of electrical disturbances and faults within power systems. Its versatility has made it an essential technique in modern electrical engineering and signal processing.

In summary, this study aimed to contribute to a more reliable power system by exploring innovative methods for fault detection. Previous study has provided valuable insights and methodologies, yet it has also highlighted the need for further exploration. By merging the fields of power system engineering and digital signal processing, this study intends to expand the knowledge in this critical area. The goal was not limited to filling the gaps in existing studies but involved introducing fresh approaches for fault detection and identification. These new methods will lead to innovative advancements in the field.

1.2 Problem Statement

In modern power systems, the reliable and uninterrupted supply of electricity is essential for the functioning of society. However, achieving an utterly fault-free power system is impractical due to various factors, including equipment failures, environmental conditions, operational errors, and other unforeseen events. These faults disrupt power supply and pose significant challenges for timely detection and accurate identification.

Existing fault detection methods face difficulties when distinguishing between different fault types, especially in the presence of noise and disturbances. Therefore, the central problem addressed in this thesis is the need for a practical and accurate fault detection approach in three-phase power systems. By bridging the gap in current literature and exploring the potential of Wavelet analysis, this study sought to provide valuable insights and methodologies to enhance the reliability and stability of power systems.

The study investigated how a mix of Wavelet transforms (WT), the threshold technique, and Wavelet coefficients' energy analysis (WCEA), combined with qualitative insights, can contribute to accurate short-circuit fault detection and identification in three-phase power systems. By addressing this problem, this thesis sought to advance the

understanding of fault detection methodologies and provide practical solutions to improve the reliability of the power system to benefit society.

1.3 Purpose, Scope, and Significance of the Study

This section outlines the study's purpose, scope, and significance. Through Wavelet analysis, it explains the importance of investigating fault detection in three-phase power systems. In addition, this section highlights the assumptions used for the analysis and the limitations.

i. Purpose of the Study: the primary objective of this study was to address the critical need for accurate fault detection and identification in three-phase power systems because of the increasing demand for a reliable and uninterrupted power supply in modern society. This study used Wavelet analysis and exploration of various Wavelet transforms combined with the threshold technique to enhance fault detection methodology. The goal was to fill the gap in the existing power systems fault detection studies by developing a method to improve power systems' reliability and stability.

ii. Scope of the Study: this study applied Wavelet analysis and other related techniques for fault detection in three-phase power systems. The study investigated different Wavelet transforms, including Daubechies 4 (db4), Haar, Symlet 5 (sym5), and Discrete Approximation Meyer (DAM). The threshold technique detects and identifies the short circuit faults. The Wavelet coefficients energy technique introduced. Utilizing both qualitative and quantitative research methodologies to investigate the optimal Wavelet for fault detection involves connecting numerical data with expert insights.

iii. Significance of the Study: this study addressed the need for enhanced fault detection in power systems to maintain reliability. This study is significant because it

provided a methodology for fault detection to reduce the downtime of the power supply. Moreover, this study fills a critical gap in the existing literature by exploring integrating qualitative and quantitative methodologies in power systems fault detection—the insights obtained from expert consultations, combined with a quantitative data perspective precise understanding of the findings.

iv. Assumption of the Study: the study assumed that the methodologies employed, including Wavelet analysis and the threshold technique, applied to power systems' fault detection. In addition, the study assumed the three-phase power system model simulated by the MATLAB/Simulink would provide accurate data for the analysis.

v. Limitations of the Study: the study focused only on three-phase power systems, and the fault under study is the short circuit fault only in the three-phase power system. In addition, the study did not explore faults related to renewable energy sources, which means it is applicable only to the three-phase conventional power systems. Another limitation is that fault detection accuracy depends on the predefined manual set value for the threshold, which means variations in the threshold value could influence the results.

1.4 Study Questions

This section introduces the study questions that established the investigation into short-circuit fault detection in three-phase power systems using Wavelet analysis. The study questions guided the study, providing a clear focus and purpose. Each study question and sub-question carefully listed to address specific aspects of the study, ensuring a comprehensive examination of the topic. These questions enabled exploring the concept and advantages of Wavelet analysis, the threshold technique, and the Wavelet coefficients energy.

i. Primary Study Question: How can Wavelet analysis enhance detecting and identifying short-circuits faults in three-phase power systems?

Sub-questions:

- How can various Wavelet transforms, including db4, Haar, sym5, and Discrete Approximation Meyer, be effectively applied to detect and identify short-circuit faults in a three-phase power system?
- How the accuracy of short-circuit fault detection is affected by various Wavelet families (db4, Haar, sym5, Discrete Approximation Meyer)?
- How do the selected Wavelets distinguish between fault types, such as line-to-line, line-to-ground, three-phase, and three-phase-to-ground faults?

ii. Secondary Study Question: What role and impact does the threshold-selected technique have on enhancing the accuracy of fault detection when applied to the current signal detailed coefficients obtained through Wavelet decomposition?

Sub-questions:

- What are the optimal threshold values for each selected Wavelet that maximize the precision and recall of fault detection?
- Can the same selected threshold value be applied universally across the selected Wavelets to detect faults in this study accurately?
- How do threshold value variations influence the fault detection process's overall accuracy and reliability?

iii. Third Study Question: How can Wavelet coefficient energy analysis determine the optimal Wavelet for short-circuit fault detection?

Sub-Questions:

- What methods can be employed to analyze Wavelet coefficients' energy for the various Wavelets used in fault detection?
- How do different Wavelets perform regarding energy distribution within their coefficients when applied to short-circuit fault signals?
- What criteria can be established to define the 'optimal' Wavelet concerning energy analysis results in short-circuit fault detection?
- What is the relationship between the energy of Wavelet coefficients and the effectiveness of different Wavelets in detecting short-circuit faults in a three-phase power system?
- What specific Wavelet coefficients should be considered in the energy analysis for identifying the optimal Wavelet for short circuit fault detection?
- Is there a universal Wavelet that is optimal for all fault types?

These study questions and sub-questions guided this study, enabling it to explore the effectiveness of various Wavelet techniques, the role of the threshold, and the optimal Wavelet for fault detection in the three-phase power system.

1.5 Significance

The importance of this study understood in two main ways. First, it contributes to the academic world by deepening knowledge of Power System Engineering and Digital Signal Processing Engineering. Second, it has practical significance for those two fields of engineering. We intended to bridge the gap and increase knowledge of these two distinct but related fields: Power System Engineering and Digital Signal Processing Engineering.

From an academic standpoint, this study adds to what known about these two engineering fields. It explores how we can use advanced digital signal processing

techniques to improve the reliability and stability of power systems. Essentially, it is about finding more innovative ways to be more efficient, reducing downtime, saving money on repairs, ensuring the power keeps flowing smoothly, and ensuring modern society always has electricity without interruption.

From a practical standpoint, this study contributes to the growing demand for power systems fault detection, particularly for three-phase systems. By exploring Wavelet transform analysis and Wavelet coefficients energy analysis to detect faults and find the optimal Wavelet for fault detection, this study offers valuable tools for power systems and digital signal processing engineering practitioners.

In summary, this study sought to increase the knowledge of fault detection in power systems and provide practical tools for those working in the field. The results of this study are a valuable resource for both fields of power systems and digital signals processing engineers to improve the reliability and stability of three-phase power systems.

1.7 Expected Contributions

This section outlines the anticipated contributions of the study, leveraging the MATLAB/Simulink for power system simulations and integrating Wavelet algorithms to extract detailed coefficients for fault detection. By investigating diverse Wavelet transforms, assessing threshold techniques, and delving into Wavelet coefficient energy analysis, the research aimed to elevate the precision of short-circuit fault detection. These contributions collectively advance the efficacy of Wavelet analysis in improving fault detection within three-phase power systems.

- i. Employ the MATLAB/Simulink and algorithm to simulate the power system and generate fault scenarios, then apply Wavelet algorithms to the simulated current signals to extract detailed coefficients for comparison.
- ii. Explore the practical application of various Wavelet transforms—db4, Haar, sym5, and Discrete Approximation Meyer—for short-circuit fault detection in three-phase power systems.
- iii. Evaluate the impact of the different selected Wavelet families on the accuracy of short-circuit fault detection, considering line-to-ground, line-to-line, double-line-to-ground, three-phase, and three-phase-to-ground faults.
- iv. Identify optimal threshold values for each selected Wavelet, maximizing short-circuit fault detection's precision.
- v. Investigate the universality of threshold values across different Wavelets and exploring variations in threshold values will provide insights into their influence on accuracy and reliability.
- vi. Pioneer methods for conducting Wavelet coefficients energy analysis and evaluating the performance of the different Wavelets concerning energy distribution within their coefficients will provide a foundation for determining the optimal Wavelet.
- vii. Investigate the existence of a universal optimal Wavelet for all fault types to guide the choice of Wavelets that excel in applying the three-phase power systems fault detection.

In summary, the study's expected contributions include advancing the understanding of Wavelet-based techniques, optimizing threshold selection, determining

the optimal Wavelet for enhanced short-circuit fault detection, offering practical insights, and guiding future research in power system fault detection.

1.7 Definition of Terms

This section defines key terms and concepts used within the study topic. The definitions adhere to the most current version of the IEEE citation style.

i. Wavelet Analysis: a mathematical technique used for signal processing, which involves the transformation of signals into various scales and resolutions for in-depth analysis.

ii. Fault: abnormal condition or a failure in the electrical network that disrupt the normal flow of electric current.

iii. Fault Detection: identifying and locating abnormalities or disturbances in a power system, indicating deviations from regular operation.

iv. Short-Circuit Fault: an electrical fault characterized by unintended connections between electrical conductors with low resistance, resulting in excessive current flow.

v. Symmetrical Fault: a balanced fault is a type of fault with uniform impedance or fault conditions across all phases, leading to a balanced distribution of currents and voltages.

vi. Unsymmetrical Fault: this is a type of fault condition where the impedance or fault characteristics vary among the different phases of the system, leading to imbalances in the distribution of currents and voltages across the phases.

vii. Threshold Technique: a method for distinguishing relevant signal components by applying a predefined threshold, effectively isolating significant data from noise.

viii. **Wavelet Coefficients Energy Analysis:** an approach that involves analyzing the energy content of Wavelet coefficients to determine the optimal Wavelet for specific fault detection applications.

ix. **Symmetrical Components:** mathematical techniques used in power systems analysis to simplify the analysis of unbalanced conditions, such as faults. The concept of symmetrical components involves decomposing an unbalanced set of three-phase phasors into three sets of balanced phasors, known as positive sequence, negative sequence, and zero sequence components.

x. **Positive Sequence Component:** represents a set of balanced phasors that rotate in the same direction and with the same angular velocity as the original system. It corresponds to the normal operation of the power system.

xi. **Negative Sequence Component:** represents a set of balanced phasors that rotate opposite to the positive sequence component. Negative sequence components are associated with unbalanced conditions caused by phase imbalances or unsymmetrical faults.

xii. **Zero Sequence Components:** represents a set of balanced phasors with zero angular velocity, implying that the phasors are in phase with each other. It is associated with unbalanced conditions where the entire system experiences a common-mode disturbance, such as a ground fault.

xiii. **Qualitative Study:** an exploratory study methodology used to gain deeper insights into human behavior and the underlying reasons, that often involving interviews, observations, or expert consultations.

xiv. **Quantitative Study:** a study approach that collects and analyzes numerical data to make statistical inferences and derive objective conclusions.

xv. **Power System:** a network of interconnected electrical components and devices designed to generate, transmit, and distribute electrical energy.

xvi. **Digital Signal Processing (DSP):** using algorithms and digital computing techniques to manipulate, process, and analyze signals or data represented in discrete form, typically in time or space, enhancing efficiency, accuracy, and capabilities in various signal-related applications.

xvii. **Signal Processing:** the manipulation and analysis of signals, such as electrical or digital signals, aimed at extracting valuable information, eliminating noise, and enhancing understanding.

xviii. **Wavelet Coefficients:** these numerical values result from applying Wavelet transforms to a signal. Wavelet transforms decompose a signal into coefficients representing its frequency components at different scales and positions. These coefficients indicate the strength or amplitude of localized waveforms within the signal.

xix. **Detailed Coefficients:** represents a signal's high-frequency components or details. When a signal undergoes a Wavelet transform, the detailed coefficients capture the signal's rapid variations or fine details at different scales. They provide information about the signal's sharp changes or sudden transitions.

xx. **Approximation Coefficients:** represents the low-frequency components or coarse approximation of the signal. These coefficients capture the signal's overall trend or smoother features at different scales. They provide information about the general behavior or trends in the signal without the fine details.

xxi. Multi-Resolution Representation: is the breakdown of a signal into different scales, capturing both high and low frequency components. In the context of Wavelet analysis, this involves detailed coefficients highlighting high-frequency details and approximation coefficients emphasizing low-frequency trends. Together, these coefficients form a multi-resolution representation, offering a nuanced understanding of a signal's intricate details and general trends across various scales.

xxii. Universal Wavelet: an optimal Wavelet function that stands out as the winner for accurately representing signals from diverse domains and types, making it valuable in applications like fault detection.

xxiii. Universal Threshold Values: a single threshold value that consistently applied across various selected Wavelets for accurate fault detection.

xxiv. IEEE Citation Style: A widely recognized academic writing and referencing style established by the Institute of Electrical and Electronics Engineers (IEEE) provides guidelines for study paper formatting, citations, and references.

These definitions clarify key terms used throughout the study and establish a shared understanding of their significance within the study while adhering to the IEEE citation style.

1.8 Organization of the Reminder of the Study

This introduction chapter provided a comprehensive summary of the world of electricity and power systems. This chapter highlighted the significance of fault detection, which affects the reliability and stability of electricity supply. The challenges posed by power system faults examined, considering their diverse origins, from equipment failures

to environmental factors, emphasizing the need for timely and accurate fault detection and identification.

The problem statement section listed the challenge and the need for this study. It discussed various factors and conditions leading to power system faults and their impacts. The purpose, scope, and significance section outlined the reasons behind the study and the significance of the identified problem. In addition, it mentioned the study's position in combining power system engineering and digital signal processing. The significance section highlights the study's contribution to the field. It emphasized the value of the study to scholars and practitioners in power system engineering and digital signal processing, bridging the gap between these two fields. The definition of terms section provides concise definitions of standard terms used within the field of the study. It adheres to the current IEEE citation style. Organization of the remainder of the section outlines the structure and content of the chapters following the introduction chapter, offering an overview of what has to come in these chapters.

Chapter 2 – Literature Review: this chapter overviews existing literature on power systems fault detection, Wavelet analysis, and digital signal processing, offering an understanding of studies conducted in these fields.

Chapter 3 – Wavelets: this chapter provides an overview of Wavelets, their mathematical foundations, and their applications in signal processing. It serves as a resource for readers to understand the core concepts related to Wavelets used in the study.

Chapter 4 – Power System Fault: this chapter overviews power system faults, covering key concepts, fault types, the effect of fault current and detailed analyses of both symmetrical and unsymmetrical faults. Also, review the symmetrical components and the

method of symmetrical components for analyzing unsymmetrical faults, contributing essential insights to enhance power system reliability.

Chapter 5 – Methodology: this chapter explores the study methodology used to collect, analyze, and interpret the data. It details the approach to Wavelet selection, threshold techniques, and data collection, clearly understanding the study process.

Chapter 6 – Results and Discussion: this chapter details the simulation setup in MATLAB, the commands for fault detection, and the use of predefined threshold values. It outlines the systematic process of simulating power system short circuit faults, applying Wavelet analysis, and detecting faults with the algorithms. Then, it presents the findings obtained through Wavelet analysis and threshold techniques to the power system data obtained from the MATLAB/Simulink. It discusses the selected Wavelets' performance in detecting various fault types and the results of applying the threshold technique to the detailed coefficient's maximum value and applying the Wavelet coefficients energy technique to highlight the optimal Wavelet for fault detection.

Chapter 7 – Conclusions: this chapter interprets the context of the initial hypotheses and study questions. It provides a conclusion summarizing the entire study, its significance, and its limitations, which leads to recommendations for future studies, such as potential methodological improvements.

This organized structure ensures a logical flow of the study's main points, guiding the reader through the process from introduction to conclusion. The study included dedicated separate chapters on "Wavelets" and "Power System Stability" to provide more understanding of the subject.

1.9 Summary

The introduction chapter laid the foundation for the entire study. It addressed various critical aspects to provide a comprehensive overview of its background, problem statement, purpose, scope, and significance, aligning it with the persistent need for enhanced fault detection methods in evolving power systems. The study questions defined to provide clarity, focus, and direction to the study. Additionally, the chapter outlined the organization of the subsequent sections in the thesis. With this foundation, the next chapter delves into the literature review, providing a comprehensive overview of existing studies, methodologies, and advancements in power systems fault detection, setting the stage for the study ahead.

2. LITERATURE REVIEW

The detection and localization of short-circuit faults in three-phase power systems are essential for maintaining electrical network reliability and ensuring uninterrupted power supply. With the increasing complexity of modern power grids, there is a growing need for advanced fault detection methods that are both accurate and efficient. This chapter delves into the existing body of knowledge in the field of short-circuit fault detection, with a particular focus on using Wavelet-based approaches. These approaches have gained significant attention recently due to their potential for precise fault detection and localization. By examining the prior study and methodologies employed by experts in the field, this literature review aims to shed light on techniques for fault detection.

This chapter explores the knowledge related to power systems, fault types, detection methods, and the significance of Wavelet analysis. By delving into the works of researchers, this chapter enables, a deeper understanding of Wavelet-based approaches in short-circuit fault detection. It offers valuable insights for future work in the field.

2.1 Three-Phase Power System Short Fault Detection and Classification Techniques

In the world of power systems fault detection, various techniques invented to ensure the reliability and stability of power systems. These techniques used different methodologies, ranging from well-established conventional protection schemes such as over-current relays and distance protection, which are effective for detecting faults like short circuits. Additionally, advanced technologies have emerged, including synchronized phasor measurement units (PMUs) and fault location algorithms, enhancing fault detection accuracy and response times. Integrating fault detection and signal processing has offered many helpful power systems fault detection techniques. The Fourier transform techniques provide insights into frequency domain characteristics, while Wavelet-based approaches offer a superior understanding of time-frequency representations. Furthermore, the integration of artificial intelligence, machine learning, and signal processing methods have given rise to intelligent fault detection systems capable of handling complex fault scenarios and disturbances.

As the power grid continues to evolve with the integration of renewable energy sources and smart grid technologies, fault detection techniques remain dynamic and adaptable to meet the evolving requirements of contemporary electrical networks.

E. Mengistu et al. [6] investigated the effective identification of different types of faults in a distribution system using the Fast Fourier Transform (FFT). Their study showed

that when a line-to-ground fault occurs, the affected phase experienced a significant drop in maximum voltage (around 50%) and a phase shift of approximately 180 degrees. In the case of a double phase-to-ground fault, the affected phases exhibit voltage and phase angle characteristics similar to the healthy phase. In contrast, a three-phase-to-ground short circuit fault resulted in a voltage drop in any phase. The study revealed that the current magnitudes for double-phase-to-ground and three-phase-to-ground faults were similar, making it challenging to use current as a distinguishing variable for identifying the nature of the short circuit fault. To overcome this challenge, the authors proposed using FFT to analyze the peak potential and phase angle shift to identify and classify the three-phase short circuit fault type. This approach eliminated manual evaluation of output voltages from multiple buses, significantly reducing the time required for fault identification and enhancing network reliability.

Z. Zhou et al. [7] presented findings on detecting transmission line short-circuited faults using a lifting Wavelet approach. Their study outlined a method to improve fault detection in power systems, explicitly emphasized single-phase short-circuit faults. The results indicated that the lifting Wavelet approach holds promise in enhancing the accuracy and effectiveness of fault detection. By applying Wavelet-based methods, the researchers could identify and locate short-circuit faults in transmission lines more precisely and efficiently than traditional approaches.

P. Broniera et al. [8] discussed using artificial neural networks to diagnose stator winding inter-turn short circuits in three-phase induction motors. The widespread use of induction motors in industry has led to various studies on analyzing and predicting motor failures. This paper introduced an alternative approach to traditional fault detection

methods, specifically for identifying short circuits between the inter-turns of the stator winding. The proposed method employed artificial neural networks (ANN) to analyze stator current signals in the time domain. The authors conducted experiments involving 134 samples of stator current signals, which trained and validated using three different network architectures. Among these, Network Architecture 3 demonstrated the best performance, achieving a test set accuracy of 94.54%.

2.2 Power Systems Fault Detection Wavelet-Based Techniques

Numerous fault detection and classification techniques developed, offering solutions to identify and categorize different types of faults that may occur. One approach that has emerged is Wavelet-based techniques. This section explores some of the studies for fault detection in three-phase power systems, focusing on Wavelet-based methodologies. By delving into the principles and applications of Wavelet-based techniques, this section aims to provide a comprehensive understanding of their role in enhancing the robustness and accuracy of fault detection and classification systems for three-phase power systems.

Reviewing the existing literature in this domain helps uncover the wealth of knowledge and insights accumulated by researchers in the field, providing understanding that can contribute to advancing more efficient solutions for detecting and identifying faults in three-phase power systems.

2.2.1 Wavelet-Based High-Impedance Fault Detection in Power Systems

In electrical systems, a high-impedance fault is a type of fault with a partial electrical disconnection or increased electrical impedance in a circuit. It does not necessarily mean an open circuit in the sense of a complete break in the conductive path.

High-impedance faults can occur when there is a partial fault or a poor electrical connection, leading to arcing and posing a safety hazard. These faults can be challenging to detect with traditional protection methods, making them an essential study area of power systems fault detection.

S. Huang et al. [9] focused on detecting high-impedance faults, a particularly challenging aspect of power system reliability. The approach introduced in this study was based on the Morlet Wavelet transform. By harnessing Wavelet transforms, this work addressed the intricate task of high-impedance fault detection, demonstrated its potential to enhance the dependability of power systems. The Wavelet transform is a valuable tool in distinguishing these high-impedance faults from routine switching events, which can occur during transient conditions or arcs under normal system operation. This differentiation is crucial, as the most common method for detecting high-impedance faults involves overcurrent protective devices, leading to unscheduled service interruptions due to the limited distinction between harmful and harmless current variations. The discussion also introduced the Wavelet transform and its properties. Notably, the Wavelet transform offered the advantage of simultaneous time and frequency knowledge, making it a superior choice for understanding time-varying signals when compared to the fast Fourier transform, which lacks insights into time domain characteristics. Huang and Hsieh emphasized the critical role of advanced signal processing techniques, particularly the application of Wavelet transforms, in improving the safety and efficiency of electrical grids.

S. Koley et al. [10] presented a Wavelet-based technique for detecting faults and identifying faulty phases in transmission lines. This approach utilized current signals from

both ends of the transmission line to identify accurately the faulty phase, particularly excelling in detecting high impedance faults, a challenging task for traditional relays. By analyzing the phase's angle differences in positive sequence current signals before and after the fault achieved the discrimination between internal and external faults. The technique calculated alienation coefficients based on the first level of approximation coefficients of current signals within a quarter-cycle-length-sliding window. A predetermined fault index threshold effectively identified the faulty phase for single line-to-ground faults within a quarter cycle from the fault's inception. The proposed method boasted a high accuracy rate across various fault scenarios, makes it a reliable and computationally efficient solution for fault detection without needing voltage signal input. This technique achieved identifying faulty phases for both low and high fault resistances.

2.2.2 Wavelet-Based Various Fault Types Detection in Power Systems

This section explores study papers based on Wavelet-based techniques, which have emerged as a powerful tool for improving the detection and classification of different fault types. With their inherent ability to analyze signals in both the time and frequency domains, Wavelets offer a powerful tool for fault detection. Their versatility and adaptability make them well-suited for addressing a variety of fault scenarios. This section aims to unravel how Wavelets effectively used for diverse fault types in power systems.

Huang et al. [11] introduced an approach to compute continuous Wavelet transforms for visualizing disturbances within electric power systems. This innovative Wavelet function derived from the B-spline function and offers unique advantages. The bandwidth-to-center frequency ratio determined solely by parameter settings allowed easy adjustment to accommodate various resolution requirements. Due to its piecewise

polynomial nature, this new function reduced computational intensity in the Wavelet transform process. Furthermore, its compact support enhanced integration speed and accuracy. The study incorporated this novel Wavelet function into the Wavelet transform framework and applied it to analyze disturbances recorded in a steel plant situated in southern Taiwan. The computational results demonstrated the effectiveness of this approach as a valuable tool for monitoring power system disturbances. The method additionally provided promise for extension to other industrial applications where electric power quality is paramount.

B. Reddy et al. [12] simulated a network comprising two interconnected regions connected by a 500 kV transmission line spanning 200 kilometers, which developed using MATLAB. This network modeled to account for distributed parameters. Subsequently, an algorithm based on Discrete Wavelet Transform (DWT) created using the "C" programming language to detect and precisely locate faults within the transmission line. The study's findings revealed that for line-to-ground faults employing a moving window algorithm, the error in fault location varied within the range of -10 % to 13%. The percentage error increased as the fault resistance within the system grew, with a notably rapid increase observed at higher fault resistances. Additionally, they explored the use of circuit reactance during both fault and healthy conditions to calculate fault distances. It observed that an increase in fault resistance led to an escalation in the percentage error in distance measurement. This phenomenon attributed to the rising resistance of the circuit under fault conditions, potentially overshadowing the influence of reactance, thereby causing an increase in percentage error.

A. Contreras-Valdes et al. [13] presented an approach to data compression and fault detection for short-circuit faults in transformers. The paper's primary focus was addressing the challenge of handling a large volume of data generated by the monitoring of electrical transformers, which necessitates efficient data compression techniques for storage and high-speed transmission. The methodology outlined in the paper emphasized using a data compression algorithm based on the Discrete Wavelet Transform. This algorithm has been applied to a database of current signals, demonstrated its effectiveness through a high compression ratio that makes it suitable for storage and transmission. The storage organized in a hierarchical data format, and it confirmed that the compressed files significantly reduced their size, achieving a compression ratio exceeding 78. Moreover, the paper extended its contribution to fault detection. It demonstrated that the decompressed signals obtained using the proposed compression algorithm can effectively detect short-circuit faults in single-phase transformers.

P. Chiradeja et al. [14] introduced a technique for identifying fault locations in three-terminal transmission systems using the Discrete Wavelet Transform (DWT). The paper's primary objective was to improve fault location detection in such systems, and the methodology relies on DWT and traveling wave theory. The proposed technique compared the peak time in the transmission system's first scale of each terminal (bus) to detect faults. As determined through comparison, the two fastest first peak times then utilized as input data for the traveling wave equation. The paper explored and compared the results obtained from three types of mother Wavelets: db4, sym4, and coif to enhance the approach's effectiveness. The comparative analysis aimed to identify the most suitable mother Wavelet for improving fault location accuracy. The proposed technique successfully

identified fault locations in the three-bus transmission system based on DWT and traveling wave theory. Various case studies conducted, considering factors such as different fault inception angles, locations along transmission lines, and fault types. The results illustrated that the 'db4' mother Wavelet consistently outperformed 'sym4' and 'coif4,' with a mean error of less than 400 meters, provided greater accuracy in fault location detection. The paper presented an approach for fault location detection in three-terminal transmission systems using the Discrete Wavelet Transform and traveling wave theory. The results underscored the superiority of the 'db4' mother Wavelet in enhancing fault location accuracy in these systems.

2.3 The Significance of the Proposed Study in Comparison with the Literature

Power systems fault detection has been a focal point in numerous studies, each contributing distinct methodologies and insights. This section provides a comparative analysis combining findings from the literature [6] with the literature [14] while highlighting the unique significance of the proposed study focused on short-circuit fault detection in three-phase power systems.

i. Fast Fourier Transform for Distribution System Faults [6]:

- Methodology: utilized Fast Fourier Transform (FFT) for fault identification.
- Limitation: limited application for specific fault types and challenges in distinguishing fault characteristics.

ii. Lifting Wavelet for Transmission Line Faults [7]:

- Methodology: introduced lifting Wavelet approach for fault detection in transmission lines.

- Limitation: focused primarily on transmission line faults, limiting applicability to broader power system scenarios.

iii. Stator Winding Faults in Induction Motors using Neural Networks [8]:

- Methodology: applied artificial neural networks for diagnosing stator winding inter-turn short circuits.
- Limitation: specialized in induction motors, not directly addressing broader power system faults.

iv. Morlet Wavelet for High-Impedance Faults [9]:

- Methodology: focused on high-impedance fault detection using the Morlet Wavelet transform.
- Limitation: specific to high-impedance faults, addressed a specific aspect of power system reliability.

v. Wavelet-Based Fault Detection in Transmission Lines [10]:

- Methodology: utilized Wavelet-based technique for detecting faults in transmission lines.
- Limitation: primarily concentrated on high impedance faults in transmission line faults, potentially lacking adaptability for broader applications.

vi. B-Spline Derived Wavelet for Electric Power Systems [11]:

- Methodology: introduced a B-spline-derived Wavelet for visualizing disturbances in power systems.
- Limitation: primarily addressed disturbance visualization, not emphasizing fault detection.

vii. DWT Algorithm for Transmission Line Fault Location [12]:

- Methodology: developed a DWT-based algorithm for fault location in a simulated transmission line network.
- Limitation: specialized in transmission line faults, focusing on fault location.

viii. Data Compression and Fault Detection in Transformers [13]:

- Methodology: applied DWT for data compression and short circuit fault detection in a transformer.
- Limitation: targeted a specific application (single-phase transformers) and emphasizes data compression.

ix. Fault Location in Three-Terminal Transmission Systems [14]:

- Methodology: relied on DWT and traveling wave theory for fault location in specific three-terminal transmission systems.
- Limitation: specialized in three-terminal transmission systems.

x. Proposed Study: Short Circuit Fault Detection in Three-Phase Power Systems:

- Methodology: integrated Wavelet decomposition, thresholding, and optimal Wavelet selection for short-circuit fault detection.
- Significance and justification: offered a solution applicable to diverse three-phase power system configurations. This study complemented and extends the scope of existing studies, addressing a broader range of faults in power systems.
- Existing studies often focused on specific fault types or system configurations, whereas the proposed study offered a methodology applicable to a wide range of three-phase power system configurations.

2.3 Summary

This chapter explored various studies and scholarly works on power systems fault detection, specifically on Wavelet-based techniques. This literature review chapter aimed to provide a comprehensive overview of existing knowledge and study findings and establish a solid foundation for the study on optimizing short-circuit fault detection in three-phase power systems using Wavelet-based approaches.

The chapter began with an introduction to the relevance and importance of fault detection in power systems, emphasizing the critical need for accurate and efficient detection methods to ensure the reliability and stability of power distribution networks. We highlighted the challenges posed by different types of faults, including short-circuit faults and the potential consequences of not addressing them promptly.

The literature review section delved into various fault detection techniques, including traditional methods such as overcurrent protection and advanced approaches like Fourier transform-based, Wavelet-based, and artificial intelligence applications. The literature review highlighted findings and insights from the study papers to provide a holistic view of the current state of knowledge and identify areas for further study.

3. WAVELETS

In power systems fault detection, Wavelet analysis has become a powerful tool. Wavelets advanced the way approaches fault detection in electrical power systems because of their unique ability to represent both time and frequency domains simultaneously. As the complexity of power systems continues to grow, the need for more advanced and efficient methods to detect and diagnose faults increases. Wavelet analysis has provided a breakthrough approach to diagnosing electrical systems. Wavelet detects irregularities in electrical waveforms by decomposing signals into different frequency components. This chapter discusses Wavelets and their properties, exploring both continuous and discrete. In addition, this chapter talks about the Wavelet capabilities to capture transient fault signals and distinguish them from normal system behavior, which enhances the accuracy and efficiency of power system stability and fault detection.

By understanding the capabilities of Wavelet analysis, power engineers can effectively identify and respond to faults, ensuring the resilience and reliability of the power system grid.

3.1 Signal Processing Techniques for Power System Analysis: a Comparative of Wavelet Transform and Fourier Transform

In the context of Wavelet analysis, it is customary to draw comparisons with the Fourier Transform (FT), even though FT is not the primary focus of this thesis. This comparative approach aims to elucidate the operational distinctions between Wavelets and FT, facilitating a clearer understanding of why Wavelets may be preferred over FT in specific applications.

A disadvantage of the Fourier Transform lies in its ability to capture global frequency information within a signal. FT covers all frequencies that persist throughout the signal, resulting in a comprehensive but less precise representation. On the contrary, the Wavelet Transform offers a very important advantage over FT by deconstructing and reconstructing the signal with accuracy.

The Wavelet Transform (WT), much like the Fourier Transform (FT), dissects a signal into its constituent frequency components. However, a pivotal distinction arises in the flexibility of the time-frequency resolution offered by the Wavelet Transform, a feature stemming from its utilization of basis Wavelet functions. In contrast, FT relies on sine and cosine functions as its fundamental building blocks. Consequently, in Wavelet analysis, we scrutinize signals with a focus on their time-domain characteristics to unveil their frequency content, leveraging the adaptability of Wavelet functions. Conversely, in Fourier analysis, the emphasis lies in examining signals through the lens of sine and cosine functions.

This inherent advantage of Wavelet Transforms over FT has significantly enhanced the appeal of Wavelet analysis across many applications. Another distinguishing feature

between Wavelet Transforms and FT is the spatial localization of individual Wavelet functions, which contrasts with the non-localized nature of FT's sine and cosine functions [15]. The spatial localization feature, combined with Wavelet Transforms' capacity for frequency localization, has led to their extensive utilization in numerous practical domains. These applications encompass tasks such as data compression, image feature detection, noise reduction in signals, and various other valuable functions [4].

Numerous distinct families of Wavelets exist, each distinguished by specific characteristics and trade-offs governing the compactness and smoothness of the Wavelet shape. This diversity implies that we select a particular Wavelet type that aligns optimally with the specific features we seek within our signal. This feature stands in contrast to FT, which exclusively relies on sine and cosine functions and lacks the versatility of tailored Wavelet selection based on signal attributes.

Wavelets are mathematical functions that cut up data into different frequency components, each with a resolution matched to its scale. They have advantages over traditional Fourier methods in analyzing physical situations where the signal contains discontinuities and sharp spikes. A Wavelet defined as a wave-like oscillation that exhibits localization to a specific period (time domain). Wavelets possess two fundamental properties: scale and location. The scale characterizes the extent to which the Wavelet is stretched or compressed is indicating its frequency. On the other hand, the location attribute signifies the precise temporal position of the Wavelet within the signal.

Fig. 3.1 illustrates the distinctions between the Wavelet Transform and other transformative methods, providing a straightforward visual representation of the

underlying concepts for each transformation, facilitating a side-by-side comparison in this simplistic yet informative graphical depiction.

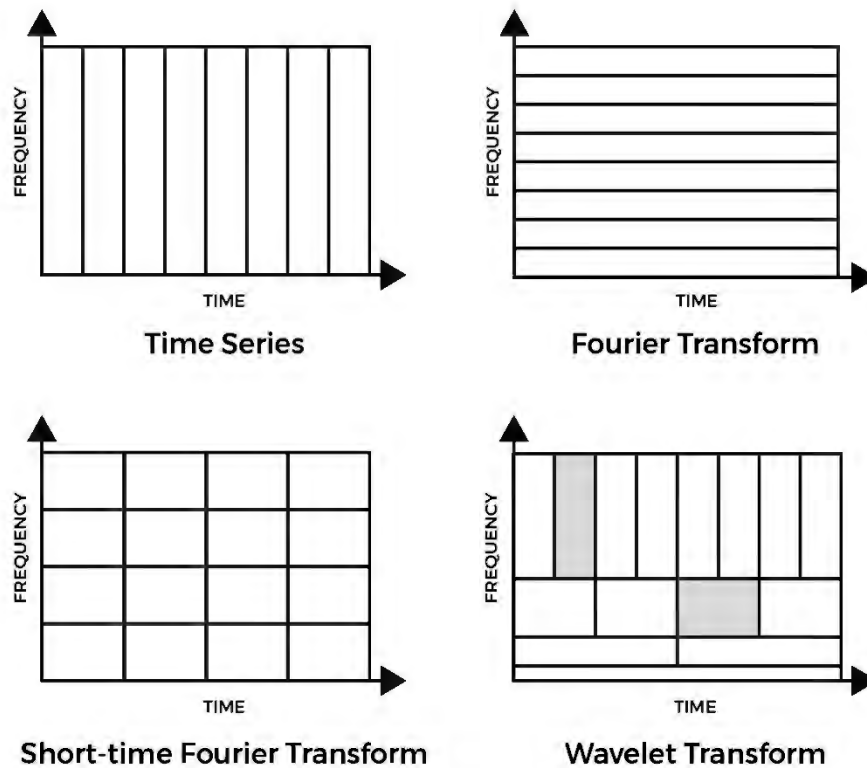


Fig. 3.1 Visual overview for the time and frequency resolutions of diverse transformations. The dimensions and orientations of the blocks symbolize the corresponding resolution sizes [16].

The visual representation allows for a clear understanding of the time and frequency resolutions associated with various transformations. The dimensions and orientation of the blocks serve as indicators of the ability to differentiate fine-scale features within the time and frequency domains. In the case of the original time series, we observe a high-resolution representation in the time domain but a lack of resolution in the frequency domain, which signifies our capacity to identify minute temporal features while simultaneously revealing the absence of discernible frequency-domain features.

In contrast, the Fourier Transform exhibits high resolution in the frequency domain but lacks resolution in the time domain. On the other hand, the Short-Time Fourier Transform offers a moderate resolution in both the frequency and time domains [15].

The Wavelet Transform exhibits distinct characteristics:

- Low-frequency values demonstrate a high resolution in the frequency domain but a comparatively lower resolution in the time domain.
- For high-frequency values, it displays a lower resolution in the frequency domain and a heightened resolution in the time domain.

The Wavelet Transform delivers a balance by prioritizing resolution in the time or the frequency domain based on the scale of interest. It allocates high resolution in the time domain when dealing with time-dependent features and, conversely, emphasizes high resolution in the frequency domain when addressing frequency-dependent features.

3.1.1 Wavelet Time-Frequency Resolutions

Time-frequency resolutions play an essential role in signal processing, offering a unique perspective on how signals evolve while providing insights into their spectral content. This duality of time and frequency analysis is a fundamental Wavelet transform characteristic. The current section explains the concept of "Wavelet Time-Frequency Resolutions," illustrated in Fig. 3.2. This concept is crucial for understanding how Wavelet transforms capture signals' time-localized and frequency-localized features and the inherent trade-off between these two aspects. By exploring the Wavelet Time-Frequency Resolutions, we gain a deeper appreciation of how Wavelet analysis can extract valuable information from signals, making it an essential tool in various fields, from image processing to audio analysis.

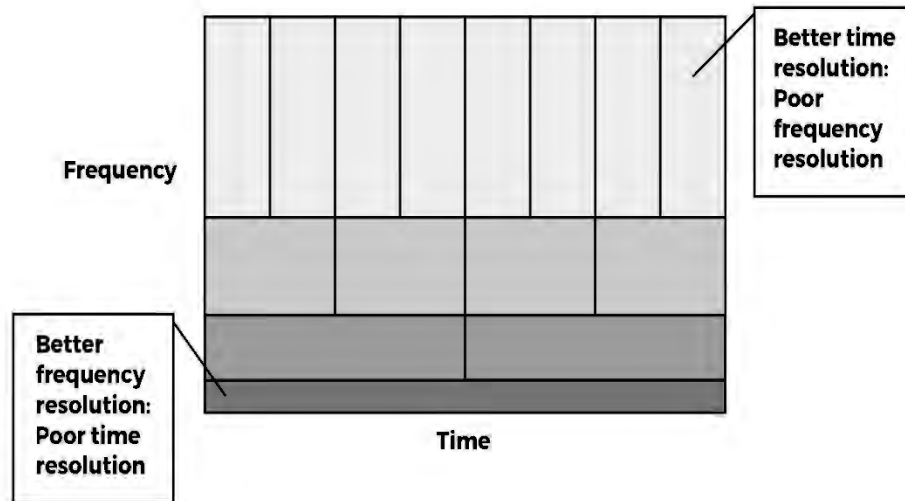


Fig. 3.2 Wavelet time-frequency resolutions.

Fig. 3.3 represents the Wavelet time-frequency resolutions concept, which provides valuable insights into how the Wavelet transform can capture different signal aspects in both the time and frequency domains. Here is an explanation of the components of such a figure:

i. Time Axis: the horizontal axis of the Fig. 3.2 represents time. It typically spans from left to right, indicating the progression of time.

ii. Frequency Axis: the vertical axis of the Fig. 3.2 represents frequency. It is divided into high and low frequencies, with low frequencies generally at the bottom and high frequencies at the top. The frequency axis illustrates how the signal's spectral content changes over time.

iii. Wavelet Transform Plot: the central part of the Fig. 3.2 is the actual Wavelet transform plot. In this plot, the signal is decomposed into its time-frequency components. The

Fig. 3.4 shows how the signal's energy distributed across various time intervals and frequencies.

- **Time Localization:** areas in the plot where the signal's energy is concentrated in a specific region along the time axis indicate good time localization, which means that the Wavelet transform can pinpoint where certain events occur within the signal.
- **Frequency Localization:** the Fig. 3.2 demonstrates how the signal's energy distributed across the frequency axis. Tight energy clusters along the frequency axis indicate high-frequency resolution, implying that the transform can accurately represent frequency information.
- **Time-Frequency Trade-Off:** the plot often shows a trade-off between time and frequency resolutions. In areas where the time resolution is high, that is, narrow in time, the frequency resolution is low, that is, spread out in frequency, and vice versa. This trade-off is a fundamental characteristic of Wavelet transforms.

iv. **Color or Intensity:** the color or intensity of the plot may vary to represent the magnitude of the signal's energy at different time and frequency combinations. Darker or more intense regions typically indicate higher energy, while lighter regions signify lower energy.

The Wavelet Time-Frequency Resolutions Fig. 3.2 provides a comprehensive visual representation of how the Wavelet transform divides a signal into its time and frequency components. It is a valuable tool for analyzing and understanding the time-

varying spectral content of signals in various applications, including image processing, audio analysis, and feature extraction from complex data.

3-2 How Wavelet Transforms Work

Wavelet transforms are based on small Wavelets of varying frequency and limited duration [5]. Wavelets are mathematical functions derived from a mother Wavelet. Dilations and translations of the mother Wavelet construct them.

The scaling parameter 'a' controls the Wavelet's dilation (expansion or contraction), and the shift parameter 'τ' controls its translation along the time axis [4]. This equation shows the relationship between these parameters:

$$\Psi_{a, \tau}(t) = |a|^{-\frac{1}{2}} \psi\left(\frac{t - \tau}{a}\right) \quad (3.1)$$

It is essential to explain the two key Wavelet concepts, translation, and dilation, to understand the functioning of Wavelet transforms.

i. Translation (Position): Wavelet shifting or translating along the time axis is translation. It allows one to analyze different signal segments at various time points, which helps capture localized features or events in the signal, which means capturing information about when an event occurs in the signal and its association with the time domain.

ii. Dilation (Scaling): dilation, however, is the process of resizing the Wavelet. It involves stretching or compressing the Wavelet function. Dilation affects the scale of analysis, allowing one to examine the signal at different levels of detail, which means capturing information about the signal's scale or frequency content and associated with the frequency domain.

Position (translation) changes the starting point of the analysis window along the x-axis, while dilation (scaling) alters the size of the analysis window. Both are distinct operations used in Wavelet analysis. By manipulating the position and dilation of Wavelets, the signal can be analyzed at different positions (times) and scales (frequencies), making Wavelets a powerful tool for understanding signal features in both the time and frequency domains.

The mother Wavelet ψ is a function with a mean value of zero, i.e., its integral over all values of 't' is equal to zero ($\int \psi(t) dt = 0$). The Wavelet transform of a signal $f(t)$ includes decomposing the signal into a group of basic functions (Wavelets) with different scales and translations [4]. This decomposition permits the representation of the signal in terms of its different frequency components at various resolutions. The Wavelet transform is suitable to use for both continuous-time and discrete-time signals. When the Wavelet transform applied to a signal, the scale components represent the signal's frequency components at different scales [17]. Low-frequency Wavelets have 'a' value greater than 1 represents larger time scales, while high-frequency Wavelets have 'a' value less than 1 represents smaller time scales. Wavelets have found numerous applications across various domains due to their ability to analyze and represent signals efficiently, such as signal analysis, power system analysis, medical imaging, and other significant fields of functionalities [4, 16, 18]. The tree of Wavelet decomposition is in Fig. 3.3. The $cA1$, $cA2$, $cA3$, and $cA4$ are the approximation levels. The $cD1$, $cD2$, $cD3$, and $cD4$ are the detail levels, while S is the signal of interest.

These are the steps for how the Wavelet Transform works:

i. **Decomposition:** the Wavelet Transform begins by decomposing the original signal into Wavelets. These Wavelets are from a predefined family of functions, each with specific characteristics.

ii. **Scale and Translation:** the decomposition involves varying the scale and translation of these Wavelets to analyze the signal at different levels of detail. Scaling modifies the frequency content of the Wavelet, while translation shifts the Wavelet along the time axis.

iii. **Convolution:** the Wavelet convolved with the original signal at each scale and translation. This convolution process measures how well the Wavelet matches a portion of the signal at that specific scale and location.

iv. **Coefficient Calculation:** the convolution results in a set of coefficients representing the similarity between the Wavelet and the signal at each scale and translation. These coefficients provide information about the signal's characteristics at different scales and times.

v. **Multi-Resolution Analysis:** the Wavelet Transform repeats this process at multiple scales and translations, creating a multi-resolution signal analysis, which allows the detection of features at various levels of detail.

vi. **Representation:** the resulting coefficients at each scale and translation represents in a two-dimensional Wavelet coefficient map or spectrogram. This representation highlights where different features and frequencies are present in the signal.

vii. **Inverse Transform (Optional):** in some cases, an inverse Wavelet Transform applied to reconstruct the original signal from its Wavelet coefficients, which is helpful for signal denoising, compression, or feature extraction.

Critical Advantages of Wavelet Transform:

i. Time-Frequency Localization: Wavelets provide excellent time-frequency localization, making them well-suited for analyzing signals with transient or rapidly changing features.

ii. Multiresolution Analysis: the ability to analyze a signal at different scales allows for the detection of both high and low-frequency components.

iii. Feature Detection: Wavelets effectively detect and isolate specific features within a signal, such as edges in images or spikes in data.

iv. Noise Reduction: Wavelet Transform can reduce signal noise by thresholding or filtering the Wavelet coefficients.

In summary, the Wavelet Transform is a mathematical technique for analyzing signals, images, and data in both the time and frequency domains. It operates by decomposing a signal into a set of Wavelet functions, each representing different scales and frequencies, offering the ability to investigate a signal's time and frequency characteristics simultaneously. It is precious for applications where traditional Fourier analysis may fall short, such as when dealing with non-stationary, which change over time, or transient signals [4, 5, 13].

A signal convolved with set Wavelets at various scales [4] to evaluate the correlation between a selected Wavelet, specified by its scale and position, and distinct components or patterns within a signal. In other words, we pick a Wavelet of a particular scale. Then, we slide this Wavelet across the entire signal, that is, vary its location, where we multiply the Wavelet and signal at each time step. The product of this multiplication gives us a coefficient for that Wavelet scale at that time step, representing the correlation

at that particular scale and time. We then increase the Wavelet scale and repeat the process. Examining how well a specific Wavelet, characterized by its scale and position, matches or fits with different parts of the signal. The scale and location parameters are essential in this analysis.

- Scale: refers to the width or frequency of the Wavelet. A smaller scale corresponds to a more localized and higher-frequency analysis, while a larger scale corresponds to a broader and lower-frequency analysis.
- Location: refers to where the Wavelet positioned or centered within the signal.

3.2.1 Wavelet Decomposition Tree

The Wavelet decomposition tree serves as a powerful analytical tool for various applications. Its multi-resolution approach provides a comprehensive understanding of signals and data. It is a significant asset in multiple fields, including signal processing, data analysis, feature extraction, and scientific and engineering disciplines.

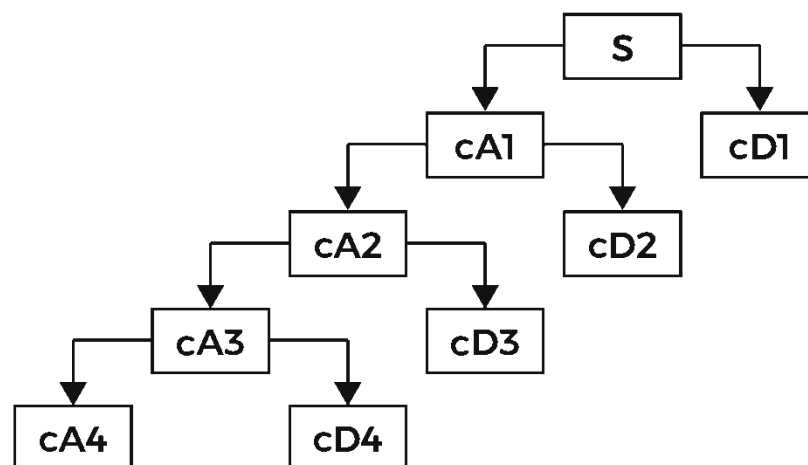


Fig. 3.3 Wavelet Decomposition Tree.

Fig. 3.3 illustrates the Wavelet decomposition tree of signal S at different decomposition levels. The signal S decomposed into detailed coefficients (CD) and approximation coefficients (CA) at multiple levels in this tree structure. Here is a breakdown of the components mentioned:

- cD1: detailed coefficients at level 1. These coefficients capture high-frequency details and rapid changes in the signal at the first level of decomposition.
- cD2: detailed coefficients at level 2. These coefficients represent the signal's high-frequency components at the second decomposition level and may capture finer details.
- cD3: detailed coefficients at level 3. These coefficients correspond to high-frequency details at the third level of decomposition, capturing even finer-scale variations in the signal.
- cD4: detailed coefficients at level 4. These coefficients correspond to high-frequency details at the fourth level of decomposition, capturing even finer-scale variations in the signal.
- cA1: approximation coefficients at level 1. These coefficients provide a lower-resolution representation of the signal's low-frequency components, summarizing the overall trends at the first level of decomposition.
- cA2: approximation coefficients at level 2. These coefficients represent the signal's low-frequency components at the second decomposition level.
- cA3: approximation coefficients at level 3. These coefficients represent the signal's low-frequency components at the third decomposition level.

- cA4: approximation coefficients at level 4. These coefficients represent the signal's low-frequency components at the fourth decomposition level.

The Wavelet decomposition tree allows analyzing the signal S at different levels, capturing both high-frequency details and low-frequency trends. This hierarchical decomposition is a key feature of Wavelet analysis, enabling multi-resolution analysis (MRA) of signals for various applications in signal processing, data compression, and feature extraction.

3.3 Two Essential Conditions for Wavelet Design

The creation of effective Wavelets depends on understanding the components that govern their design. This section explores Wavelet construction aspects, including the two essential mathematical conditions all Wavelets must satisfy.

1. Admissibility Condition: the Wavelet function must have a zero mean value. This condition represented mathematically as:

$$\int_{-\infty}^{+\infty} \Psi(t) dt = 0 \quad (3.2)$$

Where $\Psi(t)$ is the Wavelet function.

This condition ensures that the Wavelet function oscillates around the zero axes, has an equal amount of positive and negative values, and has a specific balance between time and frequency domains. This condition helps capture both high- and low-frequency components in the signal.

2. Normalization Condition: the total energy or the size of the Wavelet function must be finite. This condition ensures that the Wavelet function has a finite amount of energy.

This condition represented mathematically as:

$$\int_{-\infty}^{+\infty} |\Psi(t)|^2 dt < \infty \quad (3.3)$$

This condition ensures that the Wavelet function must be of finite duration or have compact support. It is nonzero only within a finite interval and effectively zero outside that interval to ensure that the Wavelet analysis focuses on localized features in the signal. These conditions enable the Wavelets' localization in both time and frequency domains, making them suitable for various signal-processing applications. The flexibility is because once these conditions met a wide range of Wavelet functions generated to suit specific analytical needs and objectives.

3.3 Wavelet Families

There are many different families of Wavelets, each with distinct characteristics suited for specific applications. Each family contains various Wavelet subclasses distinguished by factors such as the number of coefficients and the iteration level. The classification of Wavelets within a particular family often based on vanishing moments which is an additional set of mathematical constraints that coefficients must adhere to. The number of vanishing moments is directly linked to the quantity of coefficients within the Wavelet [4, 16, 19].

For instance, consider the Daubechies family, where Wavelets found with diverse characteristics, defined by their coefficient counts and vanishing moments. Within the Coiflet Wavelet family, one can encounter Coiflets exhibiting either two or three vanishing moments, each possessing distinct shapes, degrees of smoothness, and levels of

compactness. These variations render each type of Wavelet particularly suited to specific analytical tasks and applications.

One crucial feature of Wavelets is their flexibility in generating different Wavelet types. This flexibility arises from the minimal requirement of satisfying only two mathematical conditions, allowing for the relatively straightforward creation of customized Wavelets for specific analytical needs applications.

Here are some common types of Wavelets:

i. Haar Wavelet: the Haar Wavelet is the simplest and most basic Wavelet function. It has a compact support and often used in image compression and denoising applications.

ii. Daubechies Wavelets: Daubechies Wavelets, also known as db Wavelets, are a family of Wavelets with varying levels of smoothness. They are widely used in signal processing and image compression.

iii. Mexican Hat Wavelet: the Mexican Hat Wavelet, also known as the Ricker Wavelet, resembles a hat shape and is particularly useful in analyzing seismic data and feature detection in images.

iv. Morlet Wavelet: the Morlet Wavelet is complex and resembles a sinusoidal waveform modulated by a Gaussian function. It commonly used to analyze time-frequency data, especially in applications like EEG signal analysis.

v. Gabor Wavelet: Gabor Wavelets designed for time-frequency analysis, they are suitable for image texture analysis and feature extraction in speech recognition.

vi. Meyer Wavelet: Meyer Wavelets are a family of Wavelets known for their symmetry and smoothness. They find applications in data compression and image processing.

vii. Discrete Approximation Meyer (DAM): A specific type of Meyer Wavelet adapted for discrete signal processing. The original Meyer Wavelets, developed by Yves Meyer, are part of a continuous Wavelet family well suited for continuous functions and theoretical mathematics. When these Wavelets are adapted for digital signal processing, a discrete version created, and the "discrete approximation Meyer" is a way to distinguish it from the continuous version. The term "Meyer Wavelet" refers to continuous and discrete versions. Still, when wants to emphasize its use in discrete signal processing, the term "discrete approximation Meyer" is more specific. This distinction helps avoid confusion and indicates that it is an adapted version of the original Meyer Wavelet for digital applications.

viii. Biorthogonal Wavelets: Biorthogonal Wavelets come in pairs, with one Wavelet used for decomposition and the other for reconstruction. They are valued for their flexibility in handling various signal characteristics.

ix. Coiflet Wavelets: Coiflet Wavelets, also known as C-Wavelets, are similar to Daubechies Wavelets but offer a smoother Wavelet function. They used in applications requiring a compromise between smoothness and compact support.

x. Symlet Wavelets: Symlet Wavelets are a variant of Daubechies Wavelets designed to strike a balance between regularity and orthogonality. They employed in various tasks.

xi. Battle-Lemarié Wavelets: these Wavelets tailored for analyzing signals with singularities, making them suitable for tasks involving sharp changes or discontinuities. The choice of a specific Wavelet type depends on the characteristics of the signal or data analyzed and the particular application's requirements. Different Wavelets offer varying

levels of time and frequency localization, smoothness, and compactness, allowing practitioners to select the most suitable Wavelet for their needs.

3.4 Wavelet Transforms Two Primary Categories

Wavelet transforms are significant tools that enable one to understand the signal's structure and characteristics better. Two primary categories are continuous Wavelet transform (CWT) and discrete Wavelet transform (DWT), which have become powerful techniques for analyzing signals and data in both time and frequency domains. This section will explore these two Wavelet transform categories: principles, mathematical equations, and practical applications. Understanding CWT and DWT is essential for anyone who wants to understand the benefit of signal processing and data analysis in various fields, from image processing to power systems fault detection.

3.4.1. Continuous Wavelet Transform (CWT)

The Continuous Wavelet Transform (CWT) is a mathematical technique for analyzing signals or functions in both the time and frequency domains. It provides a continuous-time representation of a signal's frequency content over different scales. The CWT characterizes a signal by convolving it with a family of Wavelet functions, each representing a different scale and position. These Wavelet functions are often derived from a mother Wavelet by dilating (scaling) and translating (shifting). The CWT yields a time-frequency representation of the signal, highlighting how its frequency components change over time. It makes the CWT particularly useful for analyzing non-stationary signals, which change over time, or signals with transient features.

The Continuous Wavelet Transform (CWT) encompasses the utilization of every conceivable Wavelet across an extensive spectrum of scales and positions. It employs infinite scales and locations, offering a comprehensive signal analysis.

The equation for Continuous Wavelet Transform (CWT) of a function $f(t)$ concerning a Wavelet function $\psi(t)$ is:

$$CWT(a, \tau) = \int_{-\infty}^{+\infty} f(t) \cdot \left(\frac{1}{\sqrt{a}}\right) \cdot \psi^* \left(\frac{t - \tau}{a}\right) dt \quad (3.4)$$

Where

$CWT(a, \tau)$ represents the Continuous Wavelet Transform at a specific scale 'a' and translation 'b.',

$f(t)$ is the input signal or function you want to analyze,

$\psi(t)$ is the mother Wavelet, which acts as a kernel function and characterizes the properties of the Wavelet analysis,

'a' represents the scale parameter, which controls the width of the Wavelet function and is associated with the dilation of the Wavelet,

' τ ' represents the translation parameter, which shifts the Wavelet function along the time (or spatial) axis,

$\psi^*(t)$ represents the complex conjugate of the Wavelet function $\psi(t)$,

The CWT computes the inner product of the input signal $f(t)$ and a scaled and translated version of the complex conjugate of the Wavelet function $\psi(t)$ across all possible scales 'a' and position (translations ' τ ') to create a time-frequency representation of the signal. This transform provides a time-frequency model of the signal $f(t)$, showing how different frequency components are distributed in the signal over time across different time

intervals. The choice of the mother Wavelet function plays a crucial role in determining the characteristics of the Wavelet transform and the type of information it can extract from the signal.

3.4.2 Discrete Wavelet Transforms (DWT)

The Discrete Wavelet Transform (DWT) is a linear signal processing technique that decomposes a discrete-time signal into a set of coefficients representing its frequency components at multiple scales and positions [4, 20]. These coefficients capture both the approximation (CA) and detail (CD) components of the signal, providing a multi-resolution representation of the input signal. The DWT is computed through a series of convolution and down-sampling operations using low-pass (scaling) and high-pass (Wavelet) filters, with the choice of filters and decomposition levels determining the characteristics of the transformation. The DWT is widely used in signal processing, image compression, feature extraction, and many other applications.

The discrete Wavelet transform (DWT) represented as follows:

$$DWT(x) = \sum_{k=0}^{N-1} x[k] \cdot \psi(j, k) \cdot [n] \quad (3.5)$$

Where:

$x[k]$ represents the input signal values at discrete points,

$\Psi_{j,k} \cdot [n]$ represents the Wavelet function at a particular scale (j) and translation (k),

N is the total number of samples in the input signal,

This equation calculates the DWT coefficients by multiplying the input signal with the Wavelet function at different scales and translations. The Discrete Wavelet Transform (DWT) operates by discretizing the scales and positions, utilizing a finite set of scales and

locations for the Wavelet analysis. This discrete approach enables a detailed yet computationally more efficient exploration of the signal's characteristics.

3.5 Wavelet Properties

Wavelets are mathematical functions with specific properties that affect their behavior and effectiveness in signal analysis [4, 19, 20]. These are some of the Wavelet properties:

i. Orthogonality: Wavelets can be orthogonal, ensuring that the inner product between Wavelets at different scales equals zero. An example of an orthogonal Wavelet is the Haar Wavelet, which is widely used in signal compression due to its orthogonality property.

ii. Bi-Orthogonality: Some Wavelets, like the Cohen-Daubechies-Feauveau (CDF) 9/7 Wavelet, are bi-orthogonal. They possess distinct Wavelets for decomposition and reconstruction, making them suitable for tasks requiring precise analysis and synthesis filters, such as JPEG2000 image compression.

iii. Symmetry: a typical example of Symmetric Wavelets is Daubechies Wavelets, which exhibit mirror symmetry around their central point. This property is valuable in applications where preserving symmetric features is crucial, such as image edge detection.

iv. Complexity: Wavelets can be either complex or real. Complex Wavelets like the Morlet Wavelet have real and imaginary components. They are helpful in tasks like analyzing time-frequency representation in EEG signals. On the other hand, real Wavelets, like the Symlet Wavelet, contain only real components and commonly employed in applications such as denoising financial time series data. These diverse properties empower

researchers to choose Wavelets tailored to specific applications, ensuring optimal performance and accuracy in their analyses.

3.6 Summary

The Wavelet chapter serves as a comprehensive exploration of Wavelet analysis. It provided an overview of Wavelets, their mathematical foundation, and how they differ from traditional signal processing techniques. It highlighted the flexibility of Wavelets in capturing both high and low-frequency components in signals, making them suitable for analyzing power system data. The chapter explained the discrete Wavelet transform (DWT) and how it decomposes signals into different scales for detailed analysis.

4. POWER SYSTEM FAULT

In modern electrical engineering, power systems are the backbone of the energy infrastructure, ensuring the continuous supply of electricity to meet the demands of the rapidly advancing society. The efficient functioning of these systems is essential to ensure that power is reliably generated, transmitted, and distributed to customers [21]. However, the complexities of power systems raise challenges, particularly in fault management. Various factors could cause faults in power systems, from equipment failures to external interferences, disrupting the seamless flow of electricity and leading to potential outages and system failures. This chapter delves into the pivotal aspects of power system faults, aiming to contribute to the foundational knowledge necessary for improving fault detection to safeguard the robust operation of power systems facing diverse challenges.

4.1 Introduction

The continuous increase in complexity, driven by the expansion of interconnections and the integration of cutting-edge technologies marked the modern power system landscape.

Simultaneously, the imposition of financial constraints and stringent regulatory measures has given rise to novel stability challenges. Power engineers are now faced with the daunting task of ensuring high-quality, uninterrupted power supply to consumers in this intricate environment [22].

The rapid advancement of power systems has resulted in the proliferation of intricate transmission lines, making detecting power system faults increasingly challenging. Nevertheless, the smooth functioning of power systems is paramount, as these faults can significantly disrupt normal operations and people's daily lives. Hence, accurate fault detection in the power system has become critically essential.

Electric power systems, regardless of their size and structural components, share fundamental characteristics:

- i. They predominantly operate on three-phase alternating current (AC) systems, maintaining relatively constant voltage levels. Both power generation and transmission facilities employ three-phase equipment.
- ii. Power generation primarily relies on synchronous machines.
- iii. Power transmitted over extensive distances to consumers across broad geographical areas. This requires a transmission system comprising subsystems operating at different voltage levels.

Electric power generated at power stations and transported to end-users via a sophisticated network of diverse elements, including transmission lines, transformers, and switching equipment. The transmission network categorized into three main subsystems:

i. **Transmission System:** this component is responsible for conveying electricity from power generation stations to regional areas, covering significant distances through high-voltage transmission lines.

ii. **Subtransmission System:** operates at intermediate voltage levels, the subtransmission system bridges the high-voltage transmission lines and local distribution networks. It facilitates the efficient transfer of power over shorter distances.

iii. **Distribution System:** this system is the final stage in the power delivery process, distributing electricity directly to consumers within local communities. It operates at lower voltage levels and includes transformers and switching devices to regulate voltage and ensure reliable supply to homes and businesses.

In the landscape of modern power systems, ensuring a reliable power supply is increasingly challenging due to complexity and extensive interconnections. Fault detection is complicated, emphasizing the critical need for accurate identification. As we move into subsequent sections on fault concepts, types, and mathematical analysis, the focus is on addressing power system faults and developing precise detection and mitigation methodologies.

4.2 Power System Faults

Faults in power systems classified into several types based on their characteristics and origins [21]. These classifications help engineers and operators understand the nature of the fault, enabling them to implement appropriate protective measures. The two main

types of faults are short circuit faults, where the fault impedance is very low, leading to a high fault current, and open circuit faults, where the fault impedance is very high, resulting in a minimal or zero fault current. In this study, we will focus on Short Circuit Faults. Short circuits occur in the power system when equipment insulation fails due to system overvoltage caused by lightning or switching surges, insulation contamination (salt spray or pollution), or other mechanical causes. The resulting short circuit or "FAULT" current determined by the synchronous machine's internal voltages and the system impedances between the machine voltage and the fault.

A large volume of network data must also be controlled and accurately handled. Digital computers and highly developed computer programs assist the engineer in this power-system planning. Such programs include short circuits and transient programs.

The current chapter deals with fault analysis, the first introduction to the faults in power systems, transient phenomena, and three-phase short circuit, unloaded synchronous machines. Short circuits theory consists of balanced and unbalanced fault calculation in general and conventional methods for small systems. These fault types involve single line-to-ground faults, line-to-line faults, and double line-to-ground faults. The last three unsymmetrical faults studies will require the knowledge and use of tools of symmetrical components

4.3 Fault Concept

The tremendous technical advances in the design and production of commercial and scientific general-purpose digital computers since the early 1950s have placed a powerful tool at the engineering profession's disposal. This advancement has made using

digital computers for routine calculations in everyday engineering work economically feasible.

It has also provided the capability to perform more advanced engineering and scientific computations that were previously impossible because of their complex or time-consuming nature. These trends have immensely increased interest in digital computers and necessitated a better understanding of the engineering and mathematical bases for problem solving. The development of computer technology has provided the following advantages to power system engineering:

- i. More efficient and economical means of performing routine engineering calculations are required to plan, design, and operate a power system.
- ii. Relieving the engineer from tedious hand calculations lead to better utilization of engineering talent.
- iii. The ability to perform more effective engineering studies.
- iv. The capability of performing studies was impossible because of the volume of calculations involved.

Applying a computer to solving engineering problems involves several steps. The steps include problem definition, mathematical formulation, selection of a solution technique, program design, programming, and program verification. The relative importance of each of these steps varies from problem to problem.

As electric utilities have grown and interconnections have increased, planning for future expansion has become increasingly complex. The increasing cost of additions and modifications have made it imperative that utilities consider a range of design options and perform detailed studies of the effects on the system of each option based on several

assumptions: normal and abnormal operating conditions, peak and off-peak loading, and present and future years of operation.

An essential part of a power supply network's design is calculating the currents, which flow in the components when faults of various types occur. In a fault survey, the fault applied at different points in the network, and the resulting currents obtained by digital computation [23]. The magnitudes of the fault currents give the engineer the current settings for the protection used and the circuit breakers' ratings. In some circumstances, the effect of open circuits may need investigation.

When calculating short circuit currents in high-voltage installations, it is often sufficient to work with reactances because they are generally much more significant in magnitude than the effective resistances. The ratios of the rated system voltages are taken as the transformer ratios. Instead of the operating voltages of the faulty network, one works with the rated system voltage. It is assumed that the rated voltages of the various network components are the same as the rated system voltage at their respective locations. The calculation is done with the aid of the %MVA system. The ohmic resistances of low-voltage cables are usually higher than their reactances.

With widely different ratios of the real and imaginary parts, these impedances are almost always present in a series arrangement. Complex calculation with impedance $Z = R + jX$ of the equipment is necessary; therefore, a complete short-circuit is always assumed when calculating the short-circuit currents. Other influences, particularly arc resistances, contact resistances, conductor temperatures, and the inductances of current transformers, can reduce short-circuit currents. Since they are not available for calculation, they are allowed by a factor (C). The installation's apparatus and components must be designed

for maximum dynamic and thermal short-circuit stress. On the other hand, short-circuit protection devices must respond to a lower short-circuit current [24]. The terms "maximum short-circuit current" and "minimum short-circuit current" introduced to reconcile these requirements.

The maximum short-circuit currents with three, two, or single-phase faults are obtained with the short-circuit path's impedances at a conductor temperature of (20°C) and the factor ($C = 1.0$).

An electrical network under short-circuit conditions considered a network supplied by several sources like generators, with a single load connected to the node subjected to the short circuit. There are several reasons to have as accurate data as possible about short-circuiting currents and voltages in a system:

- i. Each circuit breaker's interrupting capacity in every switching locality must be based upon the most severe short-circuit case.
- ii. The protective relaying system intended to sense the fault and initiate selective switching bases its operation upon the fault current's magnitude and directions.
- iii. The magnitude of bus voltages during short circuits determines the transient generator power outputs and the "transient stability."

Fault studies form an essential part of power system analysis. The problem consists of determining bus voltages and line currents during various faults. The three-phase balanced fault information used to select and set phase relays, while the line-to-ground fault used for ground relays. Fault studies also used to obtain the rating of the protective switchgear.

For fault studies, generator behavior divided into three periods:

- i. The Sub-transient period lasts only for the first few cycles.
- ii. The transient period covers a relatively long time.
- iii. The steady-state period.

Matrices used only as research tools before 1950. They systematized the arrangement of materials that forced the research worker to be organized. Matrices reduced the computational effort; however, the absence of high-speed computers limited investigations to small sets of Equations involving only very small matrices. The first generation of small-scale computers extended the use of matrices in solving network problems of limited size.

4.4 Types of Faults

Faults in power systems classified into several types based on their characteristics and origins [25]. These classifications help engineers and operators understand the nature of the fault, enabling them to implement appropriate protective measures. In this study, we focused on Short Circuit Faults. Short circuit faults are one of the two main types of faults: Open Circuit Faults and Short Circuit Faults. Both based on fault impedance:

- i. Short Circuit Fault: a fault where the fault impedance is very low, resulting in a high fault current.
- ii. Open Circuit Fault: a fault where the fault impedance is very high, resulting in a minimal or zero fault current.

Fig. 4.1 shows the short circuit faults further subdivided into two primary categories based on the fault nature: symmetrical and unsymmetrical.

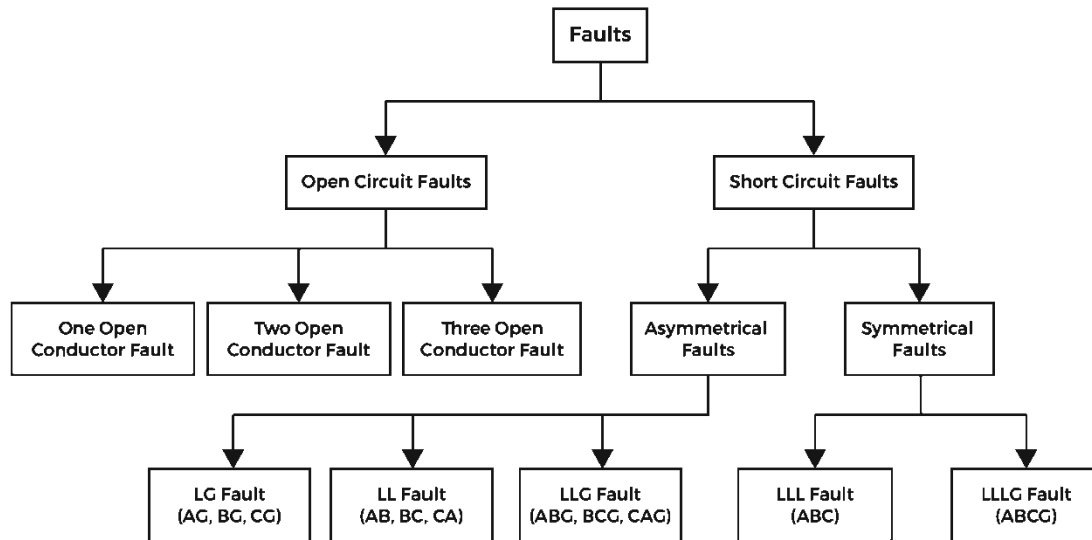


Fig.4.1 Various types of faults that occur within a three-phase power.

4.4.1 Symmetrical Faults

Symmetrical faults, also known as balanced faults, occur in a power system when all three phases, A, B, and C, simultaneously experience the same fault condition [24]. The symmetry of fault currents and voltages across all phases characterizes these faults. Short circuits or faults typically cause symmetrical faults in the power system and can have significant implications for the stability and operation of the electrical grid.

Characteristics of Symmetrical Faults:

- i. **Equal Fault Currents:** in a symmetrical fault, the fault currents in all three phases are equal in magnitude and phase, creating a balanced condition. This balanced fault current makes it easier to analyze and design protective devices.
- ii. **Minimal Voltage Imbalance:** symmetrical faults result in minimal voltage imbalances between phases, which mean the faulted system remains balanced.

iii. No Negative Sequence Component: unlike unsymmetrical faults, symmetrical faults do not introduce negative sequence components in the electrical system, simplifying fault analysis.

Common causes of symmetrical faults include short circuits due to equipment failures, such as transformer faults, transmission line faults, or the mechanical failure of electrical machinery. Power system engineers and operators must promptly analyze and address symmetrical faults to prevent equipment damage, minimize power system disruptions, and maintain grid reliability. These faults can have severe implications for the stability and reliability of power systems.

Protective relays and circuit breakers are critical to detecting and isolating symmetrical faults. These devices designed to respond quickly to symmetrical fault conditions, interrupting the fault current and isolating the faulted section of the power system to prevent further damage.

4.4.2 Unsymmetrical Faults

Unsymmetrical faults, also known as unbalanced faults, are electrical faults that occur in a power system when the fault conditions in the three phases, A, B, and C, are unequal or do not have the same phase relationship. Unsymmetrical faults introduce imbalances and asymmetry into the electrical system [21, 24]. A variety of factors can cause these faults.

Characteristics of Unsymmetrical Faults:

Unsymmetrical faults, also known as unbalanced faults, are electrical faults that occur in a power system when the fault conditions in each of the three phases, A, B, and C, are not equal or do not have the same phase relationship. Unlike symmetrical faults,

where all phases' fault currents and voltages are equal, unsymmetrical faults introduce imbalances and asymmetry into the electrical system. Unsymmetrical faults have the following distinct characteristics:

i. **Different Fault Currents:** unsymmetrical faults lead the fault currents in each phase to have different magnitudes, phases, or both. This results in an imbalance of power flowing through the system, leading to voltage and current distortions.

ii. **Voltage Imbalance:** unsymmetrical faults often lead to voltage imbalances between the phases. These imbalances can affect the performance of connected equipment and lead to issues such as unbalanced motor loads.

iii. **Negative Sequence Component:** unsymmetrical faults caused the introduction of negative sequence components in the electrical system. These components are responsible for generating magnetic fields that rotate opposite to the standard system, which can affect the operation of rotating machinery.

Common causes of unsymmetrical faults include:

i. **Phase-to-Ground Faults:** a fault where one phase comes into contact with the ground or earth, causing an imbalance in fault currents and voltages.

ii. **Phase-to-Phase Faults:** a fault where two phases come into contact, creating an unsymmetrical fault condition.

iii. **Open Circuits or Broken Conductors:** when one or more conductors in a system broken, it can lead to unsymmetrical fault conditions.

iv. **Imbalanced Loads:** significant variations in load distribution between phases can also result in unsymmetrical fault conditions.

Understanding unsymmetrical faults is crucial for power system engineers and operators because these faults can lead to equipment damage [28, 29], voltage instability, and disruptions in the power supply. Protective devices such as relays, circuit breakers, and fault detectors designed to detect and respond to unsymmetrical faults by isolating the faulted portion of the system and preventing further damage. Analyzing and addressing unsymmetrical faults are essential for maintaining the reliability and stability of the power system.

The terms "symmetrical" and "unsymmetrical" faults typically apply to short circuit faults rather than open circuit faults in power systems. Open circuit faults refer to situations where a conductor or a component in a power system becomes disconnected, resulting in a break in the electrical circuit [26]. Open circuit faults are naturally asymmetrical because they disrupt current flow in one or more phases, leading to unequal currents and voltage imbalances. However, open circuit faults are typically characterized by their impact on current flow and voltage imbalances rather than symmetrical or unsymmetrical distinctions.

In general, faults in the three-phase system classified under the following headings:

- i. Symmetrical three-phase faults.
- ii. Single line-to-ground fault.
- iii. Line-to-line faults.
- iv. Double line-to-ground faults.

Note that three fault types involve line-to-ground (Earth Fault)—most result from insulator flashovers for weather conditions and insulation quality. The balanced three-phase fault is the rarest occurrence. It is less than five percent of the total faults, and it is

the least complex of all types of short circuit studies as the calculations concerned. The types of faults commonly occurring in practice illustrated in Fig. 4.2, and the most common of these is the short circuit of a single conductor to earth. The path to Earth often contains resistance in the form of an arc, as shown in Fig. 4.2(f).

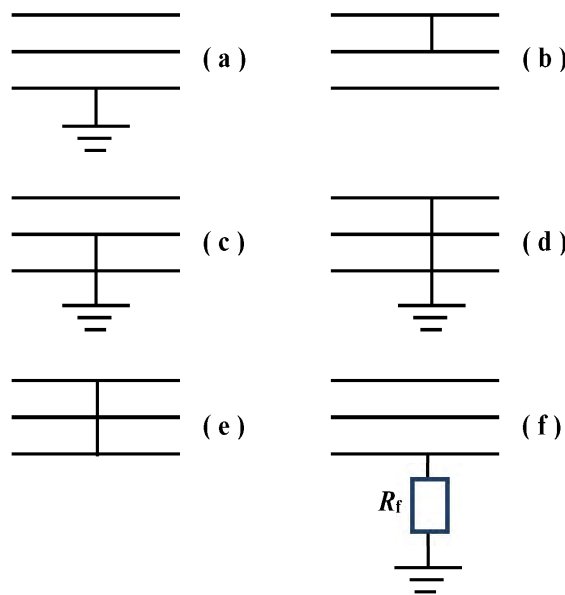


Fig. 4.2 Common types of faults.

Although the single line to ground fault is the most common, calculations frequently performed with the three-line, balanced short circuit (see Figs.4.2(d) and 4.2(e)). This fault is the most severe fault and the most interesting calculation. As well as fault current, fault MVA is frequently considered. This is obtained from the expression $\{\sqrt{3}V_L I_F \times 10^{-6}\}$, V_L is the nominal line voltage of the faulted part before the fault. The MVA often referred to as the fault level. The calculation of fault currents divided into the following two main types:

- i. Faults are short-circuiting all three phases when the network remains balanced

electrically. Typical single-phase equivalent circuits used for these calculations as in ordinary load-flow calculations.

ii. Faults other than three-phase short circuits when the network is electrically unbalanced.

iii. The primary objects of fault analysis enumerated as follows:

- To determine the maximum and minimum three-phase short-circuit currents.
- To determine the unsymmetrical fault current for single and double line-to-ground, line-to-line, and open-circuit faults.
- Investigation of the operation of protective relays.
- Determination of rated rupturing capacity of breakers.
- To determine fault-current distribution and busbar-voltage levels during faults.

4.5 Symmetrical Fault Analysis

It is necessary to perform short-circuit calculations to make the correct choice in switchgear. Such calculation enables the fault MVA due to a symmetrical 3-phase fault to be determined at a point of interest. These calculations demand the reduction of the network to that of a single source feeding single impedance. The generator reactances typically considered at their sub-transient values to account for the worst conditions, which means when analyzing or simulating power systems it is common to use the sub-transient reactance values of generators. Sub-transient reactance represents the initial response of the generator to a sudden change in electrical conditions and often considered to assess the worst-case scenario during transient events. The calculation performed by expressing

impedance in ohms or per-unit values. When a transformer is involved, all impedance referred to as a selected voltage base, which could be either the primary or secondary of the transformer or any other voltage base selected.

4.5.1 Simplified Models of Synchronous Machines for Transient Analysis

For the salient-pole, because of the non-uniformity of the air gap, the generator was modeled with direct axis reactance (X_d) and the quadrature axis reactance (X_q). However, the circuit reactance is much greater under short circuit conditions than the resistance. Thus, the stator current lags nearly $\pi/2$ radians behind the driving voltage, and the armature reaction m.m.f centered almost on the direct axis. Therefore, the machine's effective reactance assumed only along the direct axis during a short circuit, (i.e., only X_d).

The three-phase short circuit current decays from a very high initial value to a steady-state value [21, 22, 24]. This decay is because of the machine reactance change due to the effect of the armature reaction. A helpful figure obtained by considering the field and damper windings as the transformer's secondary, whose primary is the armature winding, to determine the machine's equivalent circuits during normal steady state and disturbance conditions.

There is no transformer action between the synchronous machine's stator and rotor windings during normal steady-state conditions [23, 25]. The resultant field produced by the stator and rotor revolves with the same synchronous speed, similar to a transformer with open-circuited secondaries. Its primary is described by the synchronous reactance X_d for this condition. During the disturbance, the rotor speed is no longer the same as that of

the revolving field produced by stator windings, resulting in transformer action. Thus, field and damper circuits resemble much more than short-circuited secondaries. The equivalent circuit for this condition, referred to as the stator side, shown in Fig. 4.3.

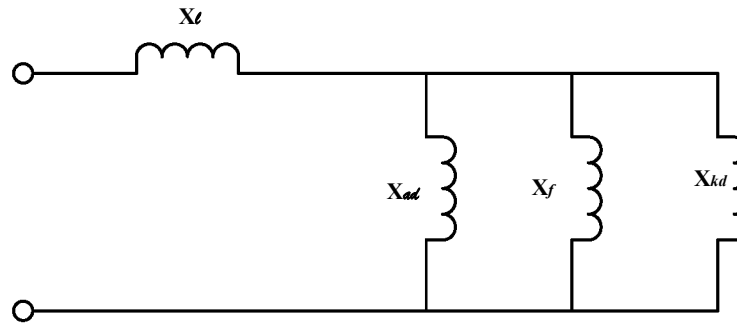


Fig. 4.3 The equivalent circuit for the sub-transient period.

Ignoring winding resistance, the equivalent reactance of Fig.4.3, known as the direct axis sub-transient reactance, is:

$$X_d'' = X_l + \left(\frac{1}{X_{ad}} + \frac{1}{X_f} + \frac{1}{X_{kd}} \right)^{-1} \quad (4.1)$$

Where

X_l - Leakage reactance of armature,

X_{ad} - Reactance of armature reaction in the d-axis,

X_f - Reactance of field circuit,

X_{kd} - Reactance of damper circuit,

If the damper winding resistance R_k inserted in Fig. 4.3, and Thevenin's inductance seen at the terminals of R_k is obtained, the circuit time constant, known as the direct axis short circuit sub-transient time constant, becomes:

$$\tau_d'' = \frac{X_{kd} + \left(\frac{1}{X_l} + \frac{1}{X_f} + \frac{1}{X_{ad}} \right)^{-1}}{R_k} \quad (4.2)$$

For 2-pole, turbo-alternator ($X_d'' = 0.07 - 0.12 \text{ p.u.}$) and for the water-wheel alternator ($X_d'' = 0.1 - 0.35 \text{ p.u.}$).

X_d'' - is only used in calculations if the effect of the initial current is important, for example, when determining the circuit breaker short-circuit rating.

τ_d'' - is very small, around 0.035 seconds, because the damper circuit has relatively high resistance. Thus, this component of the current decays quickly. It is then permissible to ignore the reactance of the damper circuit X_{kd} , and the equivalent circuit reduces to the following Fig. 4.4.

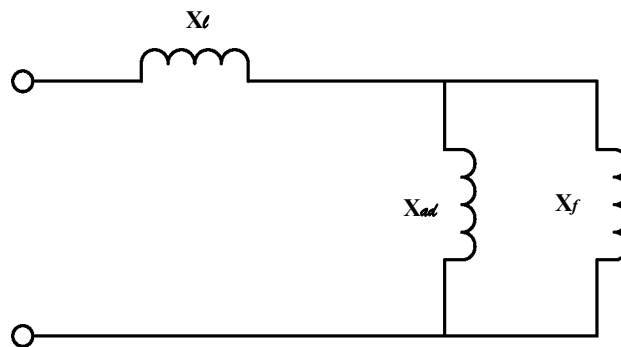


Fig. 4.4 The equivalent circuit for the transient period.

Ignoring winding resistance, the equivalent reactance of Fig.4.4, known as the direct axis short circuit transient reactance, is:

$$X_d' = X_l + \left(\frac{1}{X_{ad}} + \frac{1}{X_f} \right)^{-1} \quad (4.3)$$

If the field winding resistance R_f is inserted in the above Fig., and Thevenin's inductance seen at the terminals of R_f is obtained, the circuit time constant, known as the direct axis short circuit transient time constant, becomes:

$$\tau'_d = \frac{X_f + \left(\frac{1}{X_l} + \frac{1}{X_{ad}}\right)^{-1}}{R_f} \quad (4.4)$$

X'_d lie between 0.1 to 0.25 p.u, and τ'_d is usually in the order of (1 to 2) seconds.

The field time constant, which characterizes transient decay with the armature open-circuited, called the direct axis open-circuit transient time constant. This relation given by

$$\tau'_{do} = \frac{X_f}{R_f} \quad (4.5)$$

τ'_{do} - it is around 5 seconds. τ'_d is related to τ'_{do} by:

$$\tau'_d = \frac{X'_d}{X_d} \tau'_{do} \quad (4.6)$$

Finally, when the disturbance is over, there will be no hunting of the rotor. Hence, there will not be any transformer action between the stator and the rotor, and the circuit reduces to the following Fig. 4.5. The equivalent reactance becomes the direct axis synchronous reactance:

$X_d = X_l + X_{ad}$ is the same X_d , which is obtained in a steady-state condition.

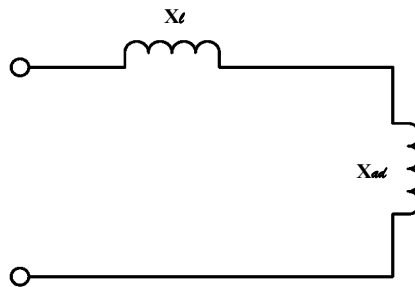


Fig. 4.5 The equivalent circuit for the steady-state period.

Similar equivalent circuits obtained for reactances along the quadrature axis. These reactances are X_q'' , X_q' , and X_q . These reactances considered when the circuit resistance results in a power factor appreciably above zero [21]. The armature reaction is not necessarily totally on the direct axis, except that the machine's equivalent circuits represented only by the direct axis's reactances. The manufacturers provide synchronous machine reactances and time constants. A short circuit test can obtain these values.

4.5.2 Transient Phenomena

To understand the synchronous machine transient phenomena, we first study a simple R-L circuit's transient behavior, as shown in Fig. 4.6.

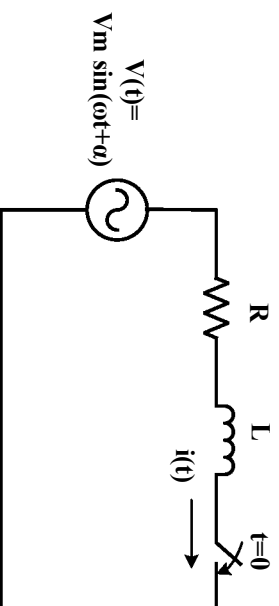


Fig. 4.6 Simple series circuit with constant R and L.

The closing of the switch at $t = 0$ represents, to a first approximation, a three-phase short circuit at the terminals of an unloaded synchronous machine. The current assumed zero before the switch closes.

$$v(t) = V_m \sin(\omega t + \alpha) \quad (4.7)$$

The angle is the phase of the voltage wave at which the switch is closed

At $t = 0^+$, the instantaneous voltage equation for the circuit:

$$Ri(t) + L \frac{di(t)}{dt} = V_m \sin(\omega t + \alpha) \quad (4.8)$$

The solution for the current shown to be:

$$i(t) = I_m \sin(\omega t + \alpha - \theta) - I_m e^{-t/\tau} \sin(\alpha - \theta) \quad (4.9)$$

Where:

$$I_m = \frac{V_m}{Z} \quad ; \quad \tau = \frac{L}{R} \quad ; \quad \theta = \tan^{-1} \omega L/R \quad ;$$

$$Z = \sqrt{R^2 + (\omega L)^2} = \sqrt{R^2 + X^2}$$

The fault current $\{i(t)\}$ in equation 4.9 called the asymmetrical fault current and consists of two components:

i. The first term is *the AC fault current* (also called symmetrical or steady-state fault current), which is a sinusoid and given by:

$$i_{ac}(t) = I_m \sin(\omega t + \alpha - \theta) \quad (4.10)$$

ii. The second term is DC offset current, which decays exponentially with a time-constant $\tau = \frac{L}{R}$ and it is often referred to as a DC component since it is unidirectional and is given by:

$$i_{dc}(t) = -I_m e^{-t/\tau} \sin(\alpha - \theta) \quad (4.11)$$

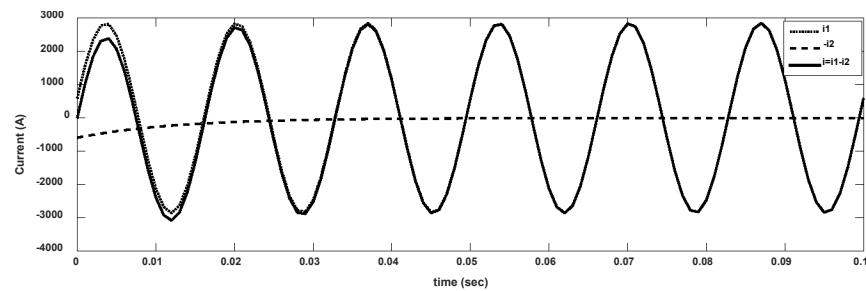
At $(t = 0)$, $i_{ac}(t)$ and $i_{dc}(t)$ are equal and opposite to satisfy the condition for zero initial currents.

The magnitude of the dc component, which depends on α (i.e., depends on the instant of application of the voltage to the circuit), varies from 0 when $\alpha = \theta$ to I_{max} When $\alpha = (\theta \pm \pi/2)$ radians.

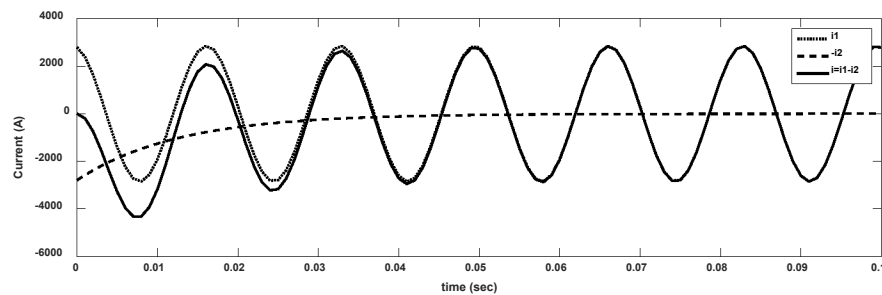
Note that a short circuit may occur at any instant during a cycle of the AC source that is, α can have any value. Since primarily interested in the largest fault current; choose $\alpha = (\theta - \pi/2)$, then $i(t)$ becomes:

$$i(t) = I_m \sin(\omega t - \pi/2) + I_m e^{-t/\tau} \quad (4.12)$$

If $\omega L \gg R$, then $\theta \cong \pi/2$, so that the circuit closer at voltage maximum ($\alpha = \pi/2, 3\pi/2, 5\pi/2, \dots$) would give no dc component, and closer at voltage zero ($\alpha = 0, \pi, 2\pi, \dots$) would cause the maximum dc component, as shown in Fig. 4.7(a) and 4.7(b).



(a)



(b)

Fig. 4.7 Current waveform (a) with no DC offset ($\alpha = 0, \pi, 2\pi, \dots$).
(b) with maximum DC offset ($\alpha = \pi/2, 3\pi/2, 5\pi/2, \dots$).

A detailed study of Equation 4.9 will show the conditions that make for the maximum possible $i(t)$. The maximum of DC offset current is usually assumed to be the result of those conditions that make $\sin(\alpha - \theta) = 1$ or $\sin(\alpha - \theta) = -1$. See Fig. 4.8.

The Fig. 4.8 below shows that $i(t)$, $i_{ac}(t)$ and $i_{dc}(t)$ when $L > R$, $\theta = 85^\circ$, $\sin(\alpha - \theta) = -1$, $\alpha = 355^\circ$, at $t = 0$, $e \approx 0$.

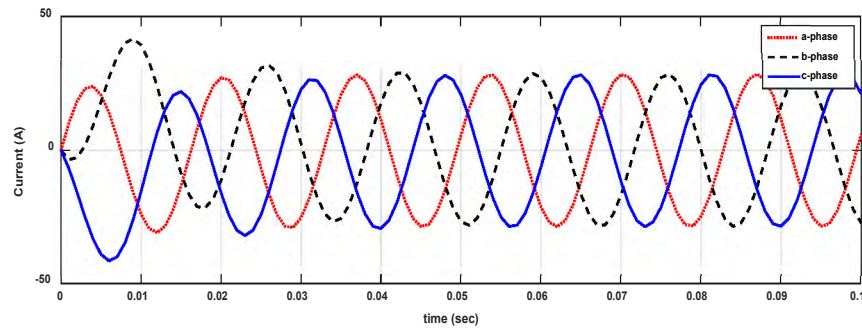


Fig. 4.8 Steady-state and transient current terms combine to form the resultant current.

4.5.3 Three-Phase Short Circuit – Unloaded Synchronous Machine

Fig.4.9 shows the waveform of the AC fault current in one phase of an unloaded synchronous machine. The DC component of the current is different in each phase. The different amounts of DC components are justified because the short circuit occurs at different points on each phase's voltage wave. Since, in a practical situation, we can never predict how much offset we will have, the DC components removed or subtracted from the current waveforms [24]. As shown, the amplitude of the sinusoidal waveform decreases from a high initial value to a lower steady-state value.

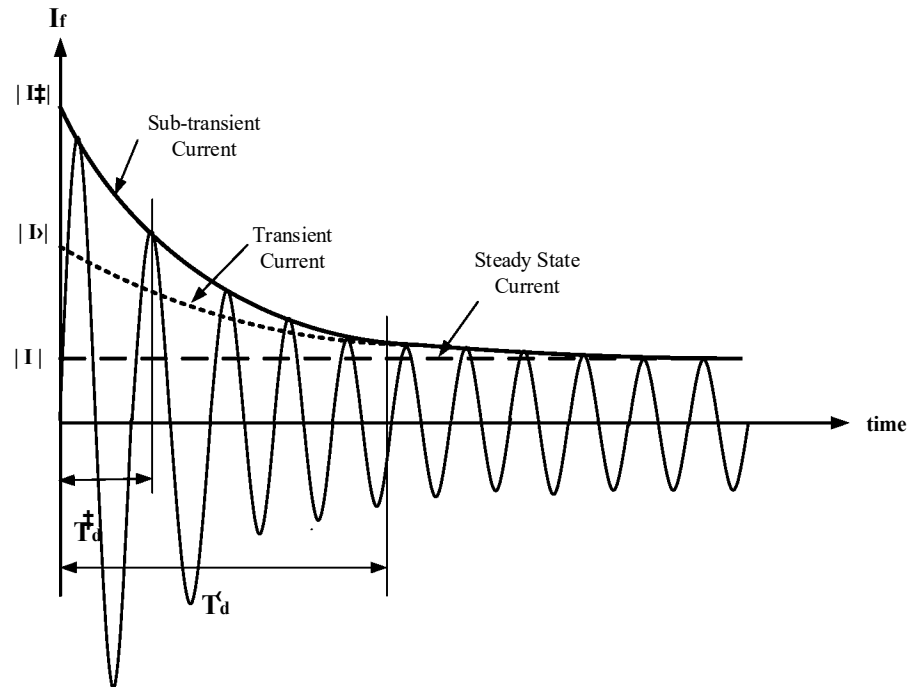


Fig. 4.9 The Fault current in one phase shows the sub-transient, transient, and steady-state currents.

A practical explanation for this phenomenon is that the magnetic flux caused by the short-circuit armature currents, or by the resultant armature m.m.f, is initially forced to flow through high reluctance paths that do not link the machine's field winding or damper circuits. This result from the theorem of constant flux linkages, which states that the flux linking a closed winding cannot change instantaneously. The armature inductance, which is inversely proportional to reluctance, is initially low. The armature inductance increases as the flux moves toward the lower reluctance path.

The AC fault current in a synchronous machine is similar to that flowing when a sinusoidal voltage suddenly applied to a series R-L circuit. However, there is one important difference: in the case of the R-L circuit, our reactance ($X = \omega L$) is a constant quantity, whereas, in the case of the generator, the reactance is not a constant one but is a function

of time [25]. Therefore, the AC fault current in a synchronous machine modeled by the series R-L circuit if a time-varying inductance $L(t)$ or reactance $X(t) = \omega L(t)$ employed. If we prefer to use r.m.s values, it is reasonable to divide the maximum values of the above Fig. 4.9 by $\sqrt{2}$, as shown in Fig. 4.10.

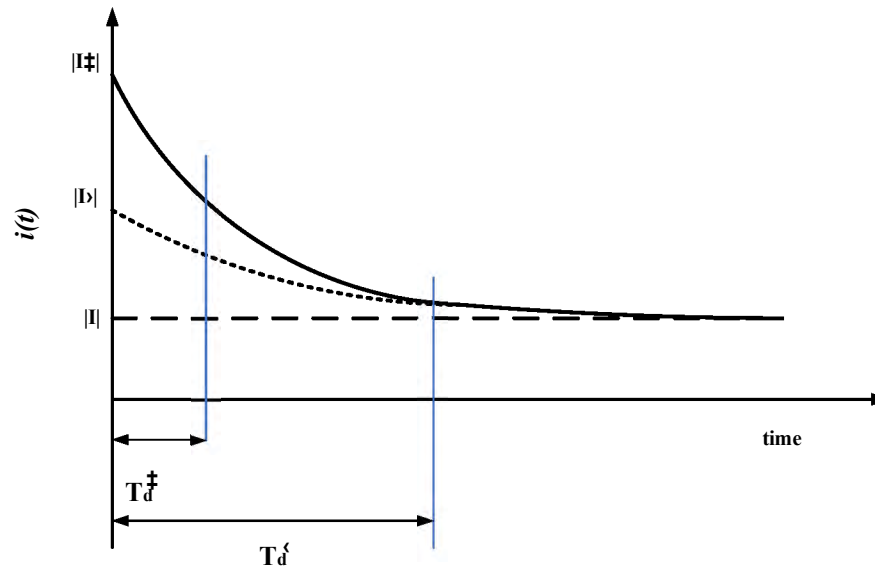


Fig. 4.10 The sub-transient, transient, and steady-state fault currents.

Referring to the above Fig., the *amplitude* of the varying ac fault current (r.m.s) as a function of time given by:

$$|I_{ac}(t)| = \left(\frac{|E|}{X_d''} - \frac{|E|}{X_d'} \right) e^{-t/\tau_d''} + \left(\frac{|E|}{X_d'} - \frac{|E|}{X_d} \right) e^{-t/\tau_d'} + \frac{|E|}{X_d} \quad (4.13)$$

The instantaneous AC fault current written as:

$$i_{ac}(t) = \sqrt{2}E \left[\left(\frac{1}{X_d''} - \frac{1}{X_d'} \right) e^{-\frac{t}{\tau_d''}} + \left(\frac{1}{X_d'} - \frac{1}{X_d} \right) e^{-\frac{t}{\tau_d'}} + \frac{1}{X_d} \right] \times \sin(\omega t + \alpha - \theta) \quad (4.14)$$

Where E is the r.m.s line-to-neutral pre-fault terminal voltage of the unloaded synchronous machine, an armature resistance neglected in Equation 4.14. Note that at $t = 0$, when the fault occurs, the r.m.s value of $i_{ac}(t)$ in Equation 4.14 is:

$$I_{ac}(0) = \frac{E}{X_d''} = I_d'' \quad (4.15)$$

Which is called the r.m.s sub-transient fault current, I_d'' . The duration of I_d'' is determined by the time constant τ_d'' . At a later time, when t is large compared to τ_d'' but small compared to the τ_d' . The first exponential term in Equation 4.14 has decayed almost to zero, but the second exponential has not decayed significantly. The r.m.s ac fault current then equals the r.m.s transient fault current, given by:

$$I_d' = \frac{E}{X_d'} \quad (4.16)$$

When t is much larger than τ_d' , the r.m.s ac fault current approaches its steady-state value, given by:

$$I_{ac}(\infty) = \frac{E}{X_d} = I_d \quad (4.17)$$

In addition to the AC fault current, each phase has a different DC offset. As in the R-L circuit, the DC offset depends on the instantaneous value of the voltage applied, that is, angle α). The time constant associated with the decay of the DC component of the stator current is known as the armature short circuit time constant (τ_a). Most of the decay of the DC component occurs during the sub-transient period. For this reason [25], the average value of the direct axis and quadrature axis sub-transient reactance used for finding τ_a . It given by:

$$\tau_a = \frac{X_d'' + X_q''}{2\omega R_a} \quad (4.18)$$

It is approximately given by:

$$\tau_a = \frac{X_d'' + X_q''}{2R_a} \quad (4.19)$$

Typical value of τ_a is around 0.05 to 0.17 seconds.

In comparison, in Equation 4.11, the r.m.s of the dc component for phase (a) is given by:

$$I_{dc}(t) = \sqrt{2} \frac{E}{X_d'} e^{-t/\tau_a} \sin(\alpha - \theta) \quad (4.20)$$

$$I_{dc}(t) = \sqrt{2} I_d'' e^{-t/\tau_a} \sin(\alpha - \theta) \quad (4.21)$$

$$I_{dc(max)}(t) = |I_{dc}(t)| = \sqrt{2} I_d'' e^{-t/\tau_a} \quad (4.22)$$

$$I_{dc(max)}(0) = \sqrt{2} I_d'' \quad (4.23)$$

The waveform of asymmetrical fault current is a superposition of DC and AC components.

$$i_{asy}(t) = \sqrt{2} E \left[\left(\frac{1}{X_d'} - \frac{1}{X_d} \right) e^{-\frac{t}{\tau_a}} + \left(\frac{1}{X_d'} - \frac{1}{X_d} \right) e^{-\frac{t}{\tau_a}} + \frac{1}{X_d} \right] \sin(\omega t + \alpha - \theta) - \sqrt{2} \frac{E}{X_d'} e^{-\frac{t}{\tau_a}} \sin(\alpha - \theta) \quad (4.24)$$

In Equation 4.24, the degree of asymmetry depends upon the point of the voltage cycle at which the fault occurs, and if $\omega L \gg R$, then $\theta \cong \pi/2$.

The r.m.s value of $i_{asy}(t)$ is of interest. Since $i_{asy}(t)$ in eq. (31) is not strictly periodic. Its r.m.s value is not strictly defined. However, treating the exponential term (dc component) as a constant, we stretch the r.m.s concept to calculate the r.m.s asymmetrical fault current with maximum dc offset, as follows:

$$I_{asy(rms)}(t) = \sqrt{[I_{ac}(t)]^2 + [I_{dc}(t)]^2} \quad (4.25)$$

Where $I_{ac}(t)$ is the magnitude of Equation 4.13, and $I_{dc}(t)$ is the magnitude of Equation 4.22.

Therefore, the maximum r.m.s current at the beginning of the short circuit $I_{asy(rms)}(0)$ is:

$$I_{asy(max)}(0) = \sqrt{\left(\frac{E}{X_d''}\right)^2 + \left(\sqrt{2}\frac{E}{X_d''}\right)^2} = \sqrt{(I_d'')^2 + (\sqrt{2}I_d'')^2}$$

$$I_{asy(max)}(0) = \sqrt{3}I_d'' \quad (4.26)$$

In practice, the *momentary duty* of a *circuit breaker (CB)* is given in terms of the asymmetrical short circuit current, that is, mean:

$$I_{momentary\ of\ CB}(t) = I_{asy(rms)}(t) \quad (4.27)$$

The factor is usually taken as 1.6 instead of $\sqrt{3}$ in assessing the momentary current for the circuit breaker above 5KV. This factor was reduced for voltage under 5KV. The momentary duty is not to be confused with the interrupting capacity of the circuit breaker. The sub-transient currents used to calculate the interrupting capacity of the circuit breaker. The calculation depends on the circuit breaker's speed, the ratio of X to R in the circuit, the distance between the fault and the generating station. If X/R is small, the DC component will decay quickly; therefore, a smaller multiplying factor must used. Of course, the faster the breaker, the higher the multiplying factor.

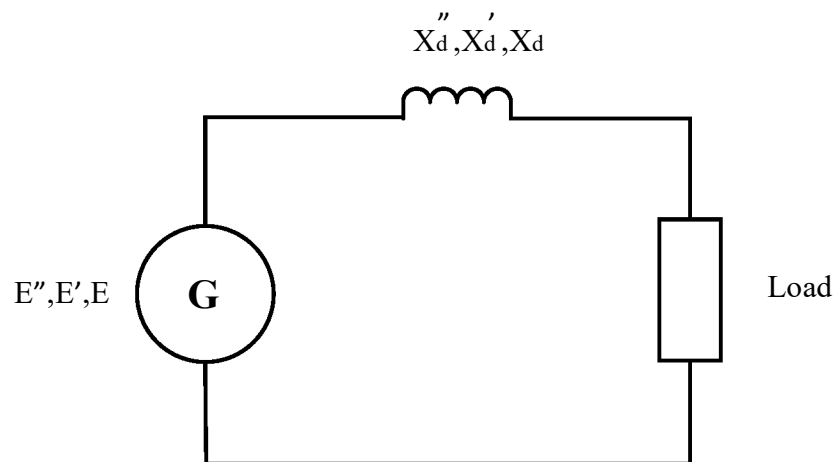
TABLE 4.1
TYPICAL VALUES OF MULTIPLYING FACTOR FOR THE
CIRCUIT BREAKERS OF DIFFERENT SPEEDS

Circuit breaker speed	Multiplying factor
1 cycle	1.6
2 cycles	1.4
3 cycles	1.2
5 cycles	1.1
8 cycles	1.0

4.5.4 Effect of Load Current

If the fault occurs when the generator delivers a pre-fault load current, two methods used to solve three-phase symmetrical fault currents.

i. Use of internal voltages behind reactances: when there is a pre-fault load current, three fictitious internal voltages E'' , E' , and E , may be considered to be effective during the sub-transient, transient, and steady-state periods, respectively, as shown in Fig. 4.11.



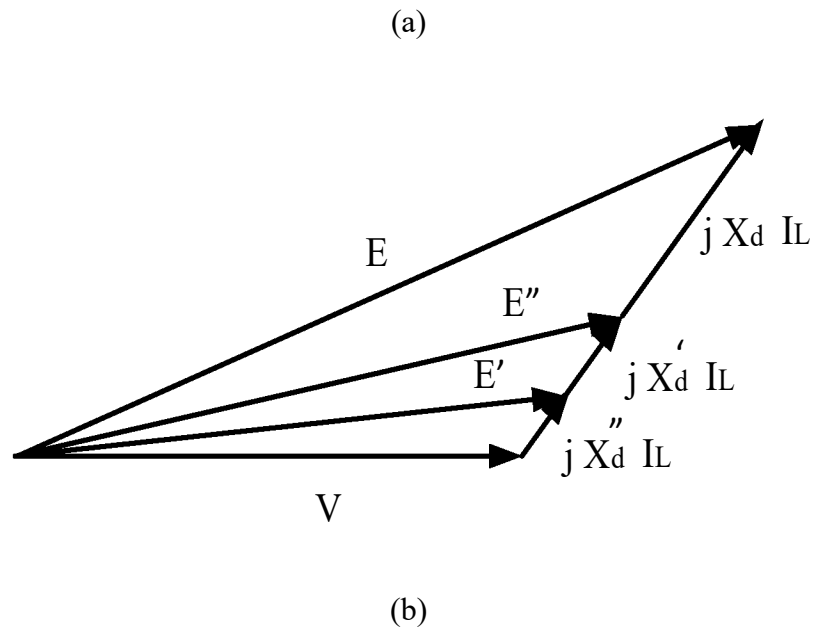


Fig. 4.11 One phase diagram showing the sub-transient, transient, and steady-state currents. (a) Circuit diagram. (b) Phasor diagram.

$$E'' = V + jX_d'' I_L \quad (4.28)$$

$$E' = V + jX_d' I_L \quad (4.29)$$

$$E = V + jX_d I_L \quad (4.30)$$

ii. Using Thevenin's theorem and superposition with load current: the fault current is found in the absence of the load by obtaining Thevenin's equivalent circuit to the point of fault. The total short circuit current is then given by superimposing the fault current with the load current.

4.6 Unsymmetrical Faults Analysis

As stated earlier, most system faults occur in practice and are unbalanced or unsymmetrical. An unbalanced power system may be defined as one in which the current or voltages are unbalanced. It will be evident that such an imbalance brought about if either

the alternator voltage is unsymmetrical or the system's circuit is so. Most faults on power systems are unsymmetrical, consisting of short circuits, unsymmetrical faults through impedances, or open conductors.

Unsymmetrical faults occur as single line-to-ground, line-to-line, or double line-to-ground faults. The path of the fault current from line to line or line to the ground may or may not contain impedance [26]. One or two open conductors result in unsymmetrical faults, either through the breaking of one or two conductors or through the action of fuses and other devices that may not open the three phases simultaneously. Since any unsymmetrical fault causes unbalanced currents to flow in the system, it is shown below the general network's sequence components and Thevenin's equivalent circuits.

4.7 Symmetrical Components

An unbalanced system of N phasors can be resolved into an N system of balanced phasors, each with phasors of equal amplitude and angles between each phasor. The systems of balanced phasors are called symmetrical components. The vector sum of the symmetrical components equals the original system of unbalanced phasors. The symmetrical components of a three-phase system, illustrated in Fig.4.12, are

i. Positive Sequence Components: these are three phasors of equal magnitude, offset from each other by 120° and rotating in the same direction as the original phasors, usually signified counterclockwise in a phasor diagram.

ii. Negative Sequence Components: three phasors of equal magnitude, offset from each other 120° in phase and rotating in the opposite direction to the original phasor, make up the negative sequence components. Usually, the rotation of the phasors considered to be in the same direction as the original phasors, but two of the phase vectors, b , and c , are

reversed, as shown in Fig. 4.11, thus, the negative sequence components phase rotation is a c b instead of a b c.

iii. Zero Sequence Components: these are three phasors of equal magnitude, with an in-phase offset between them. They are in phase. The zero sequence components are often non-rotating, like a DC voltage. However, zero sequence impedance is complex, so the zero-sequence voltage is treated as a single-phase source for calculating zero sequence impedance in relaying problems.

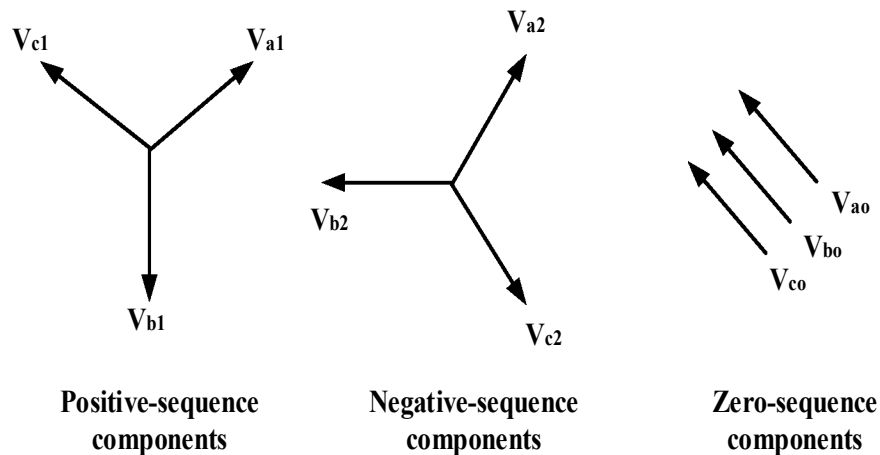


Fig. 4.12 Three sets of balanced phasors are the symmetrical components of three unbalanced phasors.

The defining Equations for the symmetrical components, where V_a , V_b , and V_c are the original unbalanced phasors, are:

$$\begin{aligned}
 V_a &= V_{a1} + V_{a2} + V_{a0} \\
 V_b &= V_{b1} + V_{b2} + V_{b0} \\
 V_c &= V_{c1} + V_{c2} + V_{c0}
 \end{aligned}
 \tag{4.31}$$

The phasor diagram is shown in Fig. 4.13.

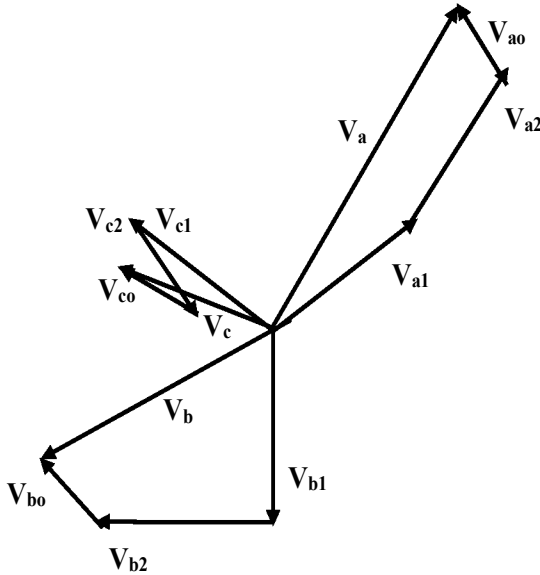


Fig. 4.13 Three phase unbalanced system phasor diagrams.

The operator is used to indicate a 120° phase shift. The three phasors' relative angular position for a three-phase voltage can be expressed as the product of the phasor's amplitude and the operator (a), referring to Fig. 4.11.

$$V_{b2} = aV_{a2}, \quad a = 1\angle 120^\circ = -0.5 + j0.866$$

$$V_{b1} = a^2V_{a1}, \quad a^2 = 1\angle 240^\circ = -0.5 - j0.866$$

$$V_{c2} = a^2V_{a2}, \quad 1 + a + a^2 = 0$$

$$V_{c1} = aV_{a1}, \quad V_{c0} = V_{b0} = V_{a0}$$

Therefore, it can use previous relations to find V_a , V_b , and V_c ;

$$V_a = V_{a1} + V_{a2} + V_{a0}$$

$$V_b = a^2V_{a1} + aV_{a2} + V_{a0} \quad (4.32)$$

$$V_c = aV_{a1} + a^2V_{a2} + V_{a0}$$

It rewrites Equation 4.32 as

$$\begin{bmatrix} V_a \\ V_b \\ V_c \end{bmatrix} = \begin{bmatrix} 1 & 1 & 1 \\ 1 & a^2 & a \\ 1 & a & a^2 \end{bmatrix} \begin{bmatrix} V_{a0} \\ V_{a1} \\ V_{a2} \end{bmatrix} \quad (4.33)$$

These transformations can do it for currents, too, as

$$\begin{bmatrix} I_a \\ I_b \\ I_c \end{bmatrix} = \begin{bmatrix} 1 & 1 & 1 \\ 1 & a^2 & a \\ 1 & a & a^2 \end{bmatrix} \begin{bmatrix} I_{a0} \\ I_{a1} \\ I_{a2} \end{bmatrix} \quad (4.34)$$

4.7.1 Effect of Symmetrical Components Impedance

To the find effect of the symmetrical component on impedance, we assumed that the start relation is:

$$V_{abc} = [Z_{abc}] \cdot I_{abc} \quad (4.35)$$

Where $[Z_{abc}]$ is a matrix of dimension (3 * 3) that gives self and mutual impedance in phases and between them.

$$[A] \cdot [V_{012}] = [Z_{abc}] [A] [I_{012}] \quad (4.36)$$

$$[V_{012}] = [A]^{-1} [Z_{abc}] [A] [I_{012}] \quad (4.37)$$

$$[Z_{012}] = [A]^{-1} [Z_{abc}] [A] \quad (4.38)$$

$$[V_{012}] = [Z_{012}] \cdot [I_{012}] \quad (4.39)$$

The critical Equation 4.38 found that $[Z_{abc}]$ is not diagonal but somewhat symmetrical, while $[Z_{012}]$ is diagonal; these make the analysis very easy.

4.7.2 Phase Shift Δ/Y Connection Δ/Y

The type of connection ($\Delta \Delta, YY$) for primary and secondary causes no phase shift between them. While for ($\Delta Y, Y\Delta$), there is a phase shift between the transformer's primary and secondary. To understand this problem, let us consider that the transformer has a ($Y-\Delta$) connection, as shown in Fig. 4.14; considering (Δ -connection) is low voltage side, then from studying the phasor diagram, as shown in Fig. 4.15, we can see that,

$$V_{AB} = V_{HV} \angle 30^\circ \quad (4.40)$$

$$V_{ab} = V_{LV} \angle 0^\circ \quad (4.41)$$

All high voltage magnitudes lead to low voltages by (30°). From many tries, it can be said that "for each star delta, delta star named the phasors as make positive sequence magnitudes in high voltage side lead more than positive sequence magnitudes in low voltage side by (30°) and vice versa according to negative sequence magnitudes."

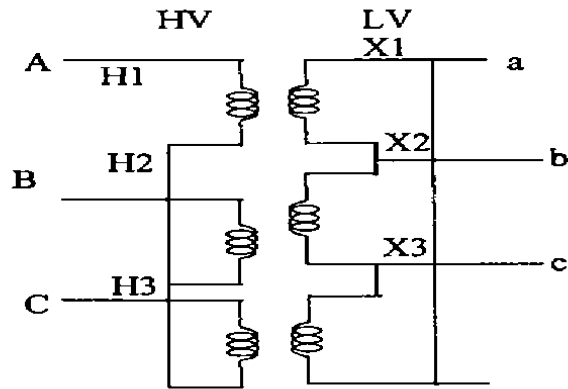


Fig. 4.14 The transformer has a (Y- Δ) connection.

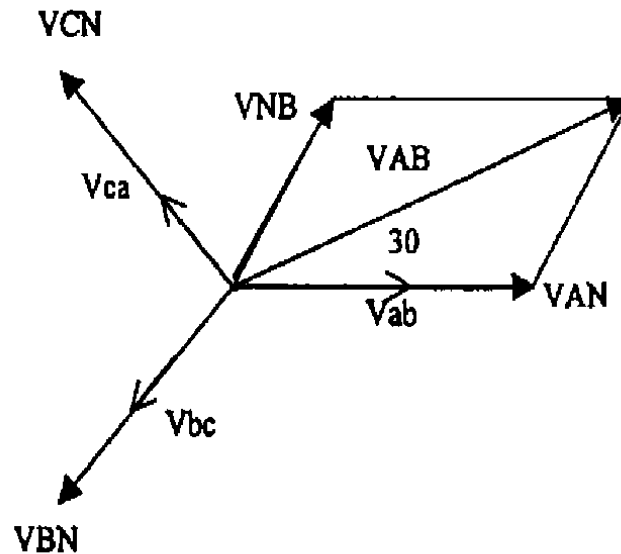


Fig. 4.15 The phasor diagram.

4.7.3 Sequence Network of Unloaded Generator

When a fault occurs at the generator's terminals, currents I_a , I_b , and I_c flow in the lines; if the fault involves ground, the current flowing into the neutral of the generator is designated (I_n). One or two of the line currents may be zero, but the currents can be resolved into symmetrical components regardless of how unbalanced they may be. Drawing the

sequence network is simple. The generated voltages are of positive sequence only since the generator is designed to supply balanced three-phase voltages. The positive-sequence network is composed of an emf in series with a positive-sequence impedance of the generator [21, 26]. The negative and zero-sequence networks contain no EMF but include the generator's impedance to negative and zero-sequence currents. A circuit diagram of an unloaded generator grounded through a reactance is shown in Fig. 4.16. The emf of each phase is E_a , E_b , and E_c .

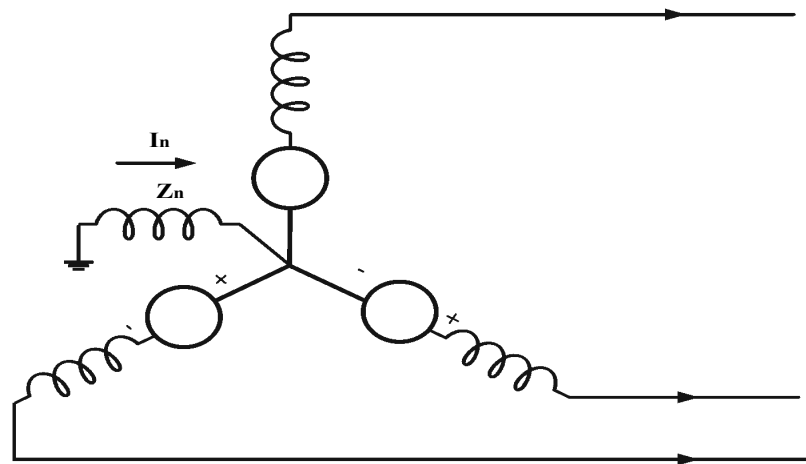


Fig. 4.16 Circuit diagram of an unloaded generator grounded.

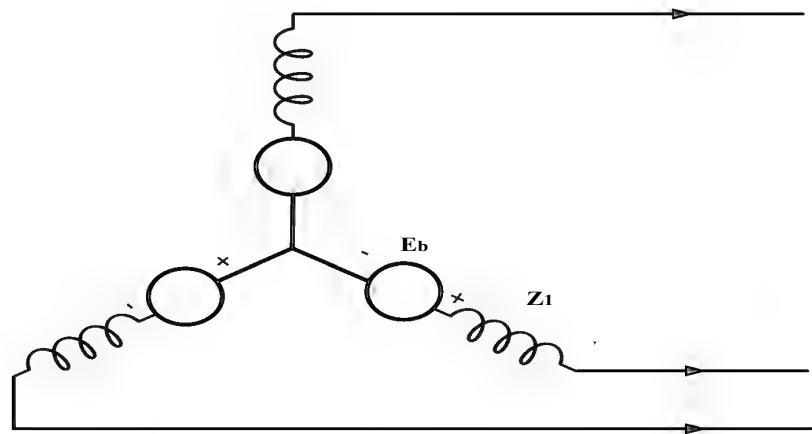
i. Positive Sequence Network: The generated emf in the positive-sequence network is the no-load terminal voltage to neutral, as shown in Fig. 4.16. It is equal to the voltage behind transient and sub-transient reactances and the voltage behind synchronous reactance since the generator is not loaded. The positive-sequence network's reactance is the sub-transient, transient, or synchronous reactance depending on whether sub-transient, transient, or steady-state conditions are being studied. From Fig. 4.17(b)

$$V_{a1} = E_a - I_{a1}Z_1 \quad (4.42)$$

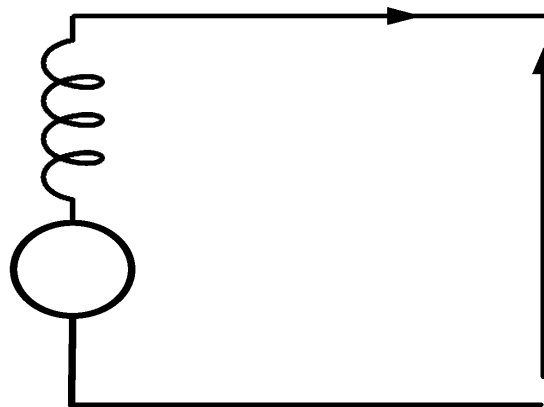
Where

E_a is the positive sequence no-load voltage to neutral,

Z_1 is the positive sequence impedance of the generator,



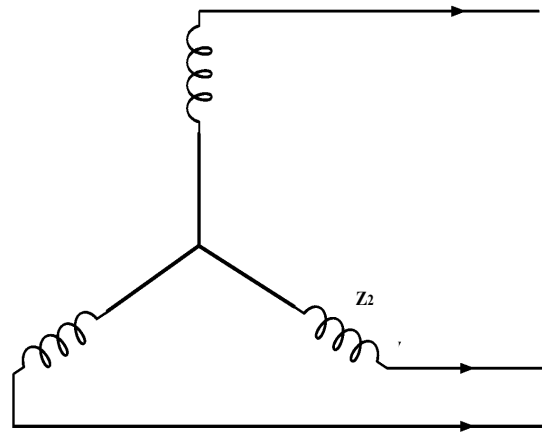
(a)



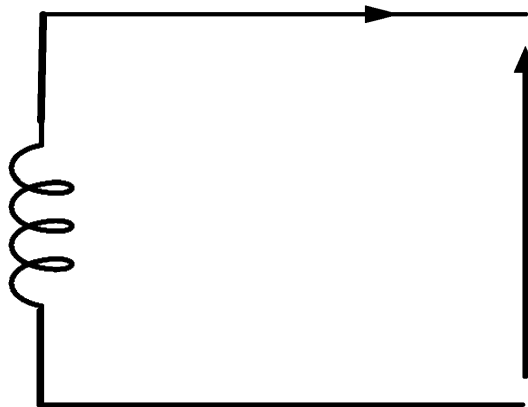
(b)

Fig. 4.17 The path for phase current of positive sequence in the generator and the corresponding sequence networks. (a) Positive Sequence current path. (b) Positive Sequence network.

ii. Negative Sequence Network: The reference bus for positive and negative sequence networks is the neutral of the generator. So far as positive and negative sequence components, the generator's neutral is at ground potential since only zero sequence currents flow in the neutral and ground impedance [21]. Fig. 4.18 shows the Path for phase Currents of the negative Sequence in the generator and the Corresponding Sequence Networks. From Fig. 4.18(b).



(a)



(b)

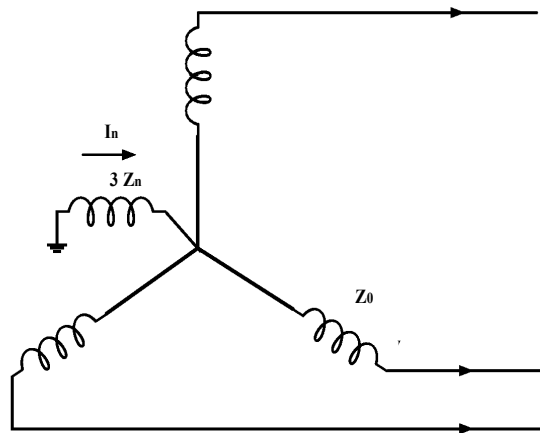
Fig. 4.18 The path for phase Current of the negative Sequence in the generator and the corresponding sequence networks. (a) Negative Sequence current path. (b) Negative Sequence network.

$$V_{a2} = -I_{a2}Z_2 \quad (4.43)$$

Where Z_2 is the negative sequence impedance of the generator.

iii. Zero Sequence: The current flowing in the Impedance Z_n between neutral and ground is $(3I_0)$. By referring to Fig.4.18.a, we see that the voltage drop of zero sequences

from point a to ground is $(-3I_{a0} Z_n - I_{a0}Z_{g0})$, where Z_{g0} is the zero sequence impedance per generator phase.



(a)

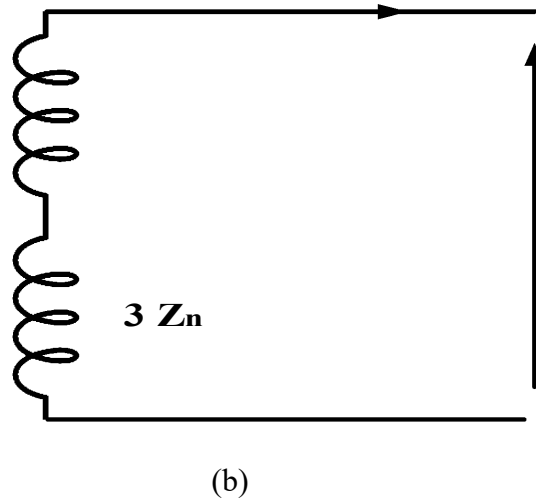


Fig. 4.19 The path for phase current of zero sequence in the generator and the corresponding sequence networks. (a) Zero Sequence current path. (b) Zero Sequence network.

The zero-sequence network, a single-phase circuit assumed to carry only the zero-sequence current of phase, must, therefore, have an impedance of $(3Z_n + Z_{go})$, as shown in Fig. 4.18(b), The total zero sequence impedance through which I_{ao} flows is:

$$Z_o = 3Z_n + Z_{go} \quad (4.44)$$

The Equations for the components of voltage drop from point (a) of phase (a) to the reference but (or ground) are, as may be deduced from Fig. 4.19.b,

$$V_{ao} = -I_{ao}Z_o \quad (4.45)$$

Where Z_o is the zero sequence impedance defined by Equation (4.44).

4.8 Analysis of Unsymmetrical Faults Using the Method of Symmetrical Component

The fault occurs at any point in the power system network represented by the interconnection between sequence components at the fault position [21, 22]. Therefore, the critical thing that must be determined accurately is the way of connecting these networks, and they must follow these steps for analysis:

- i. Make a detailed diagram for the circuit and determine all phases connected to

the fault position, as shown in Fig. 4.20.

- ii. Write down all circumstances of fault dealing with phase current and phase voltage.

- iii. Transform magnitudes of phase current and phase voltage (a-b-c) that are determined in item (2) above to sequence components (0 1 2) by using $[A]$ or $[A]^{-1}$.
- iv. Determine the connection of sequence network terminals (N, F) using the information on sequence currents is determined in item (2).
- v. Determine the connection of recent sequence components terminals of the network and all impedances concerning the fault using items (3, 4).

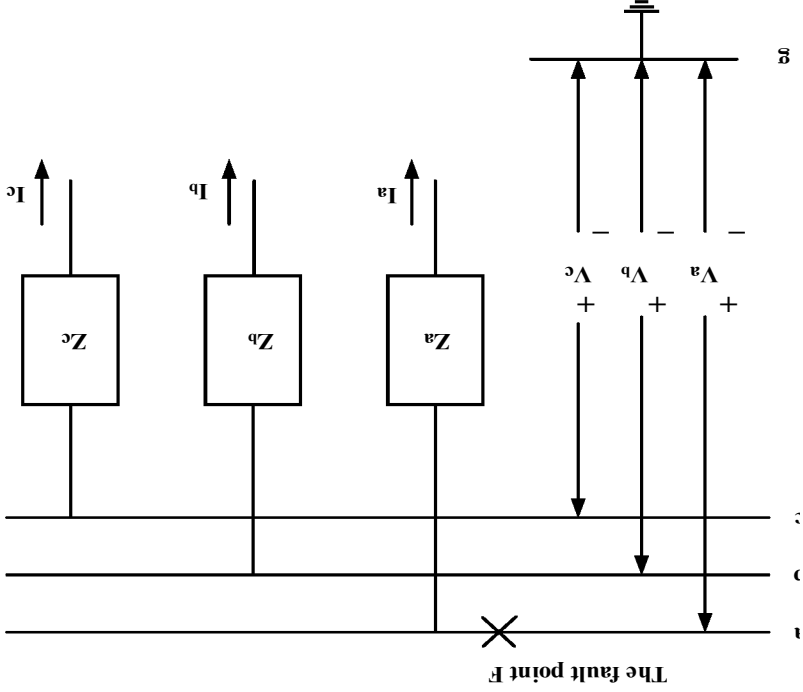


Fig. 4.20 Circuit diagram at fault point (F).

(4.46)

$$\begin{bmatrix} V^{a0} \\ V^{a1} \\ V^{a2} \end{bmatrix} = - \begin{bmatrix} 0 \\ E_a \\ 0 \end{bmatrix} - \begin{bmatrix} Z_0 \\ 0 \\ 0 \end{bmatrix} \begin{bmatrix} I^{a0} \\ I^{a1} \\ I^{a2} \end{bmatrix} + \begin{bmatrix} 0 \\ Z_1 \\ 0 \end{bmatrix} \begin{bmatrix} I^{a0} \\ I^{a1} \\ I^{a2} \end{bmatrix}$$

4.8.1 Single Line-to-Ground Fault

Consider a single line-to-ground fault from phase a to ground at the general three-phase bus shown in Fig. 4.21. For generality, we include a fault impedance Z_f in case of a bolted fault, $Z_f = 0$, whereas, for an arcing fault, Z_f is the arc impedance. In the case of a transmission line insulator flashover, Z_f includes the total fault impedance between the line and ground, including the arc and transmission tower's impedances and the tower footing if there are no neutral wires.

Fault condition in the phase domain

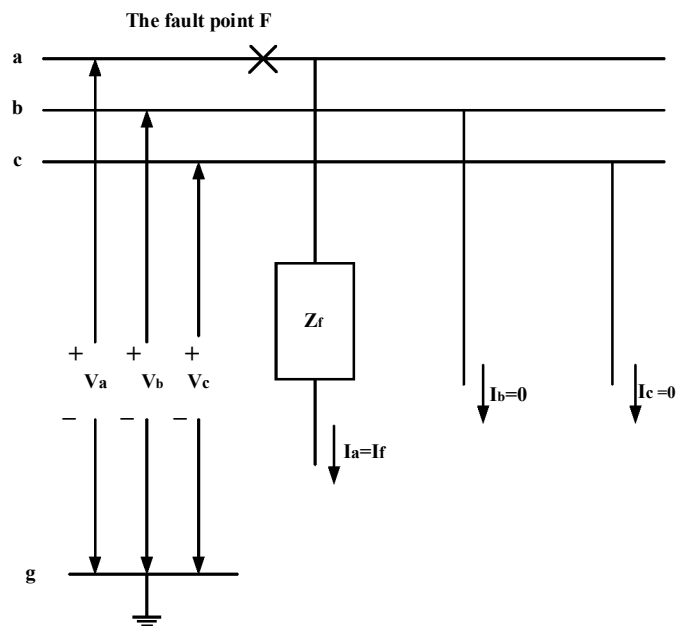


Fig. 4.21 General three-phase bus.

$$I_b = I_c = 0 \quad (4.47)$$

Single-line-to-ground

$$V_{ag} = Z_f I_a \quad (4.48)$$

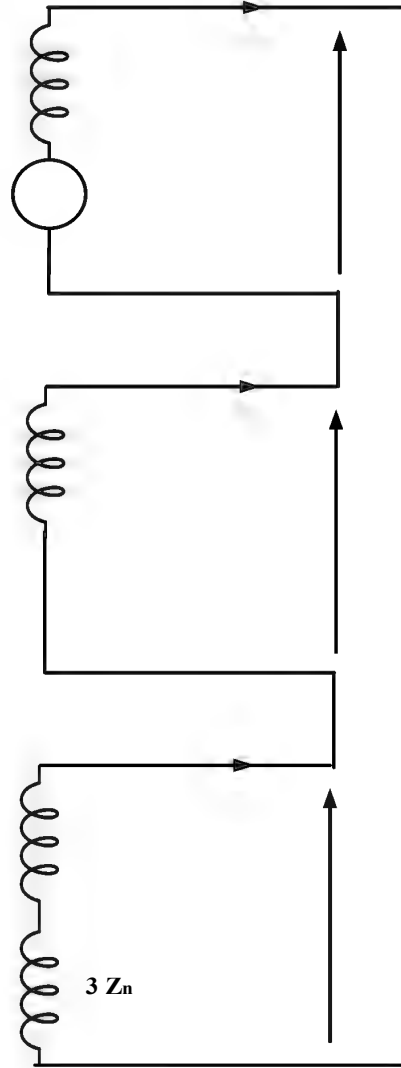


Fig. 4.22 Interconnected sequence networks for SLG fault.

As

$$V_a = Z_f I_a \quad (4.49)$$

Therefore

$$V_a = 3Z_f I_{a1} \quad (4.50)$$

$$V_{a0} + V_{a1} + V_{a2} = 3Z_f I_{a1} \quad (4.51)$$

Then, from Fig. 4.22, the sequence components of the fault current are:

$$I_{a0} = I_{a1} = I_{a2} = \frac{V_f}{Z_0 + Z_1 + Z_2 + (3Z_f)} \quad (4.52)$$

4.8.2 Line-to-Line Fault

Consider a line-to-line fault from phase b to c, shown in Fig. 4.23.

Fault conditions in the phase domain

$$I_a = 0 \quad (4.53)$$

line-to-line fault current

$$I_c = -I_b \quad (4.54)$$

$$V_{bg} - V_{cg} = Z_f I_b \quad (4.55)$$

From using the transformation Equation:

$$I_{a012} = A^{-1} I_{abc} \quad (4.56)$$

and

$$I_{a0} = 0, \quad I_{a2} = -I_{a1} \quad (4.57)$$

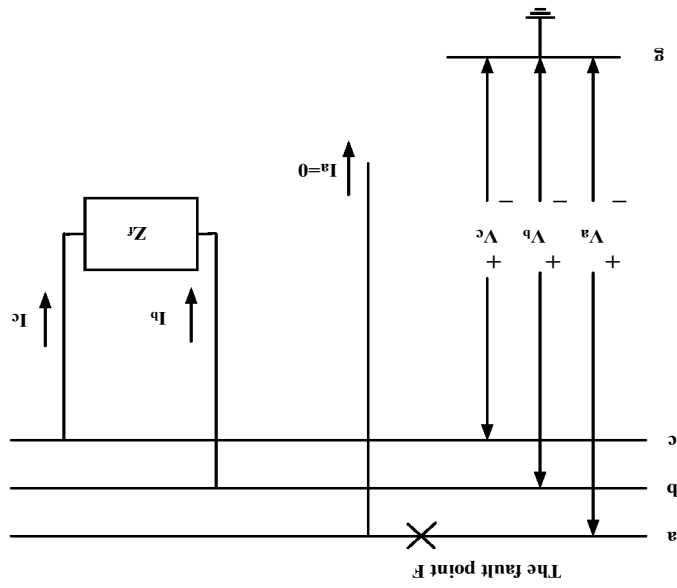


Fig. 4.23 General three-phase bus.

$$Z^f I_{a1} = V^{a1} - V^{a2} \quad (4.58)$$

Fault conditions in sequence domain

$$I_a = 0 \quad (4.59)$$

line-to-line fault

$$I_{a1} = -I_{a2}$$

$$V^{a1} - V^{a2} = Z^f I_{a1} \quad (4.61)$$

From Fig. 4.24, the fault currents are:

$$I_{a1} = \frac{V^f}{Z_1 + Z_2 + Z^f} \quad (4.62)$$

$$I_{a0} = 0 \quad (4.63)$$

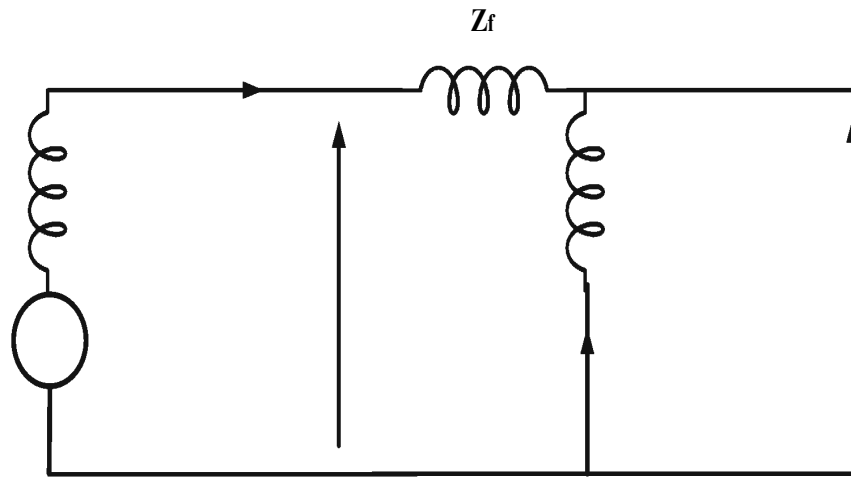


Fig. 4.24 Interconnected sequence networks.

4.8.3 Double Line-to-Ground Fault

A double line to ground fault from phase b to phase c through Impedance Z_f to the ground is shown in Fig. 4.25. From this Fig 4.25.

Fault conditions in the phase domain

$$I_a = 0 \quad (4.64)$$

Double line to ground fault

$$V_{cg} = V_{bg} \quad (4.65)$$

$$V_{bg} = Z_f (I_b + I_c) \quad (4.66)$$

Fault conditions in sequence domain

$$I_{a0} + I_{a1} + I_{a2} = 0 \quad (4.67)$$

Double line to ground fault

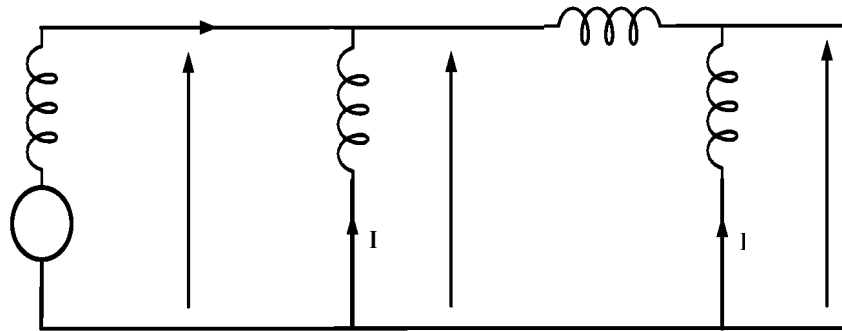


Fig. 4.26 Interconnected sequence networks.

$$I_{a1} = \frac{V_f}{Z_1 + \left[\frac{Z_2(Z_0 + 3Z_f)}{Z_2 + Z_0 + 3Z_f} \right]} \quad (4.73)$$

Using the current division in Fig .4.25, the negative and zero sequence fault currents are:

$$I_{a2} = (-I_{a1}) \left[\frac{Z_0 + 3Z_f}{Z_0 + 3Z_f + Z_2} \right] \quad (4.74)$$

$$I_{a0} = (-I_{a1}) \left[\frac{Z_2}{Z_0 + 3Z_f + Z_2} \right] \quad (4.75)$$

4.9 Fault Classification

The fault can be classified into two types according to the time:

i. Permanent fault: is defined as producing complete damage in the network's insulations and equipment, and it must change with other new ones.

ii. Instant fault: the fault may still be for a very short period of compression to a permanent fault period. The damage produced the same damage in the equipment; this fault may occur due to the conductors' contact because of heavy wind. Then, it causes an electric spark.

This type of fault is classified into two subtypes:

i. Recursion Fault: it occurs due to the contact between the conductors and comes back to normal operation and may contact conductors; hence, these cases may occur due to heavy wind.

ii. Not Recursion Fault: it occurs due to contact between the conductors, then to return to normal operation and remove the contact.

The following section deals with the balanced and unbalanced fault calculation in general and conventional methods for small systems.

4.9.1 Assumptions and Simplifications

The system data presentation assumes that the system is balanced, and only one phase in the three-phase system is considered [21, 25]. The impedances represent the per-phase impedance of transmission lines and transformers. It is assumed that the impedance to the flow of positive, negative, or zero-sequence currents is the same in each phase except at unbalanced points, and these imbalances require special treatment.

The rest of the network comprises balanced impedances, making the per-phase representation possible. The generators have different impedances to the flow of positive, negative, and zero sequence currents; however, a general simplifying assumption is made as follows:

- i. All load currents are negligible.
- ii. All generated voltages are equal in phase and magnitude to the positive sequence prefault voltage.
- iii. The positive and negative sequence networks are identical.
- iv. The networks are balanced except at fault points.

v. All shunt admittance (line charging susceptance, etc.) is negligible.

4.9.2 Fault Voltage-Amps

Voltage – Ampere is always called fault level, which it will produce by multiplying the fault current by reference voltage (V_r). In the case of a ground fault, the voltage represented as phase voltage, while in the case of a phase fault, the voltage is line voltage. This is how to compute Voltage – Ampere directly from the equivalent circuit of the fault; if per unit system is used, let (Z_t) represent the equivalent circuit of the fault.

$$Z_t = Z_1 + Z_2 + Z_0 + 3Z_f(\text{GroundFault}) \quad (4.76)$$

$$Z_t = Z_1 + Z_2 + Z_0 (\text{PhaseFault}) \quad (4.77)$$

Let (V_r) be the reference phase voltage for the faulted part of the system,

$$VA_{3ph}(\text{base}) = 3V_r * I_r = \frac{3V_r^2}{Z_r} \quad (4.78)$$

$$(\text{FaultVA}) = \frac{3V_r E_{an}}{Z_t} (\text{For Ground Fault}) \quad (4.79)$$

Then, in the per-unit system,

$$(\text{FaultVA})p.u = \frac{3V_r E_{an}}{\left[\frac{3V_r^2}{Z_r}\right] Z_t} = \frac{\frac{E_{an}}{V_r}}{\frac{Z_t}{Z_r}} = \frac{(E_{an})p.u}{(Z_t)p.u} \quad (4.80)$$

The same thing happened for phase fault:

$$(\text{FaultVA}) = \frac{\sqrt{3}V_r \sqrt{3}E_{an}}{Z_t} \quad (4.81)$$

Then, in the per-unit system:

$$(\text{FaultVA}) p.u = \frac{3V_r E_{an}}{\left[\frac{3V_r^2}{Z_r}\right] Z_t} = \frac{\frac{E_{an}}{V_r}}{\frac{Z_t}{Z_r}} = \frac{(E_{an})p.u}{(Z_t)p.u} \quad (4.82)$$

then

$$(FaultVA)p.u = \frac{1}{Z_t} \quad (4.83)$$

4.10 Summary

This chapter explored the power system faults, unraveling fundamental concepts and categorizing various fault types, including short-circuit faults. Short-circuit faults are known to introduce disturbances in the system, resulting in sudden changes in current and voltage profiles, posing a threat to the power system. The exploration extended to the essential analyses of symmetrical and unsymmetrical faults, focusing on the symmetrical components—zero, positive, and negative components, providing a thorough understanding of their significance in fault assessment. By understanding these aspects, the chapter laid a foundation for subsequent discussions, setting the stage for the in-depth examination of fault detection methodologies and applying advanced signal processing techniques in the following chapters

5. METHODOLOGY

This chapter explores the work established for detecting short-circuit faults in power systems using different Wavelet analysis, MATLAB, and Simulink simulations [4, 26]. Short-circuit faults cause significant challenges to the stability and reliability of electrical grids. The selection of Wavelet analysis arises from its unique capability to capture both time and frequency characteristics of signals, making it an excellent tool for fault detection in non-stationary signals. We used different Wavelet families, including Daubechies, Haar, Discrete Approximation Meyer, and Symlets, to identify the best fault detection and classification choice. They systematically applied to investigate their effectiveness in detecting and identifying different fault types, including single-phase, double-phase, and three-phase short circuits.

The systematic process explained from data acquisition, preprocessing, simulation, Wavelet decomposition, feature extraction, and the fault detection algorithm. The fault detection process involves threshold techniques to detect the fault and distinguish between fault and no-fault conditions. The threshold value is set strategically to identify different short circuit fault types accurately using different Wavelet families.

Recognizing the limitations of the threshold approach from the results received in determining the best Wavelet for fault detection, we went a significant step further. This step involved calculating Wavelet coefficients energy for each Wavelet family to find the most suitable Wavelet for fault detection. The goal of this study was to contribute to the advancement of fault detection techniques while using the capabilities of MATLAB [26] to enhance the efficiency of the methodology. In addition, to connect the theoretical

concepts and practical implementations to provide a reliable solution for short-circuit fault detection in the real world of power systems.

5.1 Study Design

This section of the methodology chapter discusses the rationale behind the chosen study design for the methodology approach and the specific study design applied in this short circuit fault detection in a three-phase power system using various Wavelets. The study design used the mixed methods approach, both quantitative and qualitative, to use the strengths of both [31]. The quantitative method gathers and analyzes data that involve numbers to understand things clearly and systematically. The qualitative approach gathers and analyzes information focuses on understanding observations that helps to explore the why and how behind things. Combining quantitative and qualitative methods in the study design for fault detection in a three-phase power system using various Wavelets allowed for a more holistic understanding of the subject, such as explaining why certain quantitative exist based on the qualitative observation or vice versa.

As an illustration, the process involves two steps: firstly, collecting data through quantitative methods based on numerical analysis, and secondly, engaging in communication with experts to gain a comprehensive understanding of the details. Connecting these numbers with human observations provides more understanding of power system faults. This approach helps validate the study findings.

Researchers such as Eric-Jan Manders and Pieter Mosterman at the Department of Electrical Engineering and Computer Science Vanderbilt University (2017) have used mixed methods approaches for fault isolation in continuous dynamic systems, which proved many advantages over the quantitative study design alone. This study first designed

the quantitative data on the power system current signals collected for analysis during fault and no-fault conditions. Then, the qualitative data collected through discussion with the power system, digital signal processing experts, and engineers. This approach allowed confirming quantitative findings by the qualitative and vice versa, validating the data collection.

5.2 Instruments/Measures

The instruments/measures tools used for data collection and analysis for the three-phase power systems fault detection using different Wavelets (db4, Haar, sym5, DAM) were MATLAB/Simulink and MATLAB commands. These instruments were used to extract and analyze the currents in the power system under various short-circuit fault conditions using different Wavelet transform families. MATLAB/Simulink simulates the three-phase power system that generates current signals for various short circuit fault scenarios simulated using the Three-Phase Faults Block, including line-to-line, line-to-ground, three-phase, and three-phase-to-ground faults.

The MATLAB commands applied for the Wavelet transform on the captured current signals for further analysis. Various Wavelet families, including db4, Haar, sym5, and the DAM, are used. This process allowed us to decompose the current signals extracted from the MATLAB/Simulink into Wavelet coefficients [4], which is very important for this study's fault detection methodology, especially the current signals' detailed coefficients.

5.3 Academic (Scholarly) Support

The choice of using MATLAB/Simulink to simulate the power system and capture various fault types aligned with established academic practices in power system analysis.

The academic community recognizes MATLAB's capability to capture power system behavior under different fault conditions. In addition, many study papers support MATLAB's credibility [26] as a handy, reliable study tool. Using MATLAB commands for Wavelet transformation aligns with academic practice in different fields, such as signal processing, pattern recognition, and fault detection applications. Many studies and papers use these command algorithms and prove effectiveness in extracting data needed for their study and analysis.

5.4 Data Collection

The study employed a mixed-method approach, combining quantitative and qualitative data collection methods, to investigate power systems fault detection using various Wavelets. The focus was on gaining a comprehensive understanding of the findings by connecting numerical data with expert insights. This approach aimed to enhance the depth of analysis and provide valuable insights into the complexities of power systems fault detection.

For the quantitative aspect of the study, the data collection is a critical step to gather the information needed for the study on fault detection and identification in a three-phase power system using different Wavelet transforms, db4, Haar, sym5, DAM. The quantitative data collection step executed using MATLAB/Simulink, where the current signals from the three-phase power system captured under different short circuit faults and the no-fault condition for further analysis for fault detection and identification methodology. Then, the Wavelet maximum detailed coefficients and the Wavelet coefficients energy data collected for all the various selected Wavelets for all fault types and no-fault conditions.

For the qualitative aspect of the study, we discussed with field experts their valuable insights into the meaning of signals obtained from MATLAB simulations, particularly those related to current signals during faults, to explain the significance of the data that received regarding the Wavelet coefficients energy. The expert observations with the numerical data merged to integrate these qualitative and quantitative analyses. This combination increased the understanding of the findings and validated the results effectively to gather a holistic understanding of the phenomena.

5.5 Data Analysis

This section offers a rationale for the selected data analysis techniques, justifying their relevance to the study's methodology, which is the foundation for this study on fault detection and identification in a three-phase power system using various Wavelet transform families, db4, Haar, sym5, DAM. The choice of data analysis techniques is essential to the success of any study. In this, the data analysis techniques selected based on several factors. The data analysis techniques provided the current signal behavior for each fault type in the power system, which aligns with the study objective for detecting and identifying the different fault types in a power system.

Wavelet transform analysis is capable of capturing transient high frequency features in the signal. The data collected after decomposing the current signals was the detailed coefficients. Since these detailed coefficients contained information about the signal's high-frequency components, Wavelet-based analysis techniques were rational since the power system current signals during fault conditions caused transient high-frequency features in the signal.

The Wavelet coefficients energy analysis technique then used to evaluate the energy distribution within the detailed coefficients for the current signal of the power systems. This technique was rational since it highlighted the energy content of the high frequency components of the faulty current signals. This approach helped identify the optimal Wavelet for fault detection.

5.7 Fault Detection Methodology: Comparative Flowchart Analysis

This section illustrates a comparative analysis between two fault detection methodologies, each representing distinct approaches to identifying and categorizing faults in a three-phase power system. The first methodology employed a conventional approach without the integration of Wavelet decomposition. In contrast, the second methodology used in this study introduced a novel flowchart incorporating Wavelet decomposition for enhanced fault detection and identification.

i. Conventional Methodology: Fig.5.1 illustrates the flowchart for the first methodology based on a conventional approach for fault detection techniques relying on basic analysis of three-phase current signals.

- Data Input: the process began with loading three-phase current signals as the primary input.
- Analysis: a straightforward analysis of the current signals conducted without employing Wavelet decomposition.
- Fault Identification: fault detection relied on conventional methods without detailed coefficients or a threshold comparison.
- Result: the output provides a basic indication of fault occurrence without specifying fault types or detailed information.

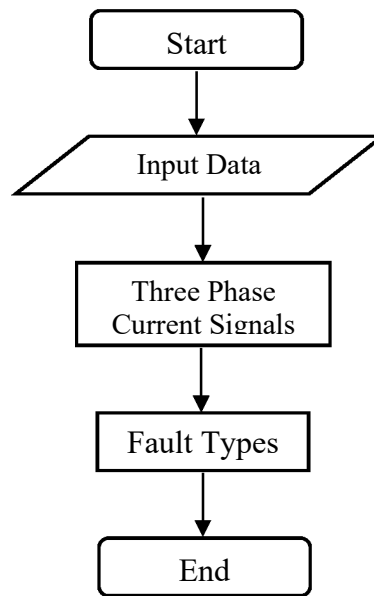
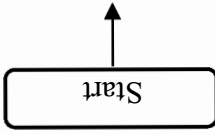


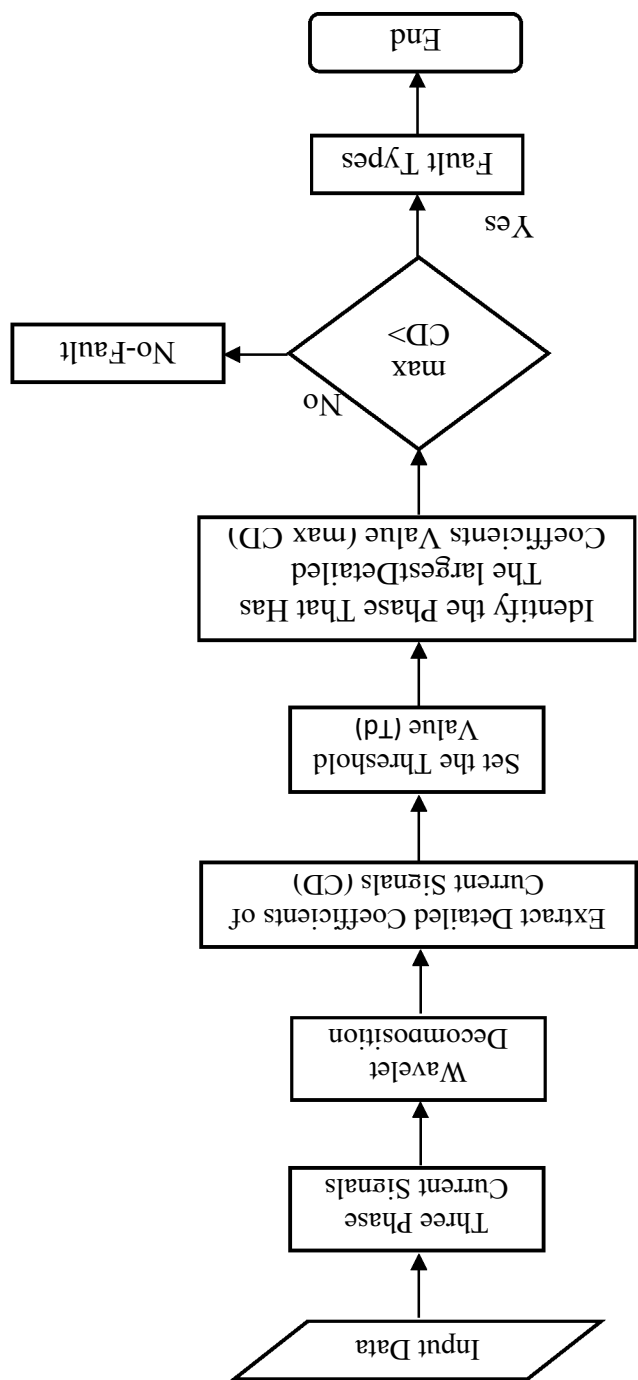
Fig. 5.1 The flowchart for conventional short circuit fault detection.

ii. Enhanced Methodology with Wavelet Decomposition: wavelet analysis is a powerful tool in power systems fault detection because it provides a multi-resolution representation of signals. This analysis involves decomposing signals into detailed and approximation coefficients, allowing for a comprehensive examination of both high and low frequency components at varying scales. This study emphasizes the significance of utilizing detailed coefficients for short-circuit fault detection. Detailed coefficients capture high-frequency information, highlighting rapid variations induced by short circuits or other transient disturbances. Focusing on these detailed coefficients, the approach aimed to enhance the sensitivity and accuracy of fault detection, enabling a more precise identification of the fault characteristics. This emphasis on detailed coefficients within the framework of multi-resolution analysis contributes to a robust methodology for improving the reliability and efficiency of power systems fault detection. Fig.5.2 illustrates the



- flowchart for the second methodology, introducing novel and advanced fault detection techniques by incorporating Wavelet decomposition into the process:
- Data Input: similar to the conventional methodology, the process starts with loading three-phase current signals.
 - Wavelet Decomposition: a crucial enhancement introduced with the application of Wavelet decomposition, breaking down the current signals into detailed and approximation coefficients.
 - Detailed Coefficients Analysis: the methodology involves extracting detailed coefficients and subjecting them to a threshold comparison.
 - Fault Identification: the phase with the most significant detailed coefficient exceeding the threshold identified as the potential faulted phase, providing a more precise fault location.
 - Result: the output clearly explains fault occurrences, including fault types and specific details about the identified faulted phase.

Fig. 5.2 The study methodology flowchart for short circuit fault detection.



iii. Comparison Analysis: the conventional methodology offers a basic indication of fault occurrences but lacks the sophistication provided by the enhanced methodology. Incorporating Wavelet decomposition enables a more detailed analysis through detailed coefficients, leading to improved fault detection accuracy. The enhanced methodology not only detects faults but also categorizes them and identifies the faulted phase, contributing significantly to the reliability and efficiency of fault detection in three-phase power systems. The comparative analysis emphasizes the value of integrating Wavelet decomposition into fault detection methodologies, setting the stage for a more advanced and accurate approach in the study.

5.7 Summary

The methodology chapter provided detailed information about the study approach used in fault detection and identification within a three-phase power system using various Wavelets transform. This chapter explored the study design using MATLAB/Simulink, the algorithm using MATLAB commands, the instruments used, data collection, and the data analysis. In summary, the study methodology involves the following:

i. Study Design Using MATLAB: the methodology used MATLAB to design and simulate the three-phase power system and to generate the three-phase short circuit faults and no-fault condition current signals.

ii. Algorithm Using MATLAB Commands: the methodology used the MATLAB commands to analyze the collected data of the three-phase power system current signals.

iii. Data Collection Instruments and Methods: the methodology provided information about the instruments used to collect data, including MATLAB/Simulink and the MATLAB commands.

iv. Data Analysis Techniques: the methodology provided the rationale and the justification for the data analysis approach, including Wavelet transform and energy analysis techniques.

In the next chapter, Chapter 6 - Results, we will present the simulation and the command process applied based on the methodology explained in this chapter. Followed by the discussion and conclusions Chapter 7, which discusses the study findings based on the methodology approach. The work we set in this methodology chapter led to exploring this study's outcomes and their importance provided valuable contributions to the power system field.

6. RESULTS

The Results chapter comprehensively presents the fault detection and identification findings in a three-phase power system using Wavelets.

6.1 Introduction

The results display the short circuit fault detection findings in three-phase power systems using various Wavelets using the methodology explored in Chapter 3. The results explain how multiple Wavelets, including db4, Haar, sym5, and DAM, performed for short-circuit fault detection and identification. The primary purpose of this chapter is to present and discuss the study's findings, explain the performance of different Wavelet transforms in detecting and identifying faults, and determine which Wavelet families were the best for detecting and identifying short-circuit faults in power systems. Two primary questions to answer: How do we use Wavelets to detect and identify faults in a three-phase power system? Then, the second question: Which Wavelet is optimal for fault detection and identification.

The results fit perfectly into the goals of this study. The results in this chapter followed the methodology chapter. The methodology chapter explained the thesis approach, data collection methods, and analysis techniques. This chapter presents the findings of applying those methods to detect faults and uncover the optimal Wavelets for fault detection in the three-phase power system.

This chapter organized into several sections. It begins by summarizing the data collection and analysis processes, highlighting the Wavelet families. It then investigates each Wavelet family's performance in capturing and classifying the short circuit faults in the three-phase power system. Next, it discusses the results of identifying the optimal

Wavelets by discussing the findings of applying the energy analysis technique since the threshold technique alone did not highlight the optimal Wavelet for fault detection.

6.2 Brief Description of How the Methodology Approach Applied to Data Analysis

This section provides an overview of how the selected methodology approach, as detailed in the methodology chapter, was applied during the data analysis step of the study on short-circuit fault detection using various Wavelets in a three-phase power system. As detailed in the methodology chapter, the data collection step involved using MATLAB/Simulink to simulate the three-phase power system and generate current signals for the different fault conditions. Then, the Wavelet transforms applied to decompose the current signals into their frequency components.

The primary focus was on extracting the detailed coefficients, which captured the high-frequency components in the signal, and the choice of Wavelet families (db4, Haar, sym5, DAM) remained consistent with the methodology. Then, the maximum detailed coefficients obtained to compare against the threshold set value to detect faults. Following that, as explained in the methodology chapter, the Wavelet coefficients' energy analysis performed to obtain the energy content within the detailed coefficients. This analysis chose to identify the optimal Wavelets for fault detection and identification.

While following the study plan, we faced a couple of challenges. In the early days of the studies, about two years ago, while enrolled in a class about Wavelets and their applications, an online presentation that furthered understanding of concepts about Wavelets and how to use the MATLAB. However, even after extensive searches, could not find that source again to include it in the references, which made it challenging to have a complete list of references. Another challenge we faced was in the performance of each

Wavelet family, comparing results across various faults required careful attention to detail. That led us to conduct more analysis, which gave us a valuable, important conclusion.

6.3 System Design and Simulation

The initial step involved obtaining current signals for the normal, no fault, and the short-circuit fault state. These current signals used as the main parameters for this thesis analysis by the characteristics of these short-circuit fault currents. The current signals associated with short circuit faults examined using Wavelet transforms in the MATLAB commands and the power system simulated by Simulink. The goal was to develop an effective method for fault detection using the capabilities of Wavelet transform to classify all short-circuit fault types in power systems effectively.

The power systems simulation model constructed using MATLAB/Simulink. As illustrated in Fig. 6.1, the complete power system was built using Simulink to generate and capture various fault currents. The system configuration included a three-phase source (generator), voltage and current measurement elements, transmission lines, current measurement devices (ammeters), visualization tools (scope), electrical loads, and three-phase fault generators. This setup was the foundation for simulating and capturing various fault scenarios within the power system, enabling accurate analysis and validation of the fault detection methodology.

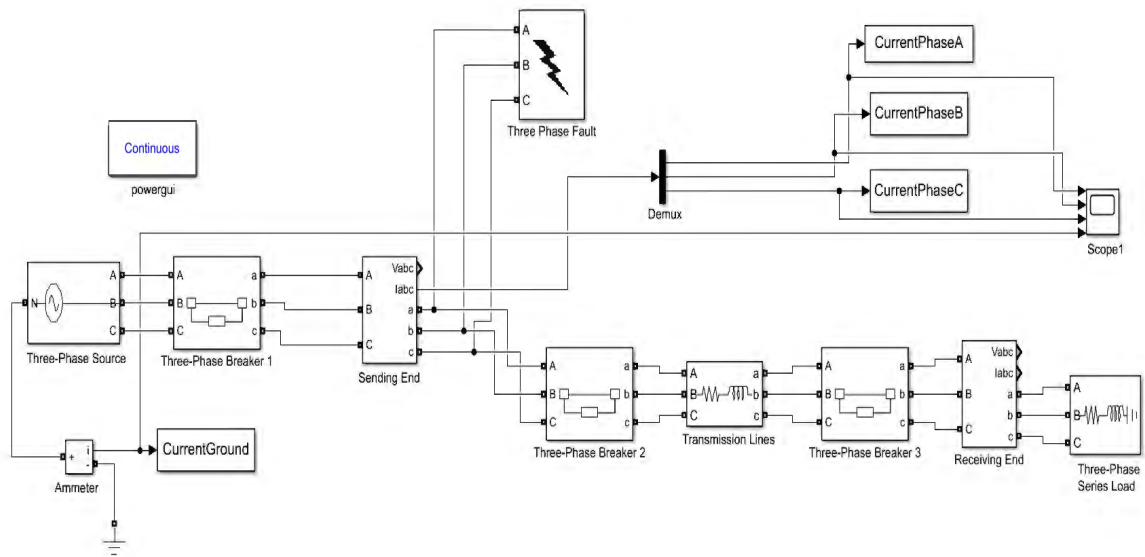


Fig. 6.1 Power system simulation using MATLAB/Simulink.

The simulation parameters of the power system model used are:

- Three Phase Source: 250 KV, 60 Hz
- Transmission Lines:
 - Resistance (R) = 6 Ohms
 - Inductance (L) = 0.053052 H
- Load:
 - 220KV
 - 60 HZ
 - Active Power: 304.8 MW
- Reactive Power: 228.6 MW

6.4 Algorithm

The methodology involved current signals for all phases and the ground signal for the three-phase power system obtained from the power system simulation in MATLAB/Simulink with the algorithm to detect and identify fault types based on Wavelet transform. We used various Wavelet families in this methodology, including db4, Haar,

sym5, and DAM, each employed separately. Fig. 5.2 in Chapter 5 presented the flowchart block diagram of the methodology. The steps detailed as follows:

i. Power System Modeling: MATLAB/Simulink to construct the power system model.

ii. Signal Acquisition: obtaining the three-phase current signals for normal operating conditions (no fault) and the various short circuit fault types simulated using the three-phase fault block in MATLAB/Simulink, 12 cases.

iii. Wavelet Transformation: applying individual Wavelet family (db4, Haar, sym5, Discrete Approximation Meyer) to extract approximation and detailed coefficients at level one for all 12 cases.

iv. Threshold Setting: setting a threshold value.

v. Coefficient Analysis: determine the maximum value among the detailed coefficients.

vi. Fault Detection: comparing the maximum detailed coefficients value with the threshold. A fault detected if the maximum detailed coefficients value exceeds the threshold value.

vii Fault Type Identification: identifying the fault type.

These steps enabled accurate fault detection and identification in the three-phase power system using various Wavelet families and the threshold concept analysis.

6.4.1 Threshold Concept

A "threshold" is generally a predetermined limit used as a boundary or for making decisions. A particular response occurs when the threshold value level reached or passed.

Thresholds used in various fields, such as technology, science, finance, and decision-making.

In power System Fault Detection and Identification, the term "threshold" refers to predefined criteria used to determine whether a fault condition exists in the power system. This threshold can be set based on different parameters, such as voltage levels, current magnitudes, or other electrical systems parameters. If the parameter exceeds the threshold, it triggers a fault detection technique to indicate the existence of the fault in the power system.

In digital signal processing (DSP), "threshold" refers to a predetermined value used to distinguish between meaningful signal components and noise or to trigger specific actions based on a signal's amplitude or characteristics. It is the main concept in different DSP applications, such as filtering, signal analysis, and detection. In Wavelet analysis, the term "threshold" refers to the Wavelet denoising concept or Wavelet-based signal processing by setting a predefined threshold value to separate relevant signal components from noise or eliminate some of the unwanted Wavelet coefficients for the specific technique.

In power systems fault detection and identification using Wavelet analysis, the term "threshold" refers to a predefined value used as a reference point for detecting and identifying faults in a power system. This study applied threshold as a fundamental technique for detecting faults and identifying the fault types in a three-phase power system using various Wavelets. The methodology was to set predetermined threshold values for the Wavelet detailed coefficients obtained from the decomposition of three-phase current and ground current signals using the four selected Wavelets. The detailed coefficients

captured the current signals' transient and high frequency components. To detect and classify the faults, we compared the magnitude of these derailed coefficients with the threshold value. A coefficient exceeding the threshold indicated a fault in the current signal.

The reason for using the threshold technique with various Wavelets (db4, Haar, sym5, DAM), was to evaluate their performance in detecting and classifying faults, ultimately helping us choose the best Wavelet for the fault detection for the given power system. It is essential to realize that threshold value selection was critical since choosing the threshold value can affect the accuracy of our fault detection results.

This thesis applied the threshold value ($T_d=350$) across all the selected Wavelets. Each of these Wavelets accurately captured and identified the fault types. The threshold technique proved successful for all the chosen Wavelets (db4, Haar, sym5, DAM) in detecting and identifying faults within the power system. However, it did not provide the means to discern which Wavelet was most optimal for the task of detecting and identifying the specific faults within our power system

6.4.2 Fault Detection

The currents and voltages within the three-phase power system were sinusoidal signals under normal no-fault conditions. However, introducing a fault disrupted this sinusoidal behavior, leading to noticeable changes in the current and voltage signals. In the case of a short-circuit fault within the transmission lines, the current signals will have transient components. The transient components that occur because of the sudden fault are important indicators for fault detection.

We used Wavelet transform because of the Wavelet's ability to capture and analyze transient components in current signals. The Wavelet transform enabled us to detect the

fault promptly and accurately, which was crucial for maintaining power systems' reliability and stability. The maximum current's detailed coefficients from the Wavelet transform for the current signals compared against the specified value for a threshold. If the maximum current detailed coefficients were below the threshold value, there was no fault within the power system. In contrast, if the current's detailed coefficients exceeded the threshold, it indicates a fault within the power system.

6.4.3 Fault Classifications

Various Wavelets, including db4, Haar, sym5, and DAM, were applied, each subjected to first-level decomposition. These Wavelets selected due to their distinctive characteristics, making them a good candidate for fault detection. The current detailed coefficients extracted from both the three-phase current and the ground current signals, and then they compared against a fixed threshold value for all Wavelets used. The faults effectively identified, and the fault types were accurate. This methodology based on the fact the detailed coefficients associated with the faulty line exceeded the threshold, leading to the detection of all faulty lines and enabling the determination of fault types, then categorize these faults into the following types:

- i. Single-phase to ground faults L1-G, L2-G, and L3-G.
- ii. Double-phase to ground faults L1-L2-G, L1-L3-G, and L2-L3-G.
- iii. Double-phase faults L1-L2, L1-L3, and L2-L3.
- iv. Three-phase faults L1-L2-L3.
- v. Three-phase-to-ground faults L1-L2-L3-G.

Here, L1 represents phase A current, L2 represents phase B current, L3 represents phase C current, and G signifies ground current. Because of this analysis, the thesis

achieved fault detection and categorizing for various fault types within the three-phase power system.

6.4.4 Selection of Wavelet Transform Families

In this section, we review the rationale behind the choice of the selected Wavelet families, db4, Haar, sym5, and DAM, for the fault detection in a three-phase power system within the scope of this thesis. The selection of these Wavelets based on their properties, making them excellent candidates for this analysis.

i. db4 (Daubechies Wavelet, Order 4):

- Orthogonality: Daubechies Wavelets, including db4, are orthogonal, ensuring an accurate representation of signals with minimal distortion.
- Compact Support: they have compact support, localized in both time and frequency domains, enabling precise localization of transient fault components.

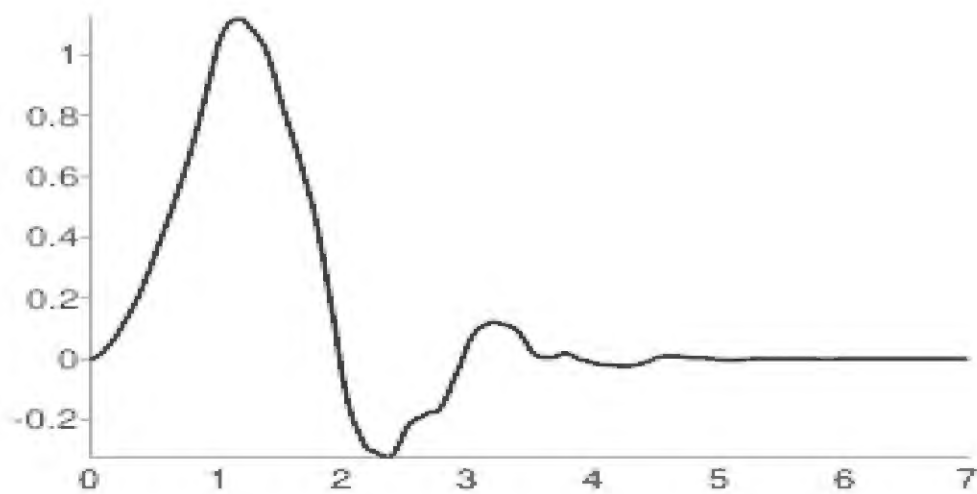


Fig. 6.2 Daubechies scaling function ϕ [19].

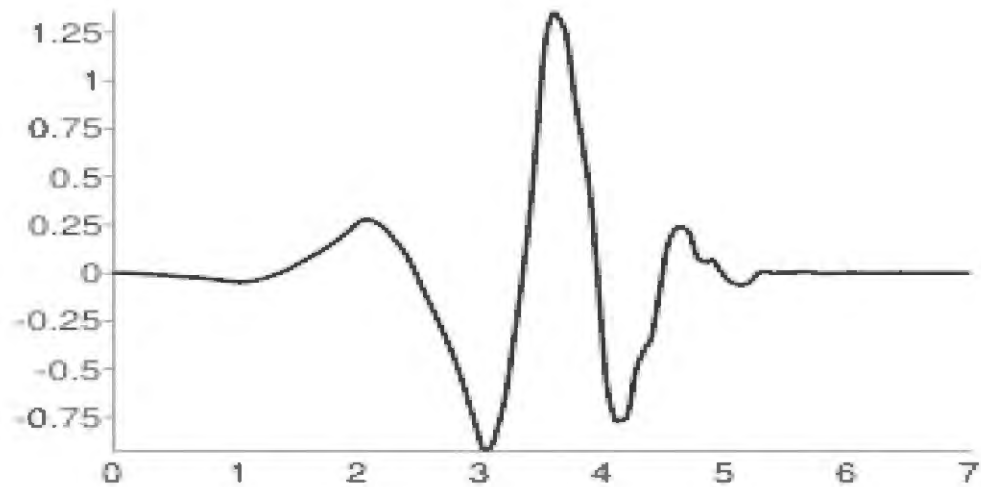


Fig. 6.3 Daubechies Wavelet function ψ [19].

ii. Haar Wavelet:

- **Simplicity:** Haar Wavelets are elementary and computationally efficient, making them ideal for rapidly analyzing and processing large datasets.
- **Step Function Representation:** Haar Wavelets can efficiently capture abrupt signal changes due to their step function-like representation, aligning well with the sudden variations typical of fault occurrences.

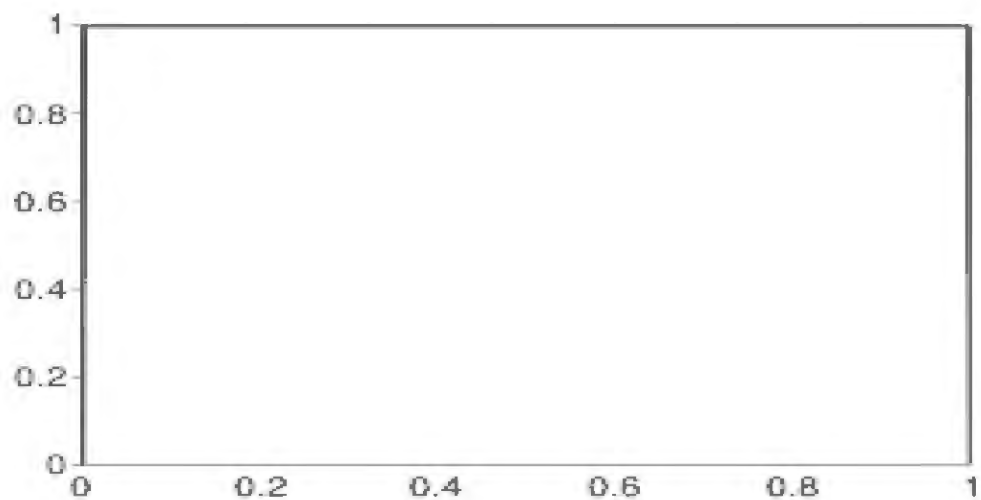


Fig. 6.4 Haar scaling function ϕ [19].

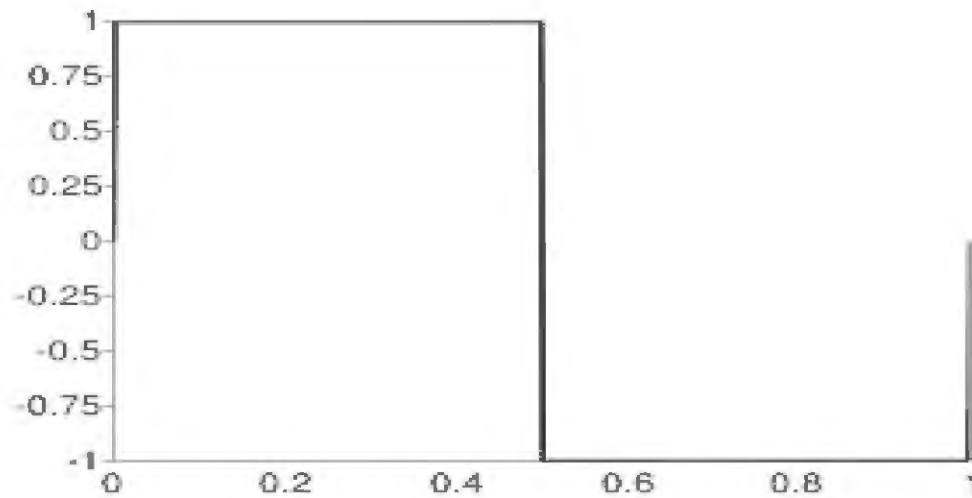


Fig. 6.5 Haar Wavelet function ψ [19].

iii. sym5 (Symlet Wavelet, Order 5):

- Symmetry and Vanishing Moments: Symlet Wavelets, including symlet 5, possess symmetry and vanishing moments, allowing them to capture signal features while minimizing noise interference effectively.
- Higher Order Coefficients: Symlet Wavelets incorporate higher-order coefficients, enhancing their ability to detect slight variations and irregularities in the signal, which is crucial for fault detection within power systems.

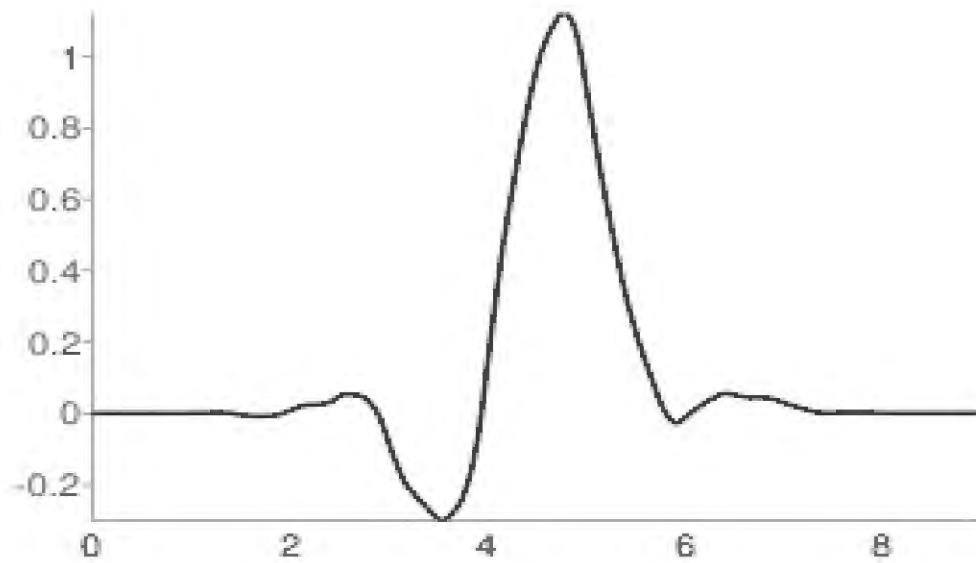


Fig. 6.6 Symlet scaling function ϕ [19].

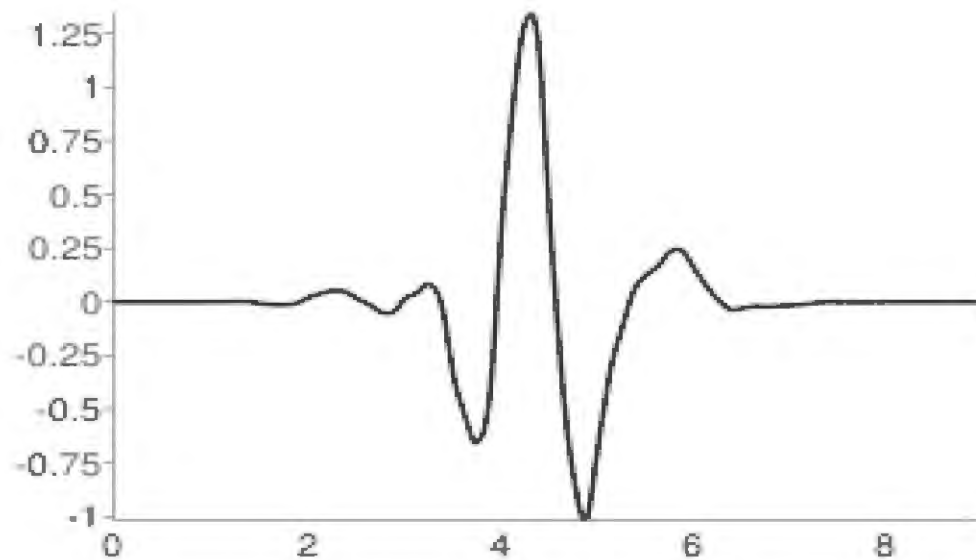


Fig. 6.7 Symlet Wavelet function ψ [19].

iv. Discrete Approximation Meyer Wavelet (DAM):

- Smoothness and Regularity: DAM Wavelets offer smoothness and regularity, ensuring an accurate representation of signals, especially in noise and distortions.

- Adaptability: their adaptability to varying signal characteristics makes them valuable for fault detection.

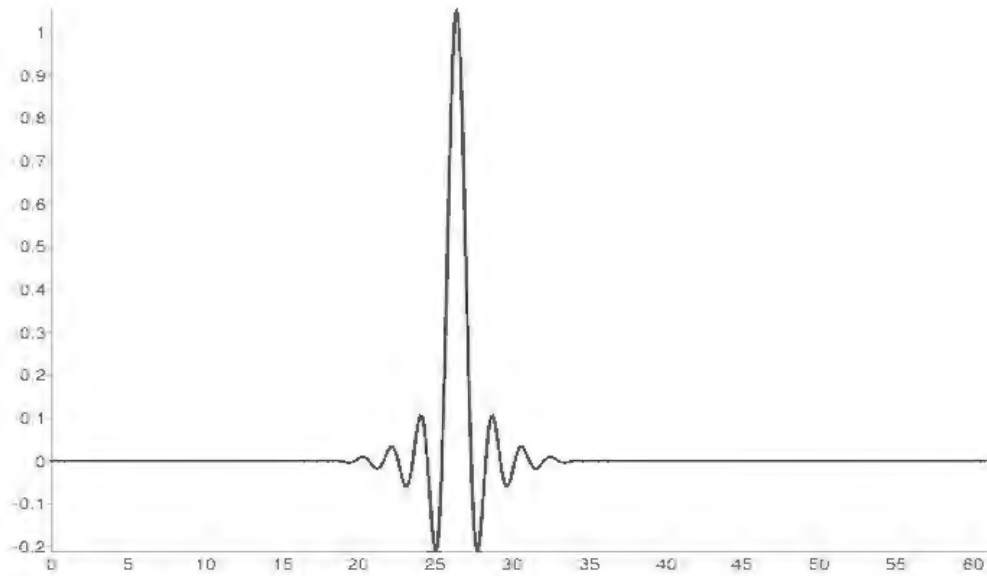


Fig. 6.8 Meyer scaling function ϕ [19].

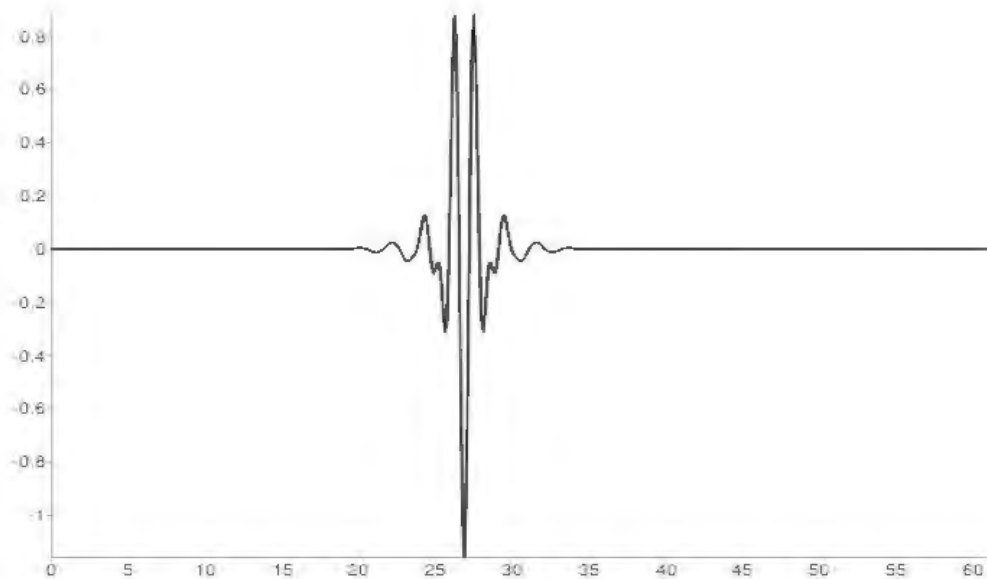


Fig. 6.9 Meyer Wavelet function ψ [19].

The characteristics of these Wavelets, such as orthogonality, compact support, simplicity, symmetry, vanishing moments, higher-order coefficients, smoothness, and adaptability to different fault scenarios, allow them to capture transient and localized features.

6.4.5 Understanding Wavelet Characteristics

This section explores each Wavelet's characteristics to provide a comprehensive understanding of how these factors contribute to the versatility and precision of Wavelet analysis.

i. Orthogonality and Compact Support: Wavelets like Haar and db4 possess orthogonality, efficiently capturing transient and localized features within signals, such as those produced by faults in power systems. Their compact support ensures that they concentrate on specific signal details.

ii. Wavelet Shape and Symmetry: the symmetrical nature of Wavelets like sym5 and db4 enables them accurately capture both positive and negative transient components in power signals, making them suitable for fault detection where signal symmetry can be crucial.

iii. High Time-Frequency Localization: Wavelets including Haar and DAM, offer excellent time-frequency localization. This characteristic is essential for pinpointing the exact timing of transient events associated with faults, allowing for precise fault detection.

iv. Multiresolution Analysis: these Wavelets support multiresolution analysis, meaning they can simultaneously capture high-frequency transients and low-frequency

steady-state components in power signals. This versatility is critical for detecting sudden fault occurrences.

v. **Adaptability and Flexibility:** the flexibility to choose from various Wavelets allows researchers to tailor their selection to the specific characteristics of the power systems under investigation.

vi. **Extensive Study and Application:** Wavelets such as db4 and Haar have a well-established record in signal processing, and have been widely used in various engineering and fault detection applications. Their reliability and extensive study literature make them excellent choices.

In summary, the selection of db4, Haar, sym5, and DAM Wavelets for fault detection in a three-phase power system was based on their distinctive characteristics, including orthogonality, localization, simplicity, and their ability to effectively capture transient features. These characteristics make them an excellent choice to extract the transient components in the faulty current signals that enhance the fault detection technique.

6.5 MATLAB Simulation and Commands to Extract Signals Detailed Coefficients

The MATLAB/Simulink simulated the short circuit faults and the normal, no-fault, conditions within the three-phase power system. By modeling the power system in Simulink correctly and then applying the different fault scenarios using the Three-Phase Fault Block; current signals corresponding to each fault type and the no-fault condition captured and plotted for analysis. These data are essential data for this methodology.

The current signals then subjected to Wavelet transform analysis. Using various Wavelet families, including db4, Haar, sym5, and DAM, the MATLAB command

'wavedec' was applied to decompose the signals into approximation and detailed coefficients. The detailed coefficients data needed here because it captured the high frequency components in a signal, which play an essential role in fault detection and identification. Both approximation and detailed coefficients plotted to visualize the signals' behavior.

This section is an overview of the Wavelet decomposition process and the calculation of the coefficient using the MATLAB commands for the three-phase current signals obtained from the MATLAB simulation for all fault and no-fault conditions for each of the selected Wavelets: db4, Haar, sym5, and DAM.

6.5.1 Wavelet Decomposition and Maximum Detailed Coefficients Process for db4

The Daubechies 4 (db4) Wavelet selected because of its ability to capture transient features and transient disturbances within the signals. The decomposition process achieved using the MATLAB's 'wavedec' command. This command breaks down the input signal into two primary components: approximation and detailed coefficients. The decomposition process can be at various levels, but we used decomposing at level 1 in this study.

One of the essential parameters we needed in this fault detection methodology was the extraction and calculation of detailed coefficients. The detailed coefficients had high frequency and transient components in the signal. That was significant for identifying transient events, such as those caused by different types of faults, including short-circuit faults because the detailed coefficients' magnitude has the information that helps in accurate fault detection and classification.

Then, the MATLAB command `max ()` was applied to determine the maximum value of the detailed coefficients for each current signal in fault and no-fault conditions.

These maximum detailed coefficient values were then compared against the threshold ($T_d=350$) for identification and fault detection. These maximum detailed coefficient values recorded in a Table. The Table detailing the maximum coefficient values presented in the Results chapter for further analysis, significantly contributing to these findings and conclusions.

Fig. 6.10 to Fig. 6.13 illustrate the power system's three-phase currents and ground current under normal conditions, including both the approximation and detailed coefficients of the current signals. The X-axis represents the sample number and the Y-axis represents the amplitude of the coefficients.

Fig. 6.10 Simulink no fault currents.

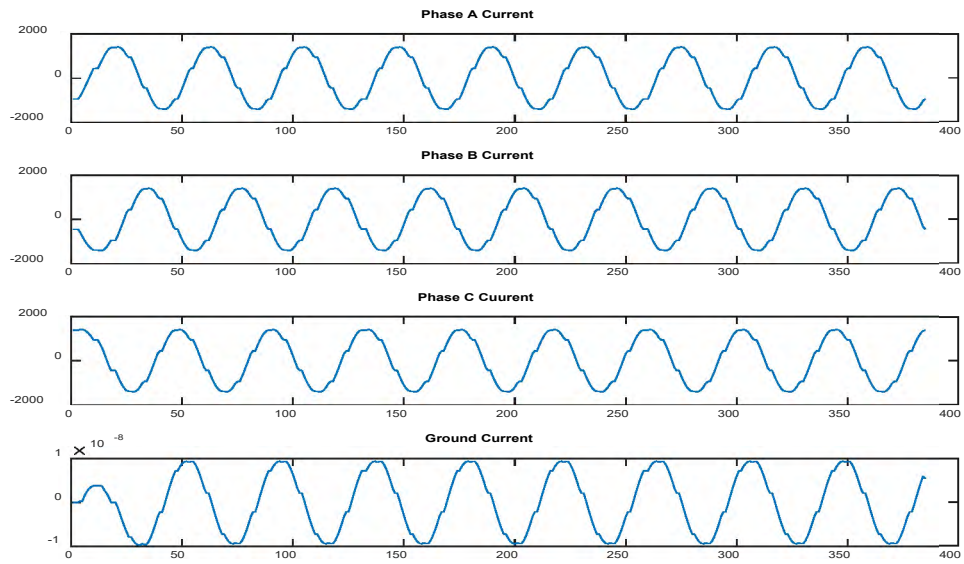


Fig. 6.11 Algorithm no fault currents.

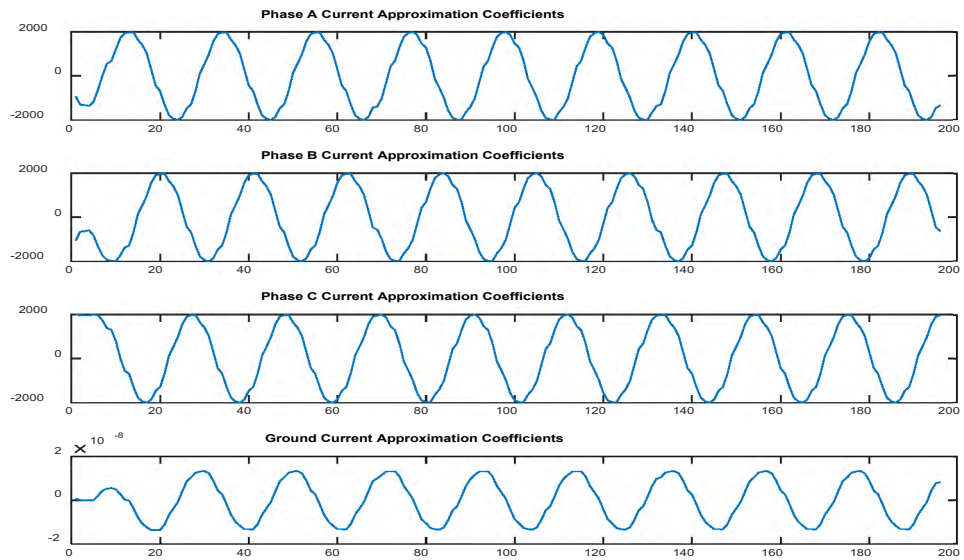


Fig. 6.12 No-fault currents approximation coefficients db4.

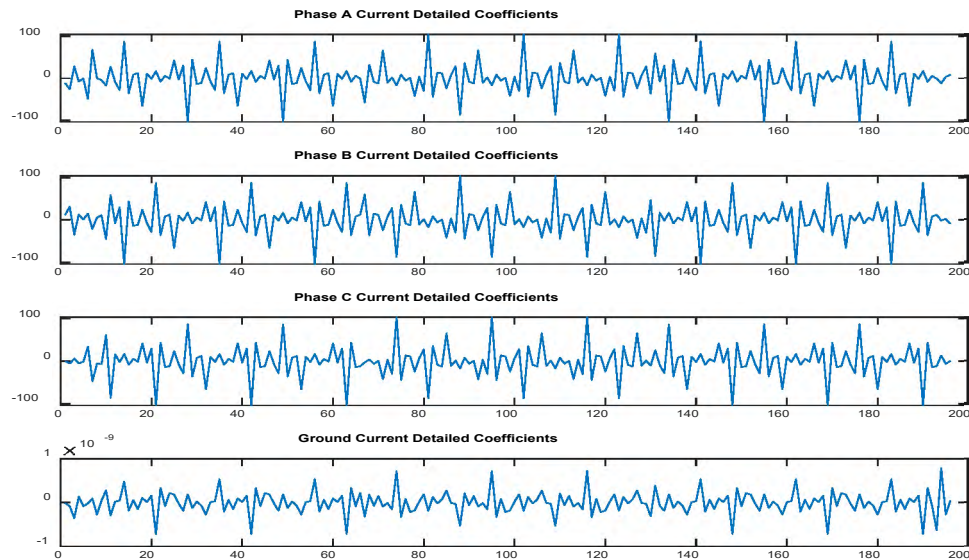


Fig. 6.13 No-fault currents detailed coefficients db4.

The analyses of Figs. 6.10 to 6.13 reveal that under normal no-fault conditions, the three-phase current signals for phases A, B, and C and the ground current remained normal. Similarly, both the approximation and detailed coefficients had a consistent pattern, confirming the no-fault condition of the system. This understanding of the power system behavior with no fault applied serves as a reference point for interpreting the other figures with fault conditions. This reference shows the importance of studying the power system behavior before investigating fault detection and analysis.

Five distinct fault scenarios examined to represent the observations concerning faulty three-phase currents visually. These scenarios included single line-to-ground, double-line, double lines-to-ground, three-phase, and three-phase-to-ground faults. The captured data, including the approximation and detailed coefficients displayed in Figs. 6.14 to 6.34.

Fig. 6.14 Simulink single-line-to-ground fault B-G Currents.

Fig. 6.15 Single-line-to-ground fault B-G (Phase A and ground currents).

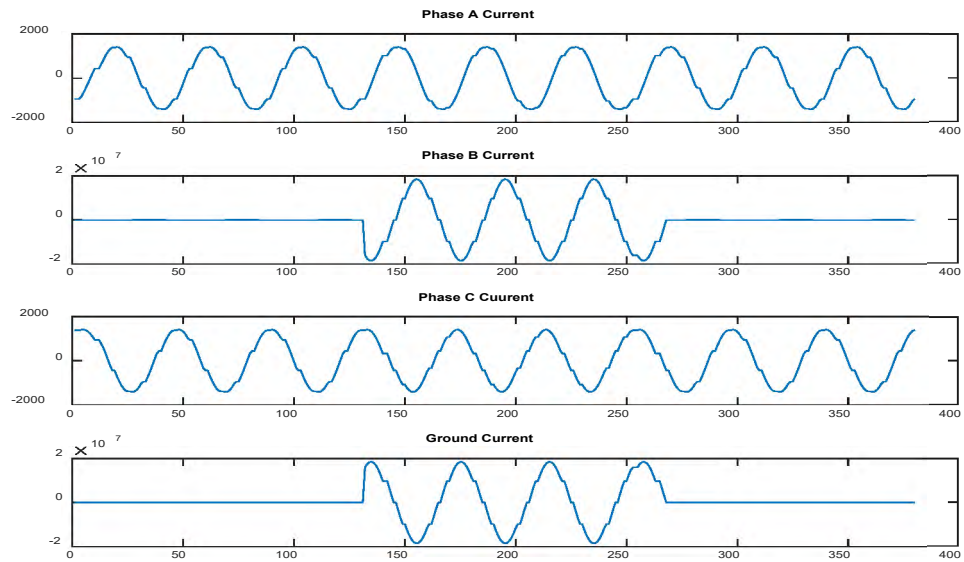


Fig. 6.16 Algorithm single-line-to-ground fault B-G.

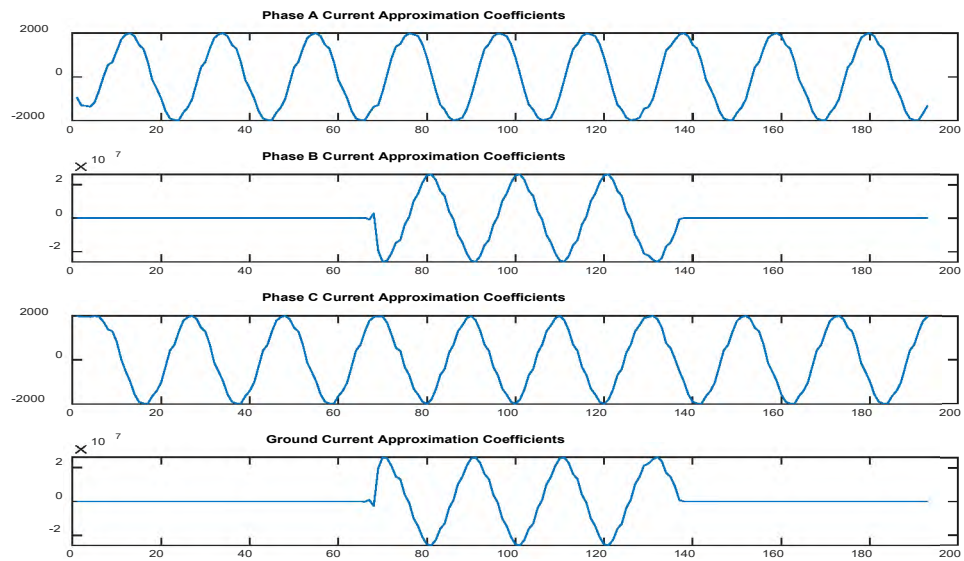


Fig. 6.17 Single-line-to-ground fault B-G currents approximation coefficients db4.

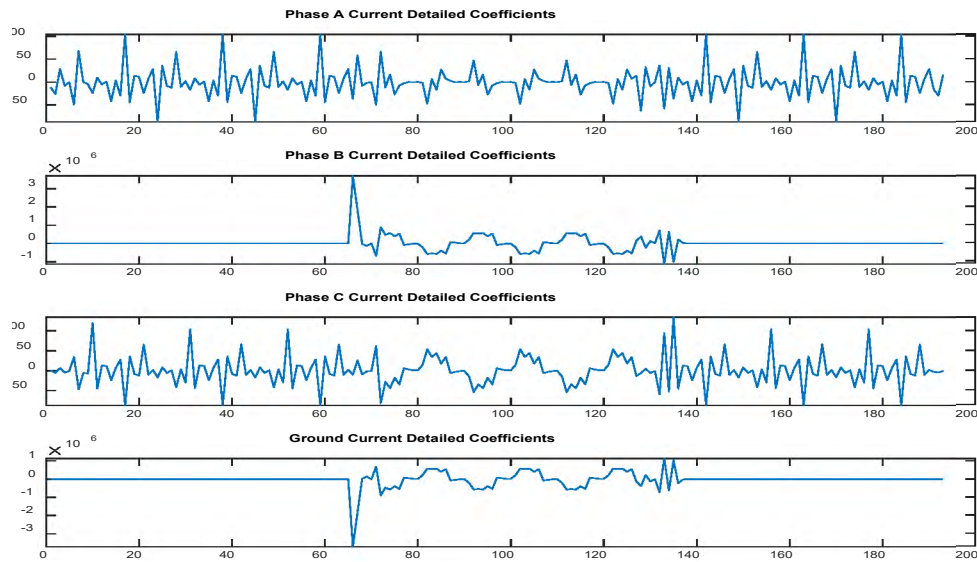


Fig. 6.18 Single-line-to-ground fault B-G currents detailed coefficients db4.

Fig.6.15 and Fig.6.18 revealed the abnormal behavior of the phase B signal and the ground current when the fault introduced. During a fault event, the current in the affected phase experienced an increase, and the maximum value of the detailed coefficients for phase B and ground currents had a very high value. In contrast, phases A and C had a minimal coefficient value. This observation is a similar consistent outcome across all fault types.

Fig. 6.19 Simulink double-line fault A-B currents.

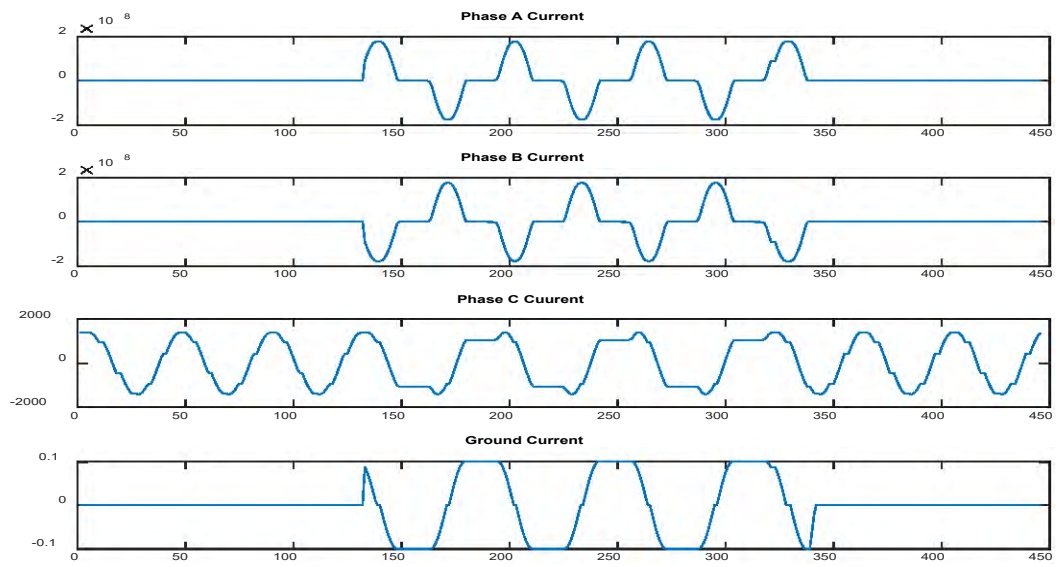


Fig. 6.20 Algorithm double-line fault A-B currents db4.

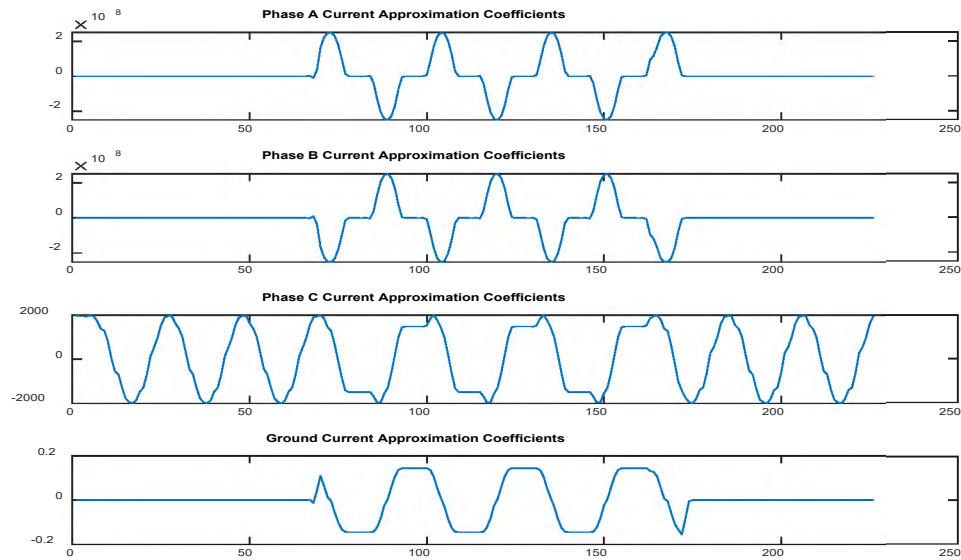


Fig. 21 Double-line fault A-B currents approximation coefficients db4.

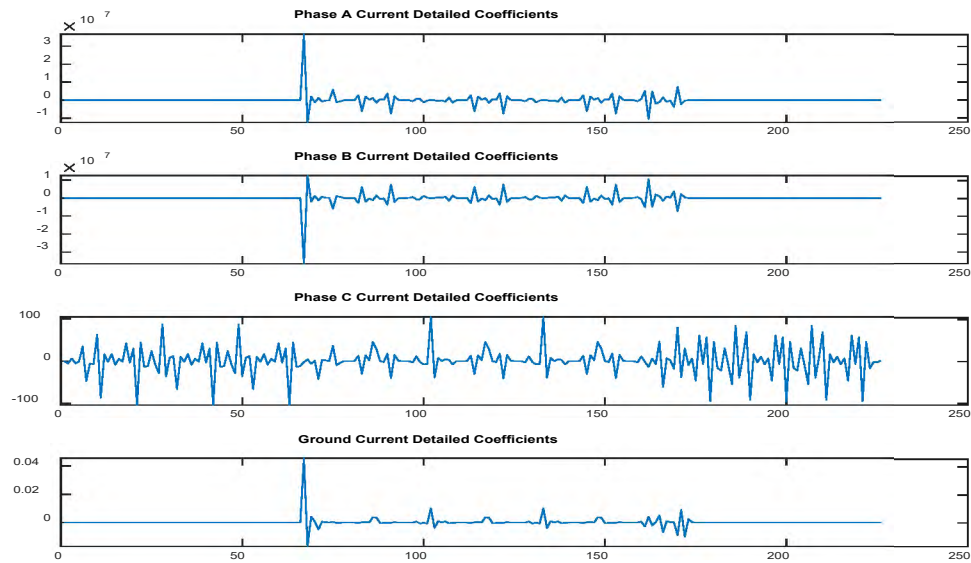


Fig. 22 Double-line Fault A-B currents detailed coefficients db4.

Fig. 6.19 and Fig. 6.22 revealed the abnormal behavior of the phase A and phase B current signals when the fault introduced. During a fault event, the current in the affected phase experienced an increase, and the maximum value of the detailed coefficients for

phase B and ground currents had a very high value. In contrast, phase C and G current had very small coefficient values.

Fig. 6.23 Simulinkdouble-line-to-ground AB-G fault currents.

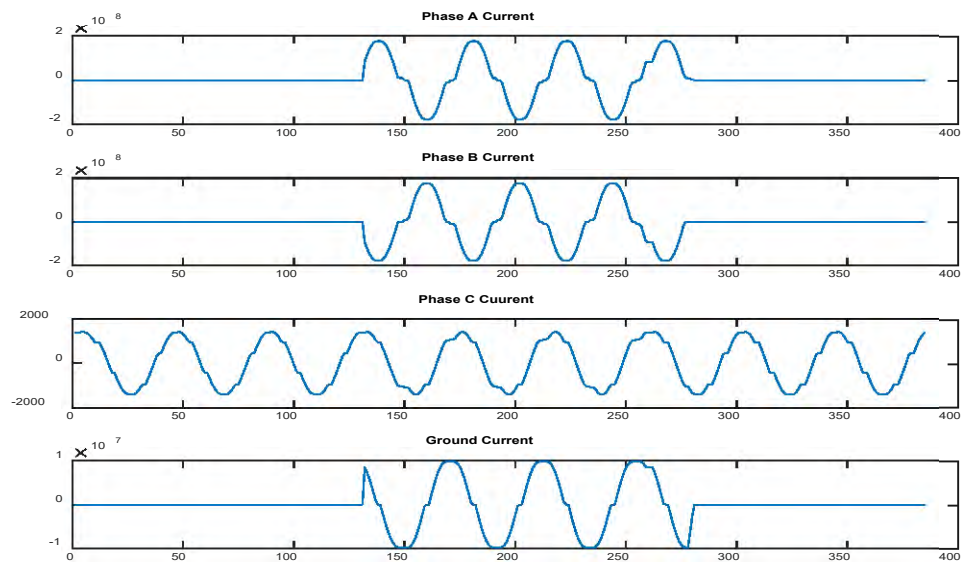


Fig. 6.24 Algorithm double-line-to-ground fault AB-G currents.

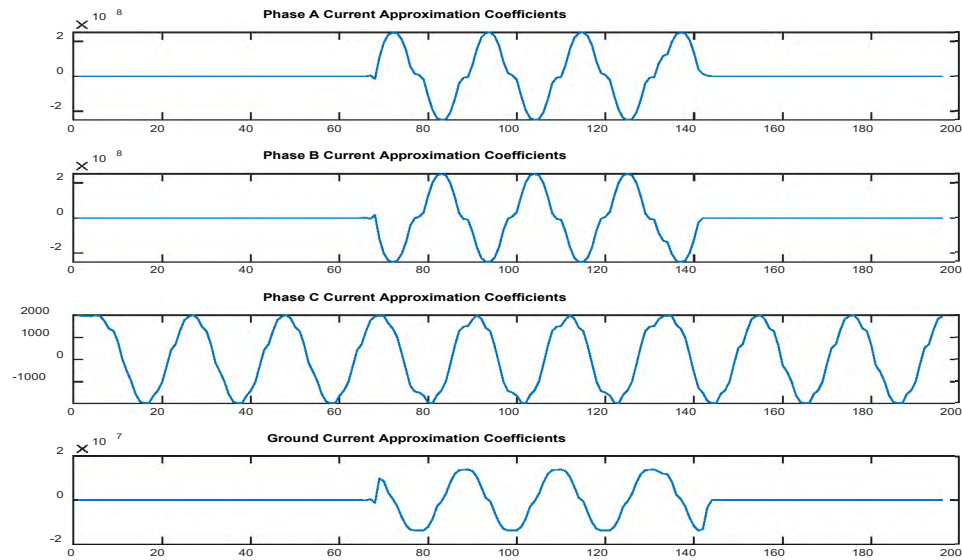


Fig.6.25 Double-line-to-ground fault AB-G currents approximation coefficients db4.

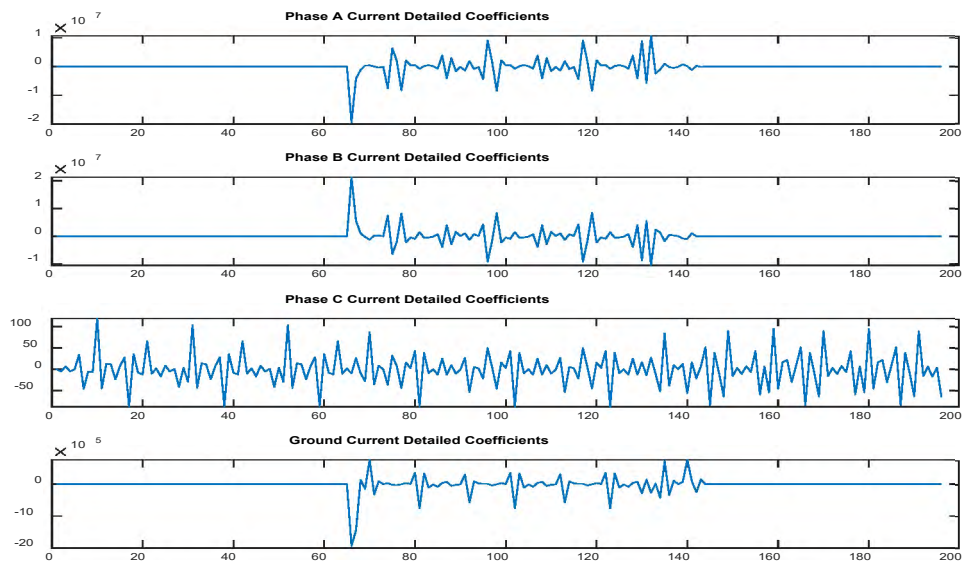


Fig.6.26 Double-line-to-ground fault AB-G currents detailed coefficients db4.

Fig. 6.23 and Fig. 6.26 revealed the abnormal behavior of phase A, phase B, and the ground current signals when the fault was introduced. During a fault event, the current in the affected phase experienced an increase, and the maximum value of the detailed

coefficients for phase A, phase B, and ground currents had a very high value. In contrast, phase C had a very small coefficient value.

Fig. 6.27 Simulink three-phase fault ABC currents.

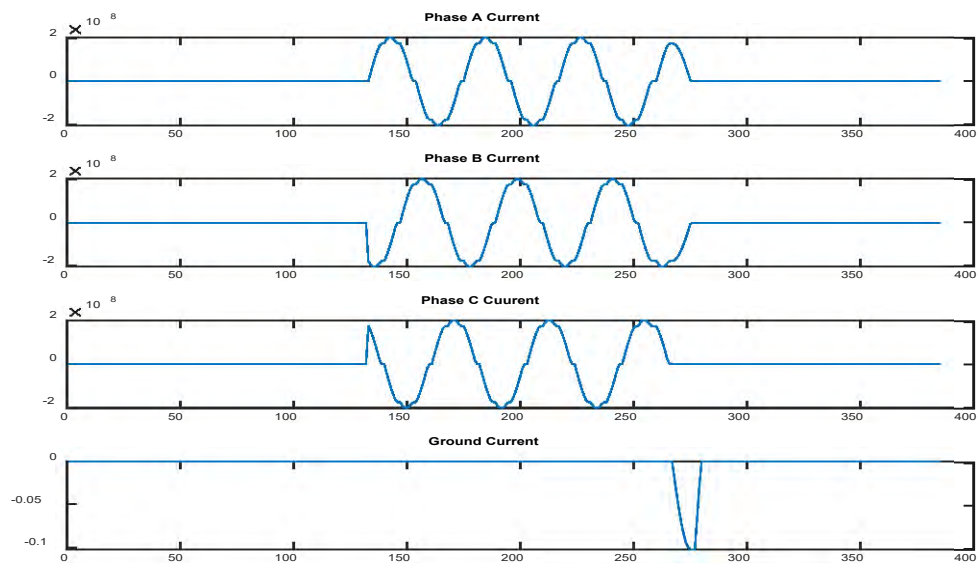


Fig. 6.28 Algorithm three-phase fault ABC currents.

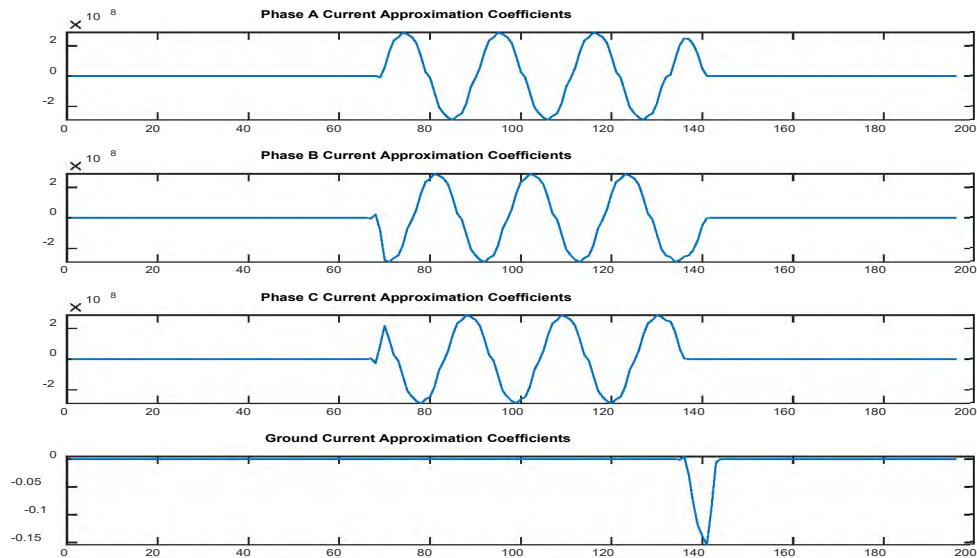


Fig. 6.29 Three-phase fault ABC currents approximation coefficients db4.

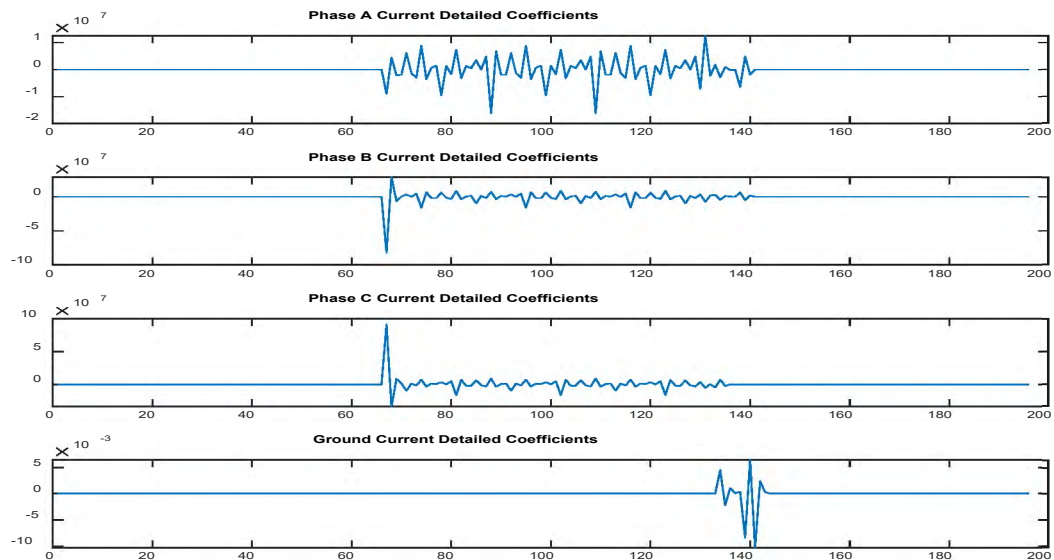


Fig. 6.30 Three-phase fault ABC detailed coefficients db4.

Fig. 6.27 and Fig. 6.30 revealed the abnormal behavior of phase A, phase B, and phase C current signals when the fault was introduced. During a fault event, the current in the affected phase experienced an increase, and the maximum value of the detailed

coefficients for phase A, phase B, and phase C were very high. In contrast, the ground current had a very small coefficient value.

Fig. 6.31 Simulink three-phase-to-ground fault ABC-G currents db4.

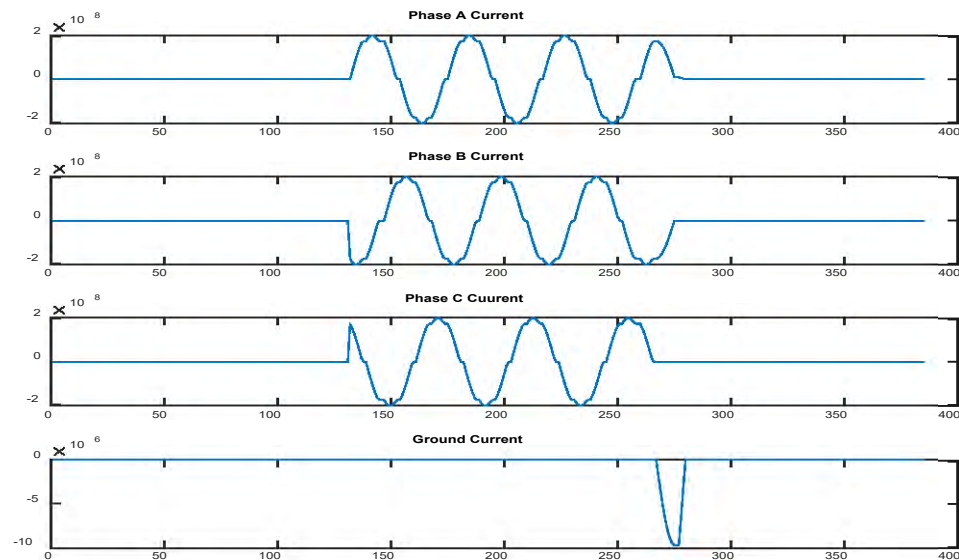


Fig. 6.32 Algorithm three-phase to ground fault ABC-G currents db4.

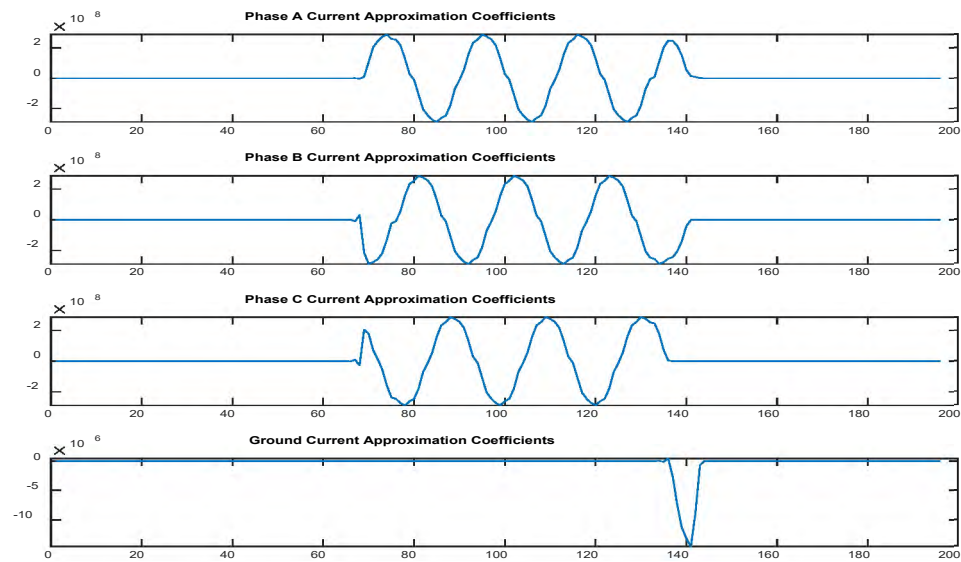


Fig. 6.33 Three-phase-to-ground fault ABC-G currents approximation coefficients db4.

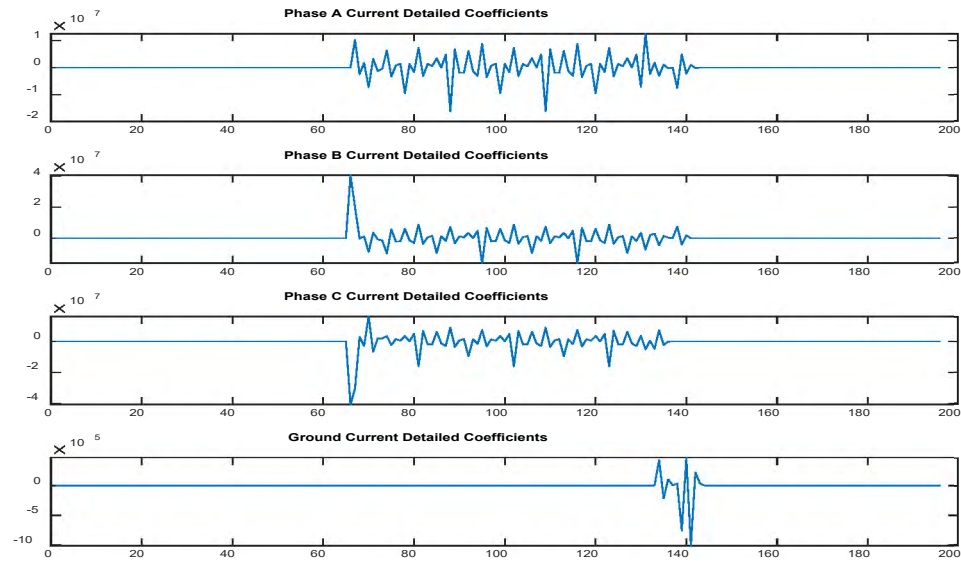


Fig. 6.34 Three-phase-to-ground fault ABC-G currents detailed coefficients db4.

Fig. 6.30 and Fig. 6.34 revealed the abnormal behavior of phase A, phase B, phase C, and the ground current signals when the fault was introduced. During a fault event, the

current in the affected phase experienced an increase, and the maximum value of the detailed coefficients for all phases and the current signals had a very high value.

6.5.2 Wavelet Decomposition and Maximum Detailed Coefficients Process for Haar

The Haar Wavelet selected because of its simplicity, orthogonality, and efficiency in capturing transient features within the signals. The decomposition process achieved using the MATLAB's 'wavedec' command. This command breaks down the input signal into two primary components: the approximation coefficients (CA) and the detailed coefficients (CD). The decomposition process can be at various levels, but we used decomposing at level 1 in this study.

One of the essential parameters we need in our fault detection methodology is the extraction and calculation of detailed coefficients. The detailed coefficients had high frequency and transient components in the signal, which were significant for identifying transient events, such as those caused by different types of faults, including short-circuit faults because the detailed coefficients' magnitude had the information that helped in accurate fault detection and classification.

Then, the MATLAB command `max ()` was applied to determine the maximum value of the detailed coefficients for each current signal in fault and no-fault conditions. These maximum detailed coefficient values then compared against the threshold ($T_d=350$) for identification and fault detection. These maximum detailed coefficient values recorded in a Table. The Table detailing the maximum coefficient values presented in the Results chapter for further analysis, which significantly contributes to these findings and conclusions.

Fig. 6.35 to Fig. 6.38 illustrate the power system's three-phase currents and ground current under normal conditions, including both the approximation and detailed coefficients of the current signals.

Fig. 6.35 Simulink no fault three-phase Currents.

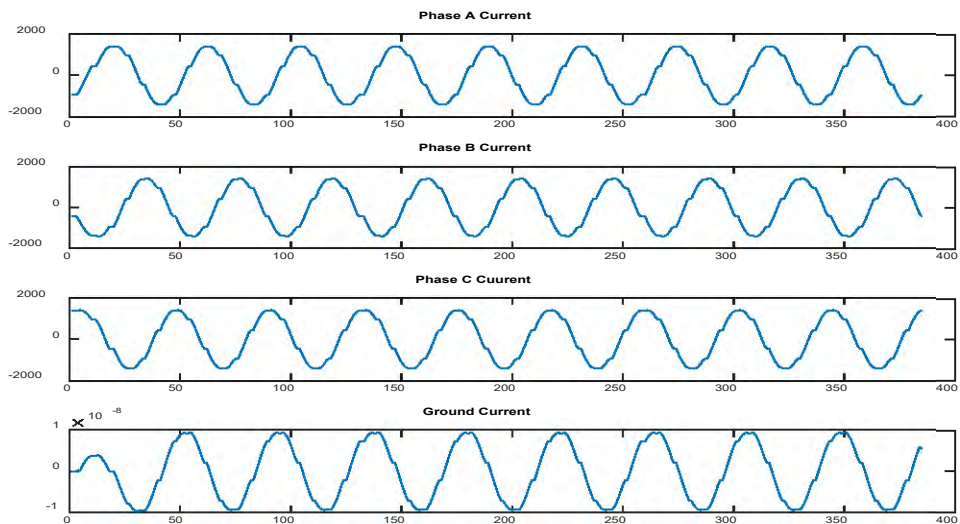


Fig. 6.36 Algorithm no fault three-phase currents.

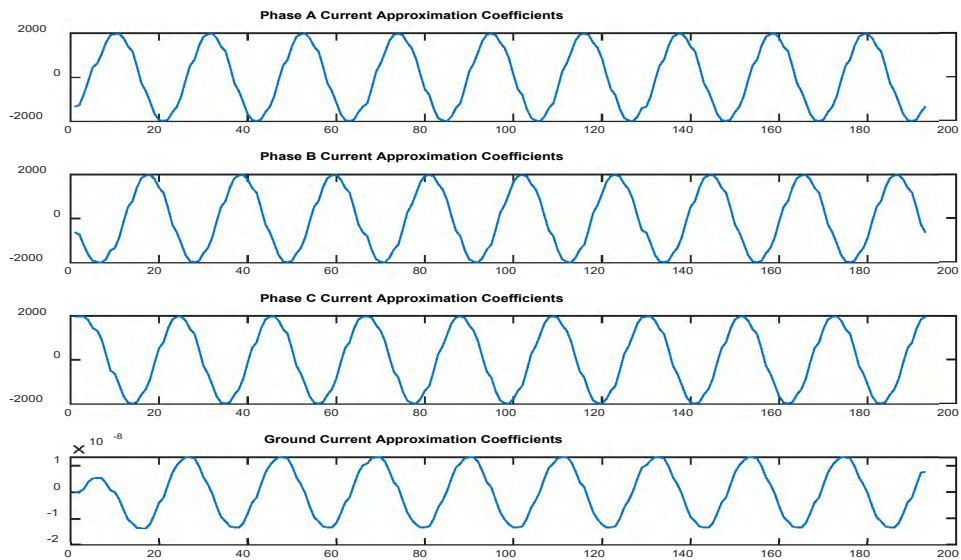


Fig. 6.37 No fault three-phase currents approximation coefficients Haar.

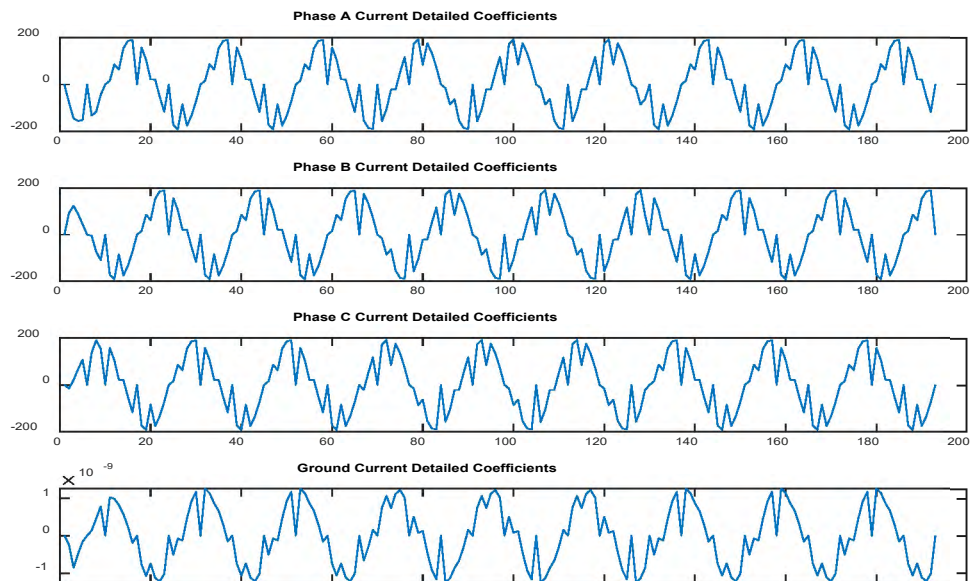


Fig. 6.38 No fault three-phase currents detailed coefficients Haar.

The analysis of Fig. 6.35 to Fig. 6.38 revealed that under normal no-fault conditions, the three-phase current signals for phases A, B, and C and the ground current

remained normal. Similarly, both the approximation and detailed coefficients had a consistent pattern, confirming the no-fault condition of the system. This understanding of the power system behavior with no fault applied serves as a reference point for interpreting the other figures with fault conditions.

Five distinct fault scenarios examined to represent the observations concerning faulty three-phase currents visually. These scenarios included single line-to-ground, double-line, double lines-to-ground, three-phase, and three-phase-to-ground faults. The captured data, including the approximation and detailed coefficients displayed in Fig. 6.39 to Fig. 6.58. The X-axis represents the sample number and the Y-axis represents the amplitude of the coefficients.

Fig. 6.39 Simulink single-line-to-ground B-G fault currents.

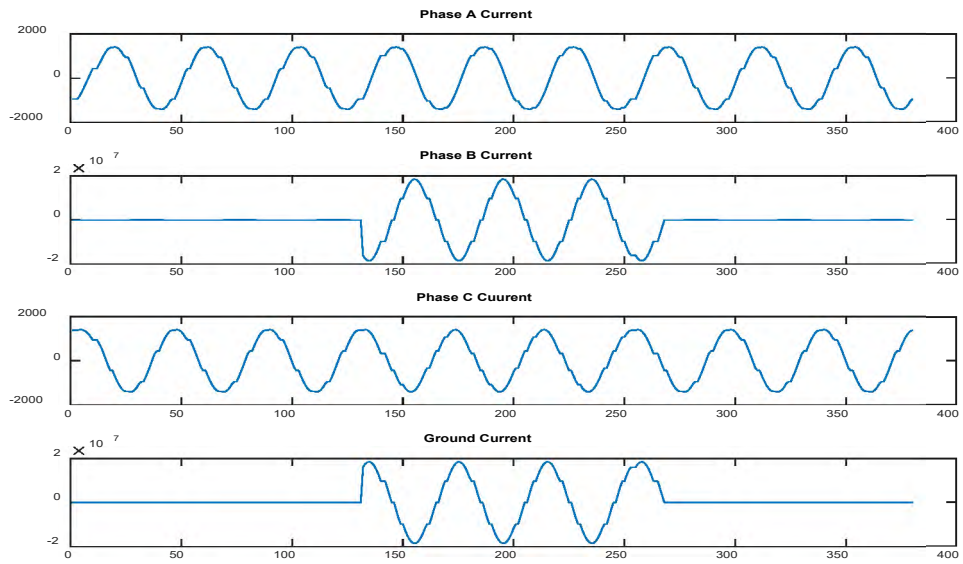


Fig. 6.40 Algorithm single-line-to-ground B-G fault currents.

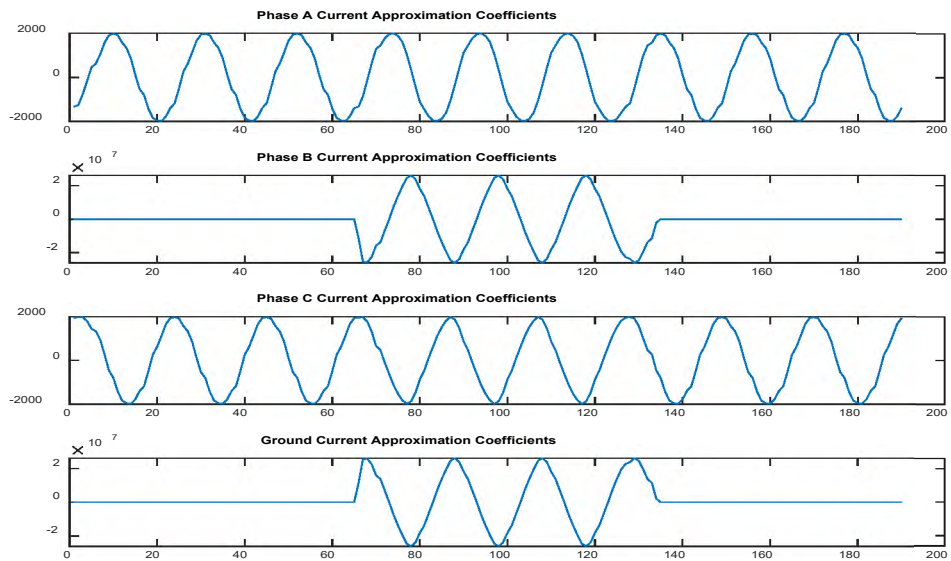


Fig. 6.41 Single-line-to-ground B-G fault currents approximation coefficients Haar.

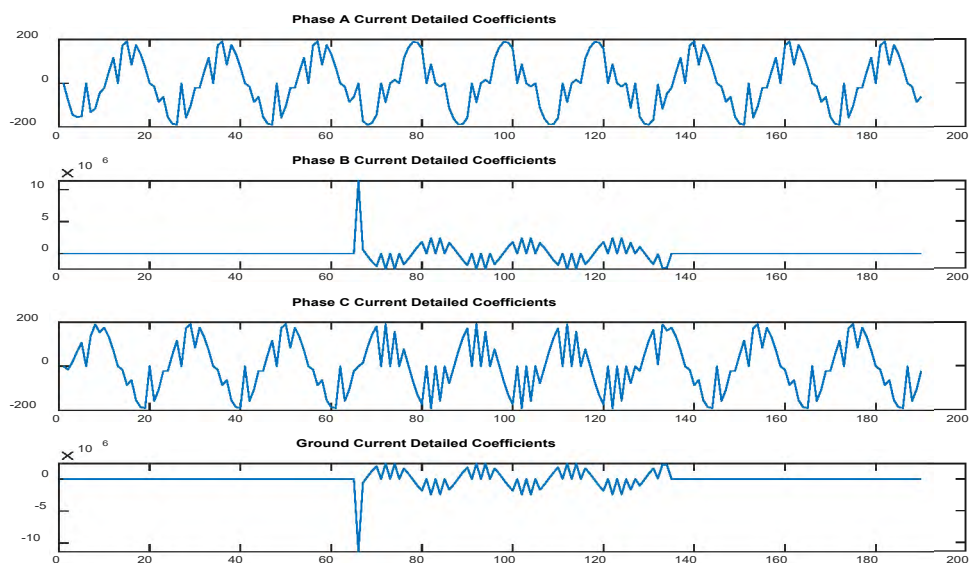


Fig. 6.42 Single-line-to-ground B-G fault currents detailed coefficients Haar.

Fig. 6.39 and Fig. 6.42 revealed the abnormal behavior of the phase B signal and the ground current when the fault introduced. During a fault event, the current in the affected phase experiences an increase, and the maximum value of the detailed coefficients for phase B and ground currents had a very high value. In contrast, phases A and C had a minimal coefficient value.

Fig. 6.43 Simulink double-line-to-ground AB-G fault currents.

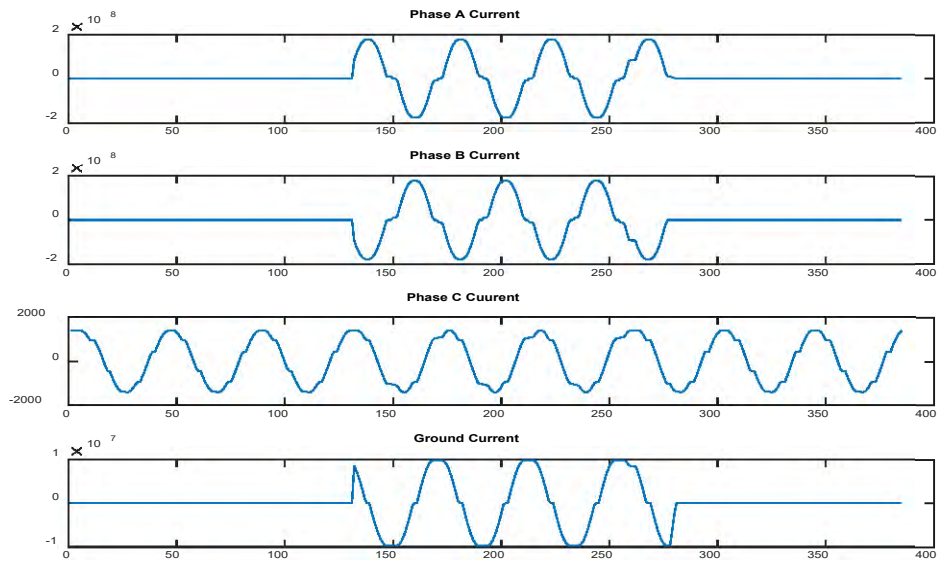


Fig. 6.44 Algorithm double-line-to-ground AB-G fault currents.

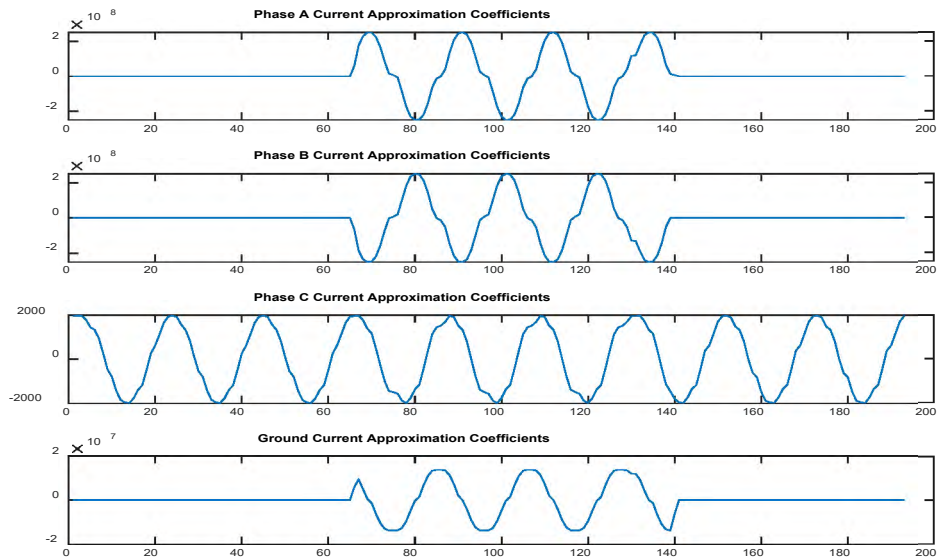


Fig. 6.45 Double-line-to-ground AB-G fault currents approximation coefficients Haar.

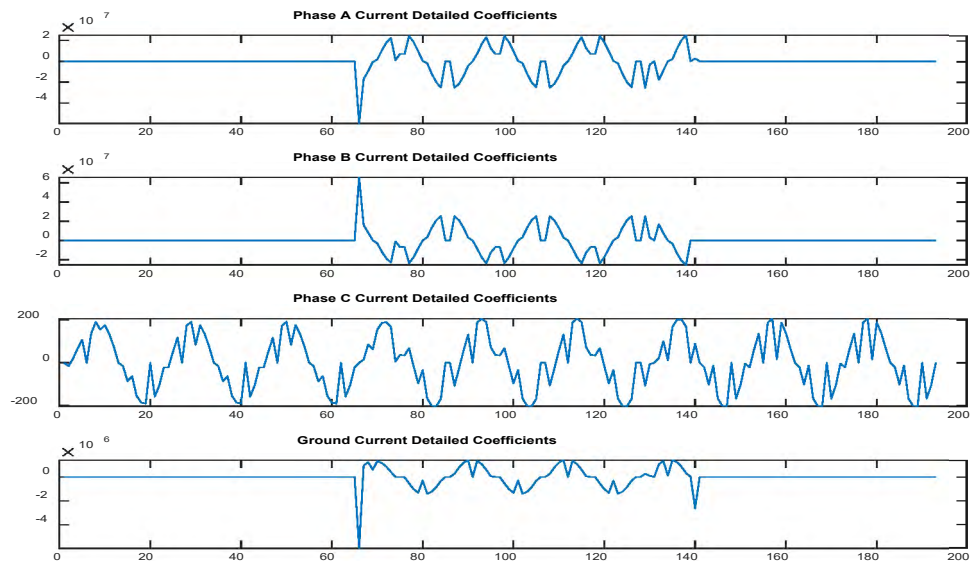


Fig. 6.46 Double-line-to-ground AB-G fault currents detailed coefficients Haar.

Fig. 6.43 and Fig. 6.46 revealed the abnormal behavior of phase A, phase B, and the ground current signals when the fault was introduced. During a fault event, the current in the affected phase experienced an increase, and the maximum value of the detailed

coefficients for phase A, phase B, and ground currents had a very high value. In contrast, phase C had a very small coefficient value.

Fig. 6.47 Simulink double line A-B fault currents.

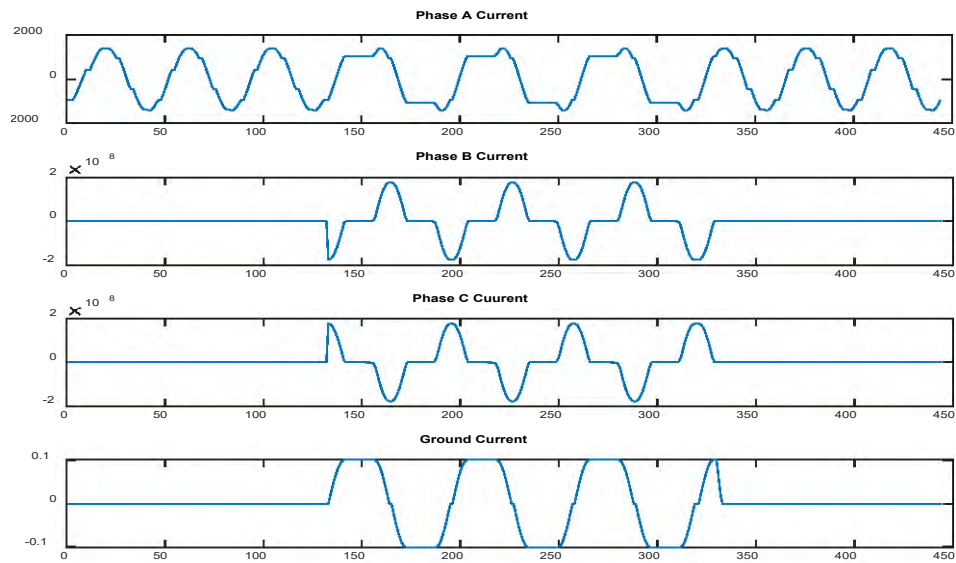


Fig. 6.48 Algorithm double line A-B fault currents.

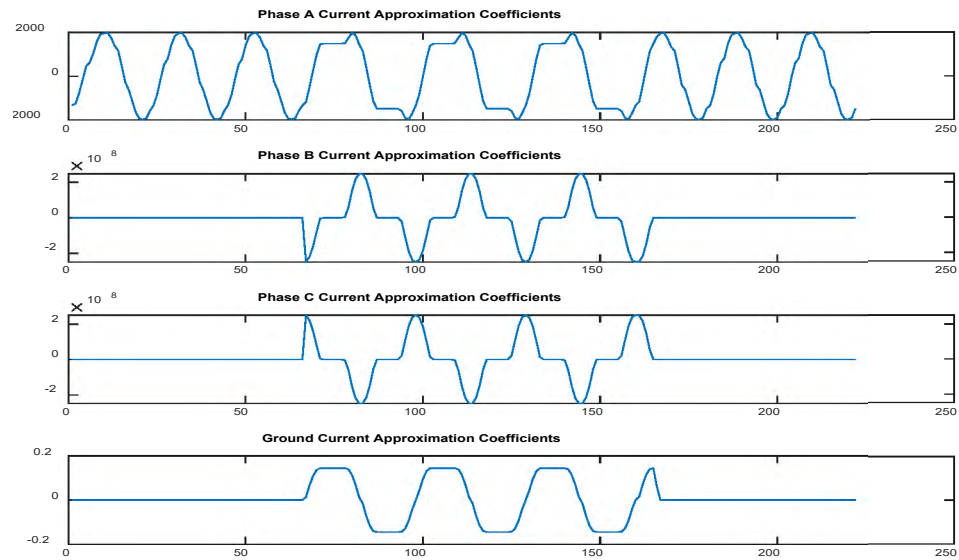


Fig. 6.49 Double line A-B fault currents approximation coefficients Haar.

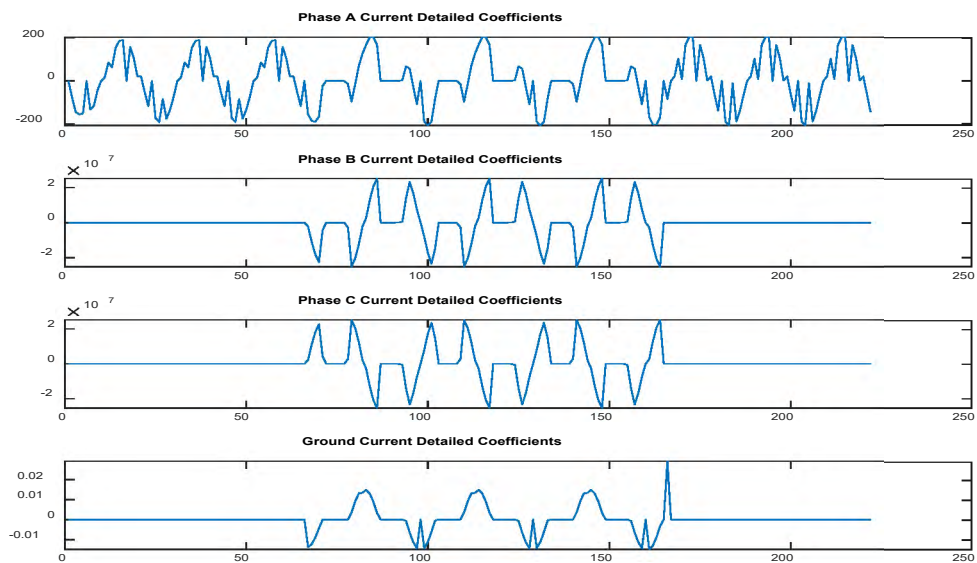


Fig.6.50 Double line A-B fault currents detailed coefficients Haar.

Fig. 6.47 and Fig. 6.50 reveal the abnormal behavior of the phase A and phase B current signals when the fault introduced. During a fault event, the current in the affected phase experienced an increase, and the maximum value of the detailed coefficients for

phase B and ground currents had a very high value. In contrast, phase C and G currents had a very small coefficient value. This is a similar consistent outcome observed across all fault types.

Fig. 6.51 Simulink three-phase ABC fault currents.

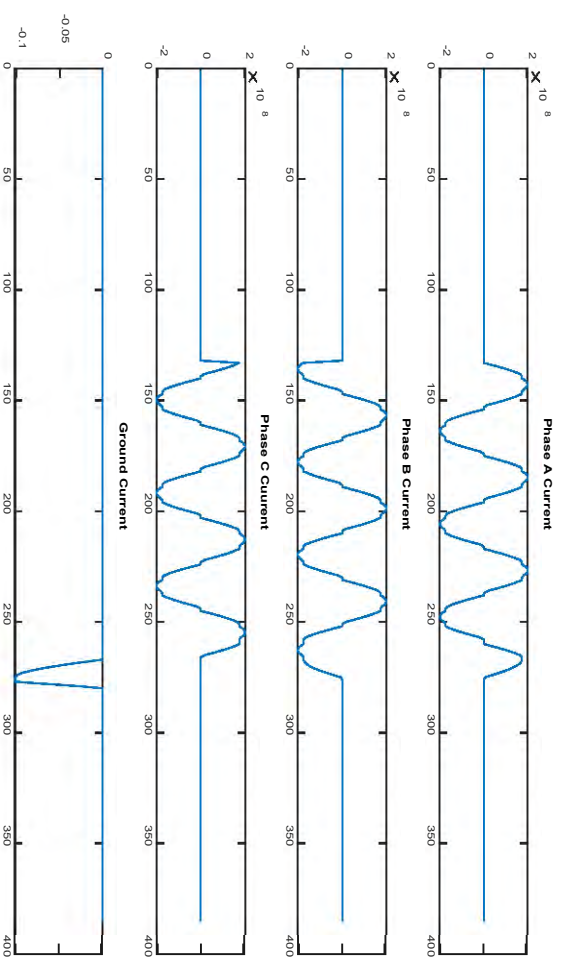


Fig. 6.52 Algorithm three-phase ABC fault currents.

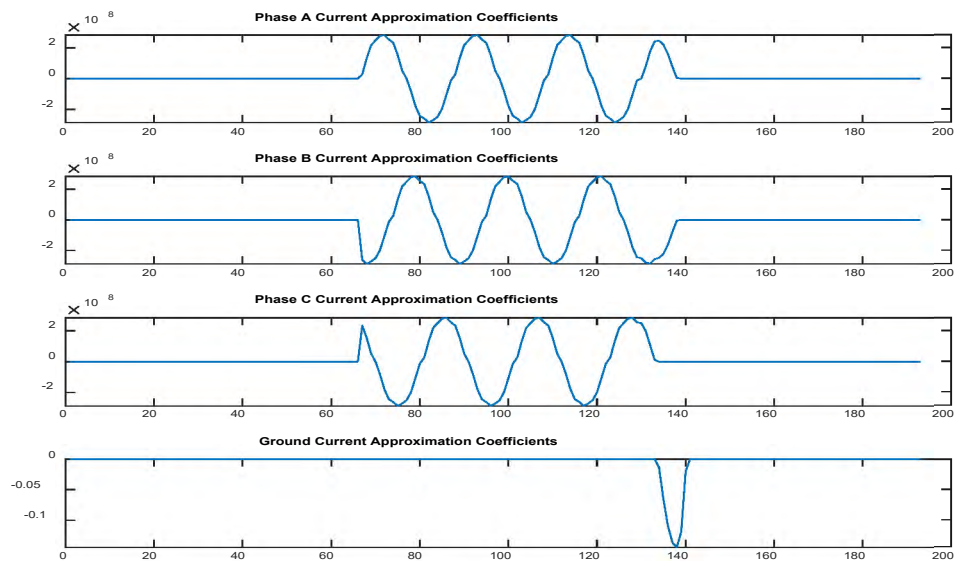


Fig. 6.53 Three-phase ABC fault currents approximation coefficients Haar.

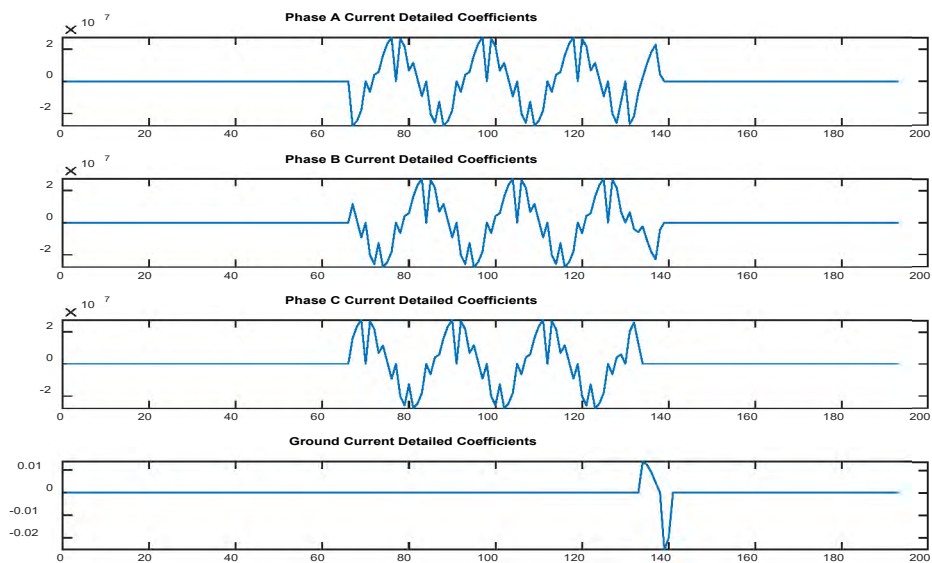


Fig. 6.54 Three-phase ABC fault currents approximation coefficients Haar.

Fig. 6.51 and Fig. 6.54 revealed the abnormal behavior of phase A, phase B, and phase C current signals when the fault is introduced. During a fault event, the current in

the affected phase experienced an increase and the maximum value of the detailed coefficients for phase A, phase B, and phase C were very high. In contrast, the ground current had a very small coefficient value.

Fig. 6.55 Simulink three-phase to ground ABC-G fault currents Haar.

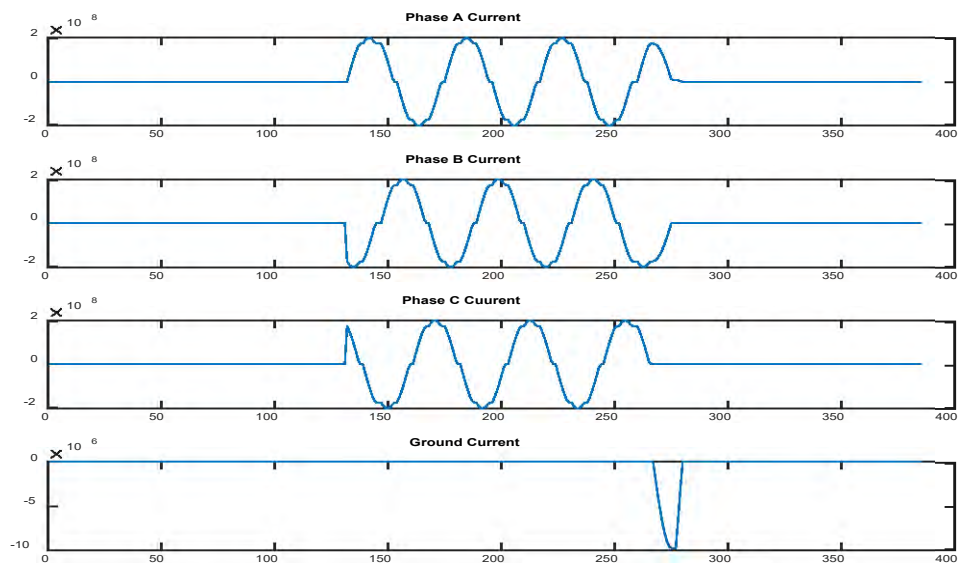


Fig. 6.56 Algorithm three-phase to ground ABC-G fault currents Haar.

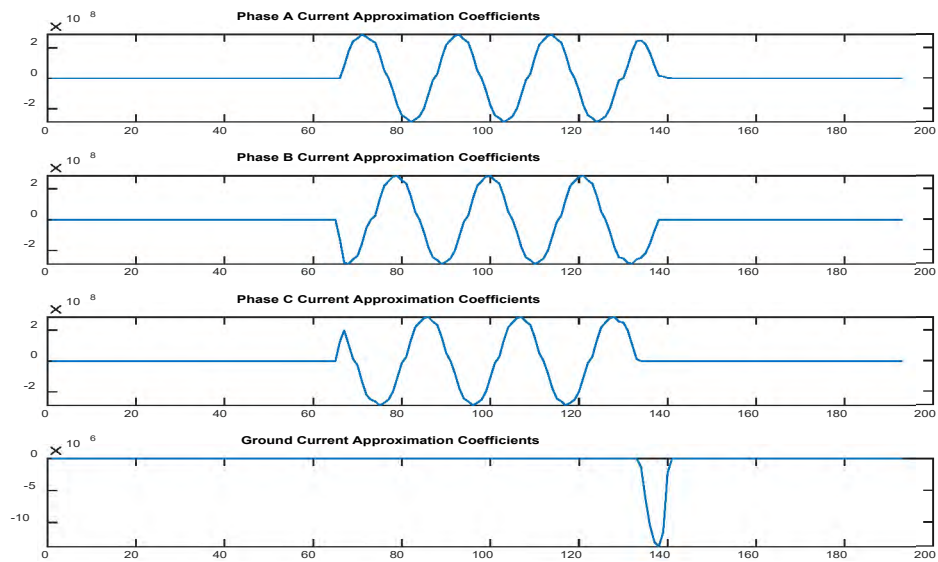


Fig. 6.57 Three-phase-ground ABC-G fault currents approximation coefficients Haar.

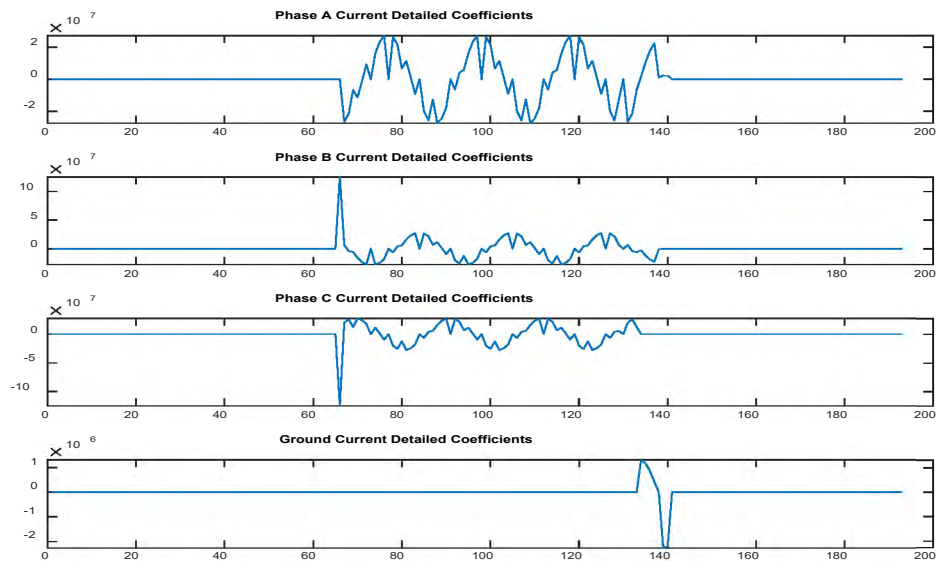


Fig. 6.58 Three-phase-to-ground ABC-G fault currents detailed coefficients Haar.

Fig. 6.55 and Fig. 6.58 revealed the abnormal behavior of phase A, phase B, phase C, and the ground current signals when the fault was introduced. During a fault event, the

current in the affected phase experienced an increase, and the maximum value of the detailed coefficients for all phases and the ground currents had a very high value.

6.5.3 Wavelet Decomposition and Maximum Detailed Coefficients Process for sym5

The Symlet 5 (sym5) Wavelet selected because of its versatility and effectiveness in capturing transient features and transient disturbances within the signals. The decomposition process achieved using the MATLAB's 'wavedec' command. This command breaks down the input signal into two primary components: approximation and detailed coefficients. The decomposition process can be at various levels, but we used decomposing at level 1 in this study.

One of the essential parameters we needed in this fault detection methodology was the extraction and calculation of detailed coefficients. The detailed coefficients had high frequency and transient components in the signal, which were significant for identifying transient events, such as those caused by different types of faults, including short-circuit faults because the detailed coefficients' magnitude had the information that helped in accurate fault detection and classification.

Then, the MATLAB command `max ()` was applied to determine the maximum value of the detailed coefficients for each current signal in fault and no-fault conditions. These maximum detailed coefficient values were then compared against the threshold ($T_d=350$) for fault detection and identification. These maximum detailed coefficient values recorded in a Table. The Table detailing the maximum coefficient values presented in the Results chapter for further analysis, significantly contributing to these findings and conclusions.

Fig. 6.59 to Fig. 6.62 illustrates the three-phase currents and the ground current of the power system under normal conditions, including both the approximation coefficients and the detailed coefficients of the current signals. The X-axis represents the sample number and the Y-axis represents the coefficients amplitude.

Fig. 6.59 Simulink no-fault three-phase currents.

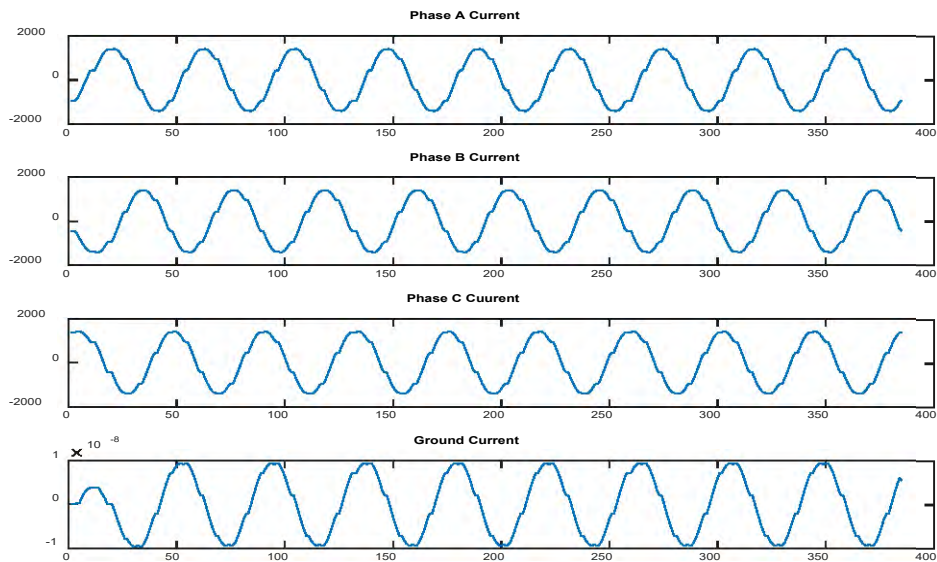


Fig. 6.60 Algorithm no-fault three-phase currents.

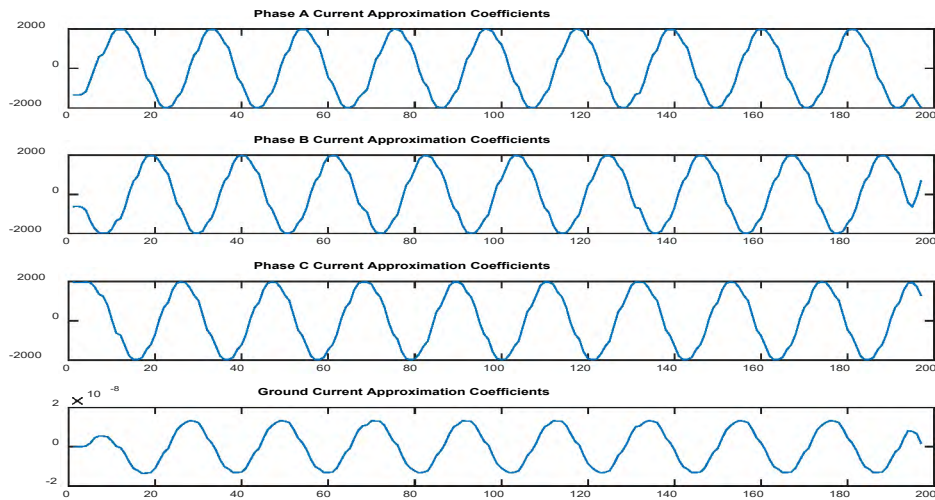


Fig. 6.61 No-fault three-phase currents approximation coefficients sym5.

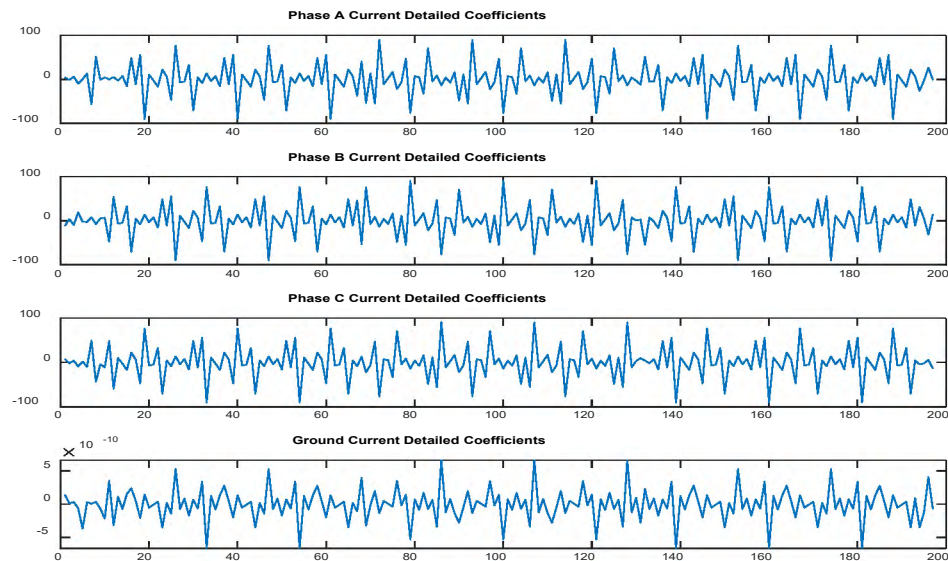


Fig. 6.62 No-fault three-phase currents approximation coefficients sym5.

The analyses of Fig. 6.59 to Fig. 6.62 revealed that under normal no-fault conditions, the three-phase current signals for phases A, B, and C and the ground current

remained normal. Similarly, both the approximation and detailed coefficients had a consistent pattern, confirming the no-fault condition of the system. This understanding of the power system behavior with no fault applied serves as a reference point for interpreting the other figures with fault conditions.

Five distinct fault scenarios examined to represent the observations concerning faulty three-phase currents visually. These scenarios included single line-to-ground, double-line, double lines-to-ground, three-phase, and three-phase-to-ground faults. The captured data, including the approximation and detailed coefficients displayed in Fig. 6.62 to Fig. 6.81.

Fig. 6.62 Simulink single-line-to- ground B-G fault currents sym5.

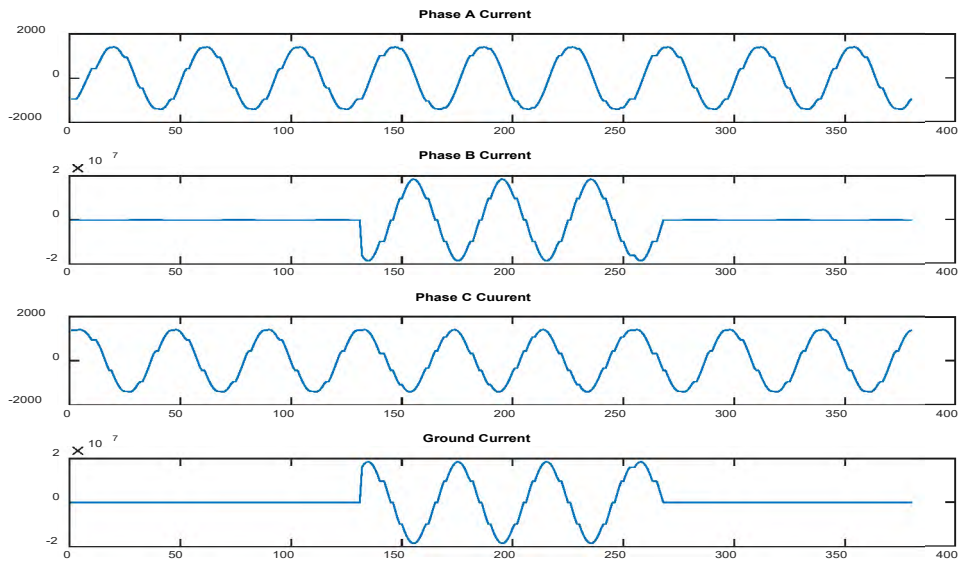


Fig. 6.63 Algorithm single-line-to- ground B-G fault sym5.

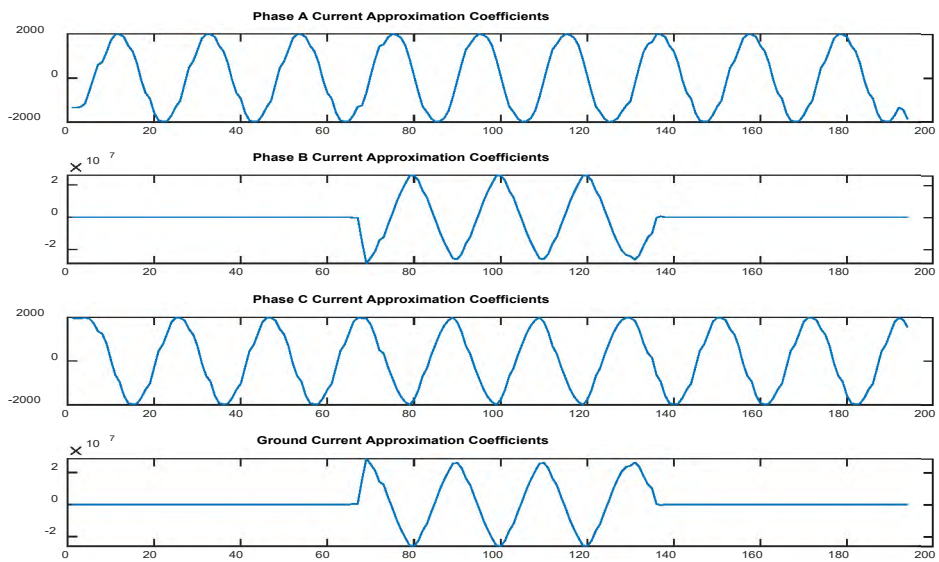


Fig. 6.64 Single-line-to-ground BG fault currents approximation coefficients sym5.

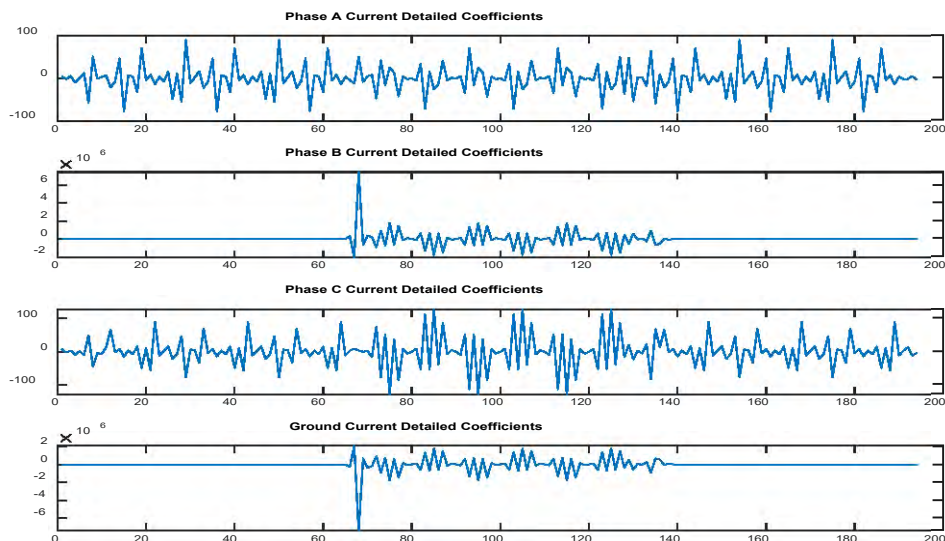


Fig. 6.65 Single-line-to-ground B-G fault currents detailed coefficients sym5.

Fig. 6.62 and Fig. 6.65 revealed the abnormal behavior of the phase B signal and the ground current when the fault introduced. During a fault event, the current in the affected phase experienced an increase, and the maximum value of the detailed coefficients for phase B and ground currents had a very high value. In contrast, phases A and C had a minimal coefficient value.

Fig. 6.66 Simulink double-line-to-ground AB-G fault currents sym5.

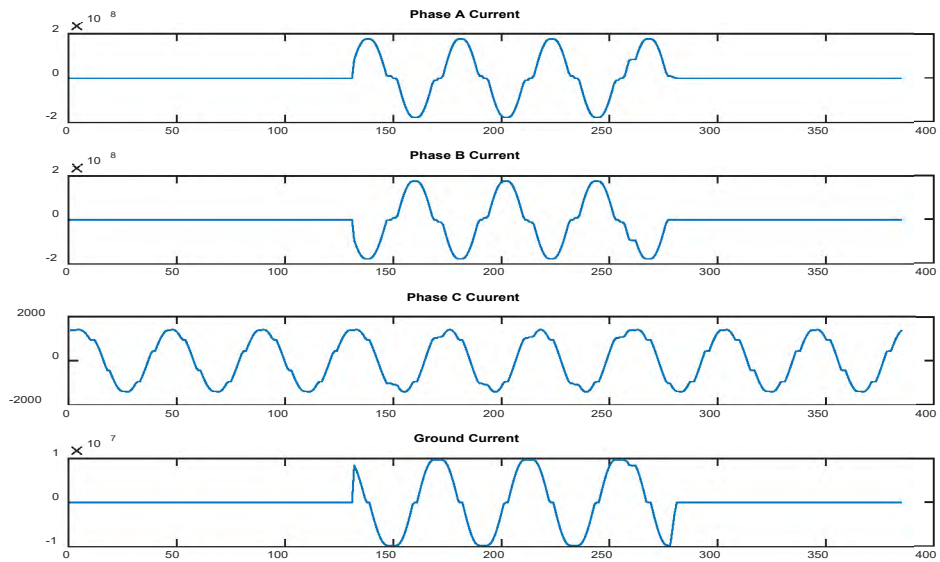


Fig. 6.67 Algorithm double-line-to-ground AB-G fault currents sym5.

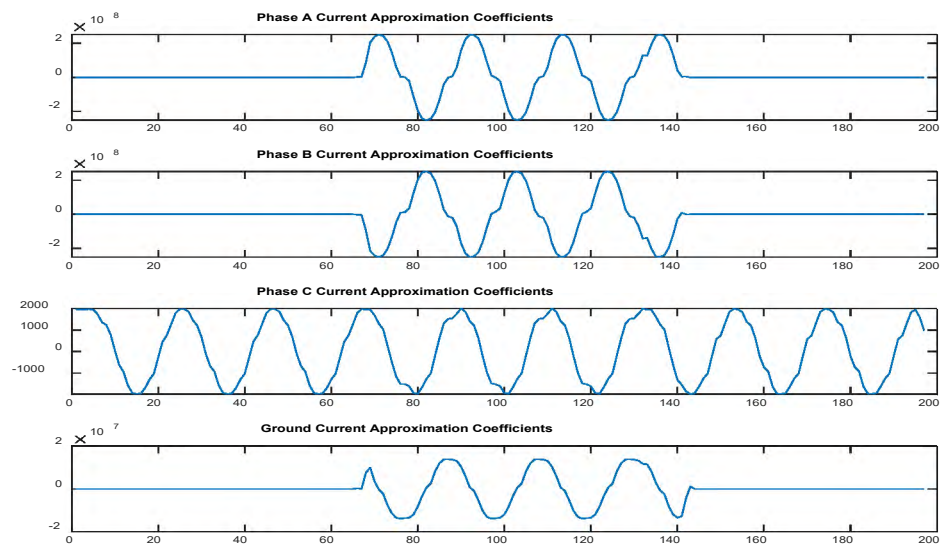


Fig. 6.68 Double-line-to-ground AB-G fault currents approximation coefficients sym5.

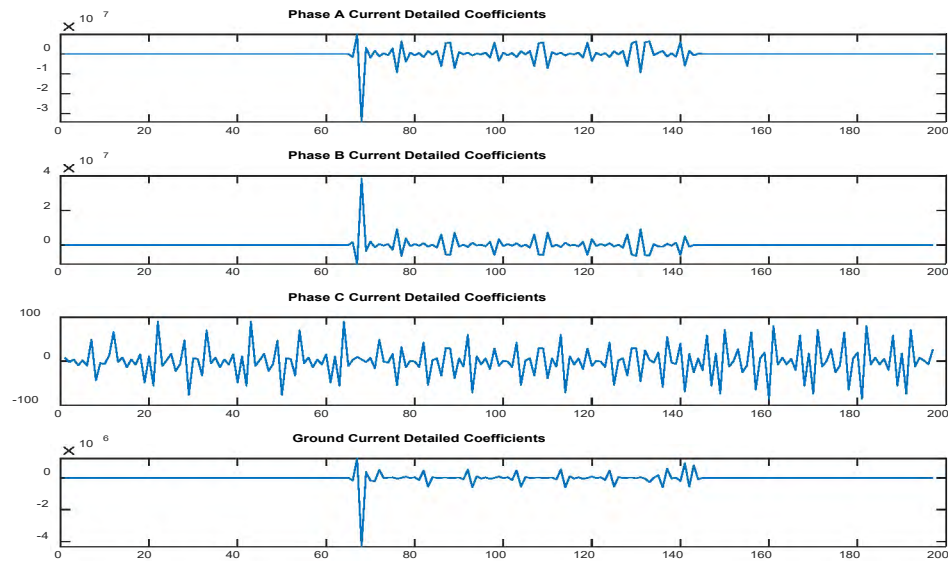


Fig. 6.69 Double-line-to-ground AB-G fault currents detailed coefficients sym5.

Fig. 6.66 and Fig. 6.69 revealed the abnormal behavior of phase A, phase B, and the ground current signals when the fault introduced. During a fault event, the current in the affected phase experienced an increase, and the maximum value of the detailed coefficients for phase A, phase B, and ground currents had a very high value. In contrast, phase C had a very small coefficient value.

Fig. 6.70 Simulink double-line B-C fault currents sym5.

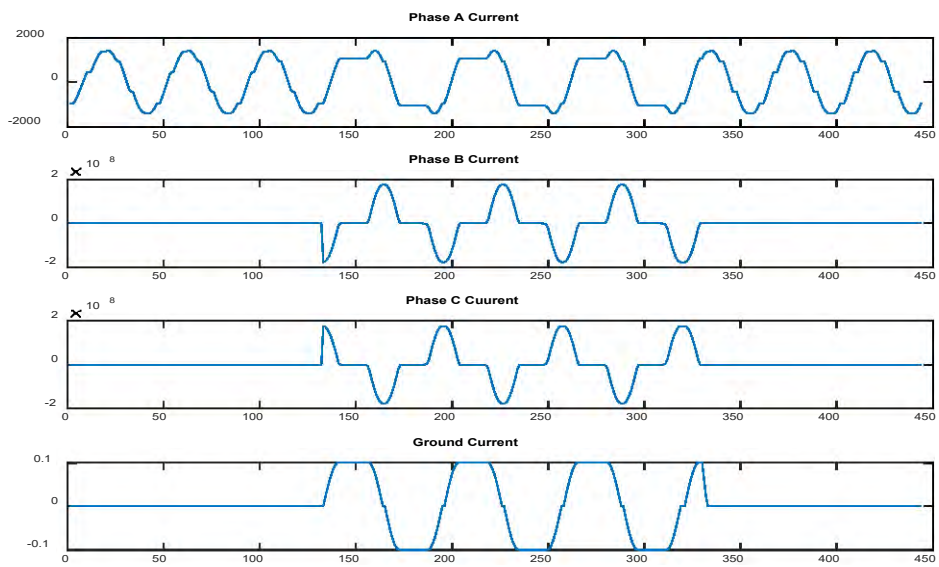


Fig. 6.71 Algorithm double-line B-C fault currents sym5.

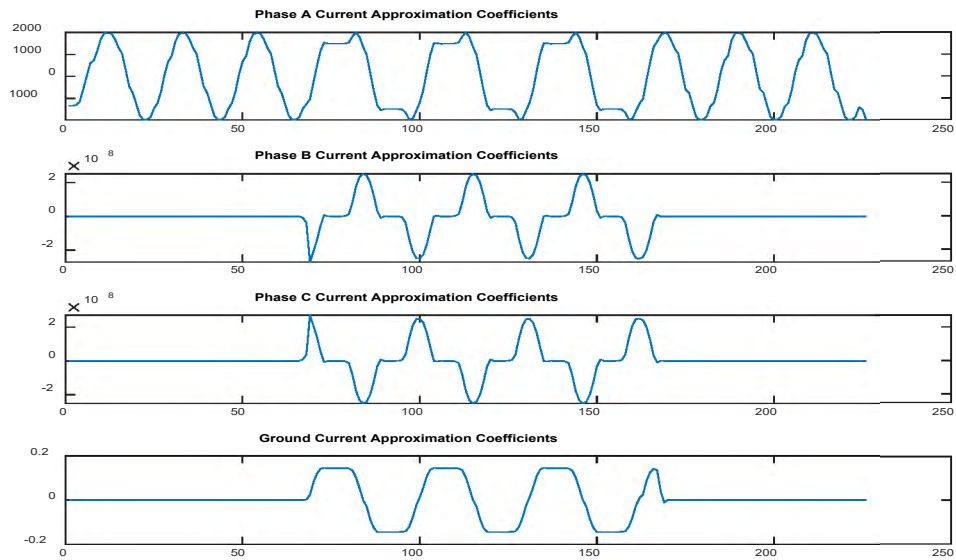


Fig. 6.72 Double-line B-C fault currents approximation coefficients sym5.

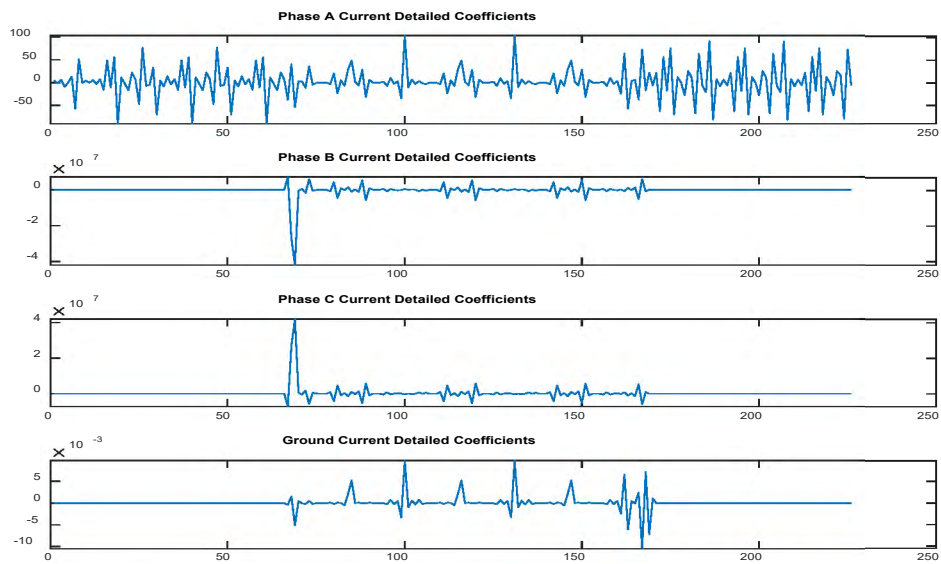


Fig. 6.73 Double-line B-C fault currents detailed coefficients sym5.

Fig. 6.70 and Fig. 6.73 revealed the abnormal behavior of the phase A and phase B current signals when the fault introduced. During a fault event, the current in the affected

phase experienced an increase, and the maximum value of the detailed coefficients for phase B and ground currents had a very high value. In contrast, phase C and G currents had very small coefficient values.

Fig. 6.74 Simulink three-phase ABC fault currents sym5.

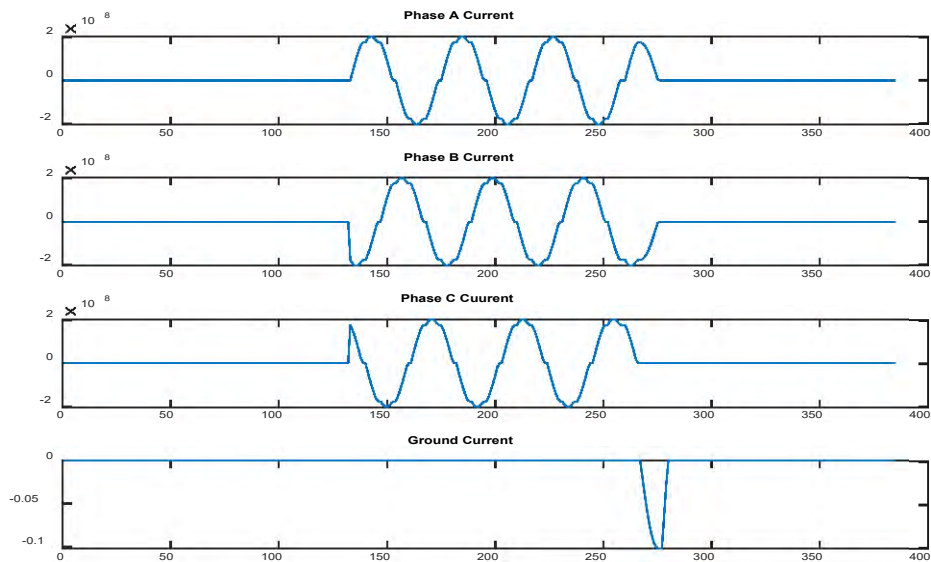


Fig. 6.75 Algorithm three-phase ABC fault currents sym5.

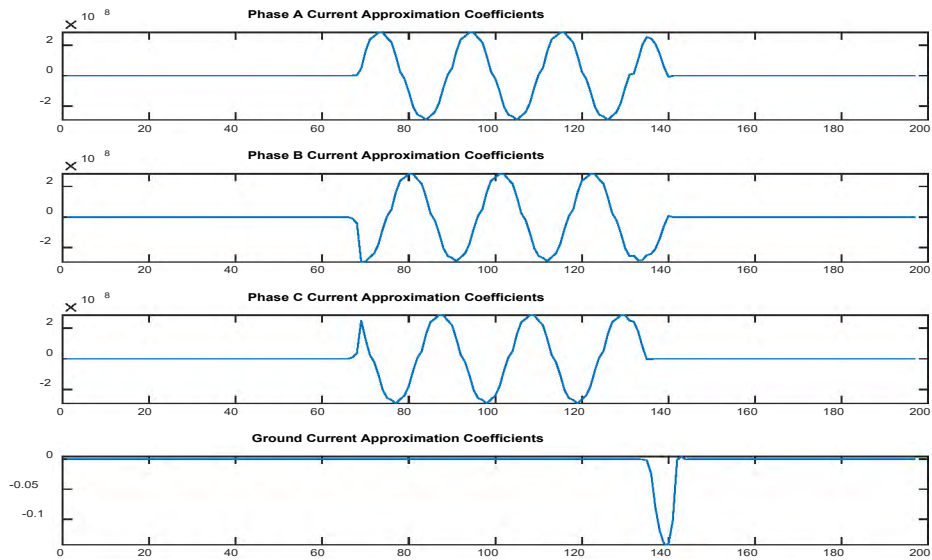


Fig. 6.76 Three-phase ABC fault currents approximation coefficients sym5.

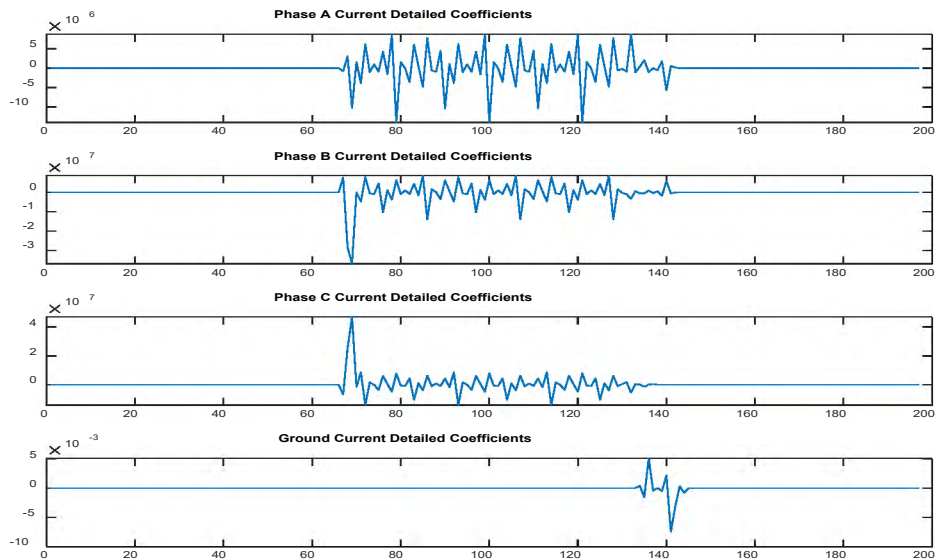


Fig. 6.77 Three-phase ABC fault currents detailed coefficients sym5.

Fig. 6.74 and Fig. 6.77 revealed the abnormal behavior of phase A, B, and C current signals when the fault introduced. During a fault event, the current in the affected phase experienced an increase, and the maximum value of the detailed coefficients for phase A,

phase B, and phase C were very high. In contrast, the ground current had a very small coefficient value.

Fig. 6.78 Simulink three-phase to ground ABC-G fault currents sym5.

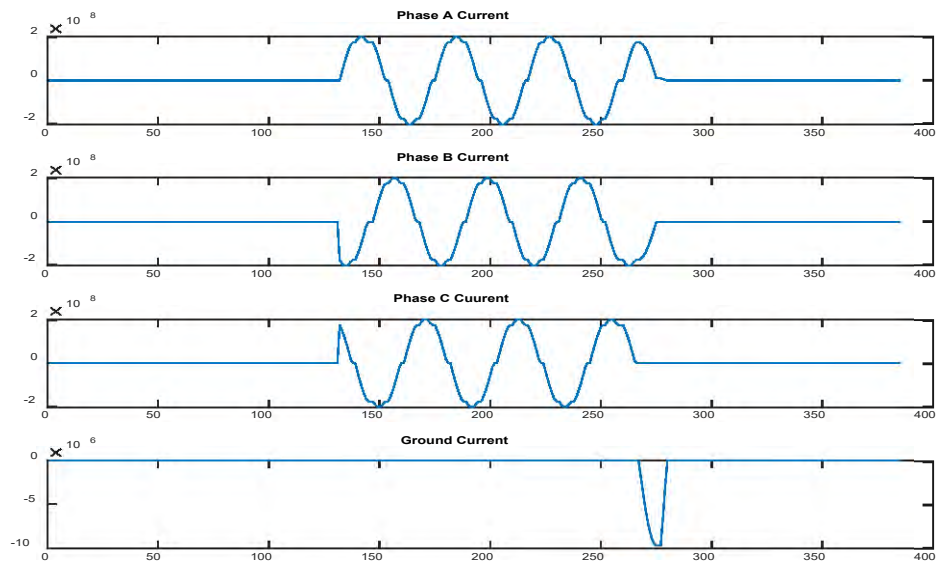


Fig. 6.79 Algorithm three-phase to ground ABC-G fault currents sym5.

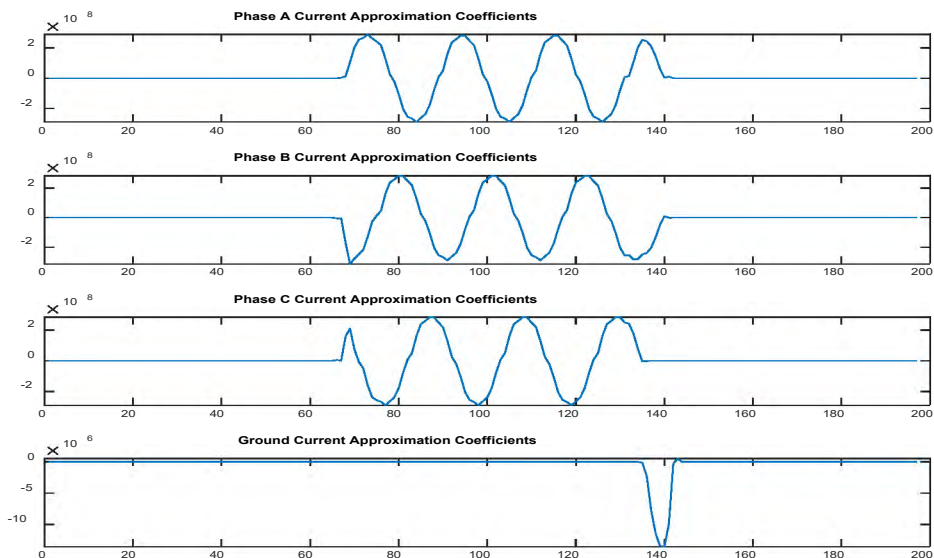


Fig. 6.80 Three-phase-to-ground ABC-G currents approximation coefficients sym5.

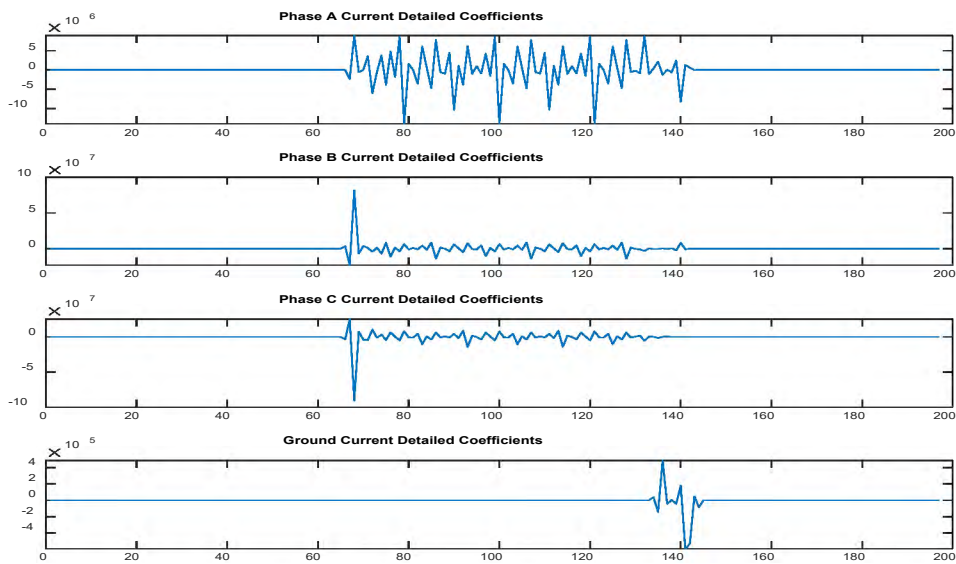


Fig. 6.81 Three-phase-to-ground ABC-G fault currents detailed coefficients sym5.

Fig. 6.78 and Fig. 6.81 revealed the abnormal behavior of phase A, phase B, phase C, and the ground current signals when the fault introduced. During a fault event, the

current in the affected phase experienced an increase, and the maximum value of the detailed coefficients for all phases and the current signals had very high values.

6.5.4 Wavelet Decomposition and Maximum Detailed Coefficients Process for DAM

The Discrete Approximation Meyer (DAM) Wavelet selected because of its localization and suitability in capturing transient features and transient disturbances within the signals. The decomposition process achieved using the MATLAB's 'wavedec' command. This command breaks down the input signal into two primary components: approximation and detailed coefficients. The decomposition process can be at various levels, but we used decomposing at level 1 in this study.

One of the essential parameters we needed in this fault detection methodology was the extraction and calculation of detailed coefficients. The detailed coefficients had high frequency and transient components in the signal, which were significant for identifying transient events, such as those caused by different types of faults, including short-circuit faults because the detailed coefficients' magnitude had the information that helped in accurate fault detection and classification.

Then, the MATLAB command `max ()` was applied to determine the maximum value of the detailed coefficients for each current signal in fault and no-fault conditions. These maximum detailed coefficient values were then compared against the threshold ($T_d=350$) for identification and fault detection. These maximum detailed coefficient values recorded in a Table. The Table detailing the maximum coefficient values presented in the Results chapter for further analysis, significantly contributing to these findings and conclusions.

Fig. 6.82 to Fig. 6.85 illustrates the three-phase currents and the ground current of the power system under normal conditions, including the approximation coefficients and the detailed coefficients of the current signals. The X-axis represents the sample number and the Y-axis represents the coefficients amplitude.

Fig. 6.82 Simulink no-fault three-phase currents.

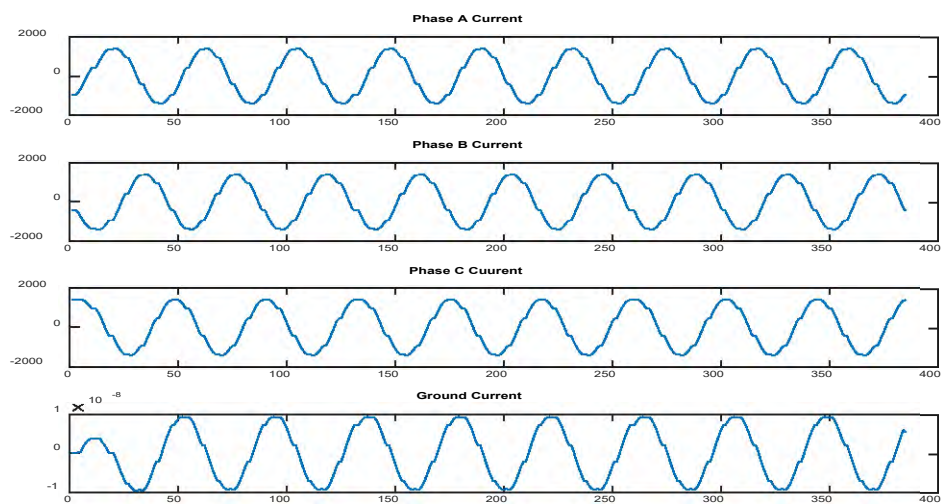


Fig. 6.83 Algorithm no-fault three-phase currents.

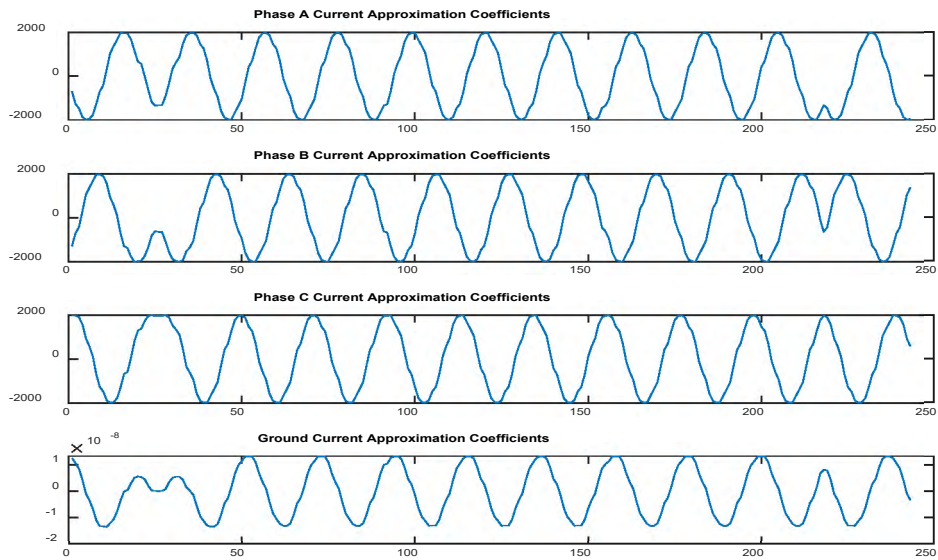


Fig. 6.84 No-fault currents approximation coefficients DAM.

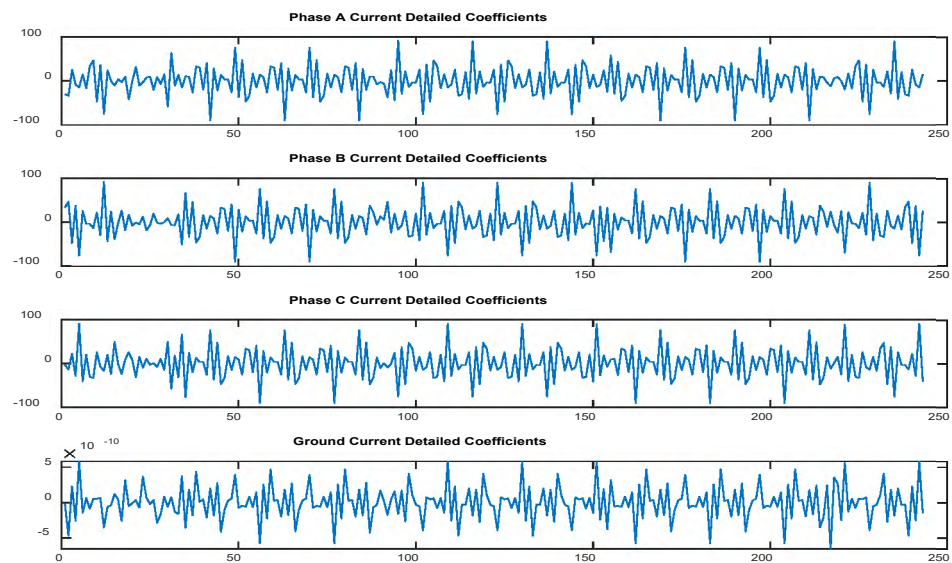


Fig. 6.85 No-fault currents detailed coefficients DAM.

The analyses of Fig. 6.82 to Fig. 6.85 revealed that under normal no-fault conditions, the three-phase current signals for phases A, B, and C and the ground current remained normal. Similarly, both the approximation and detailed coefficients had a

consistent pattern, confirming the no-fault condition of the system. This understanding of the power system behavior with no fault applied serves as a reference point for interpreting the other figures with fault conditions.

Five distinct fault scenarios examined to represent the observations concerning faulty three-phase currents visually. These scenarios included single line-to-ground, double-line, double lines-to-ground, three-phase, and three-phase-to-ground faults. The captured data, including the approximation and detailed coefficients displayed in Fig. 6.86 to Fig. 6.105.

Fig. 6.86 Simulink single-line-to-ground B-G fault currents DAM.

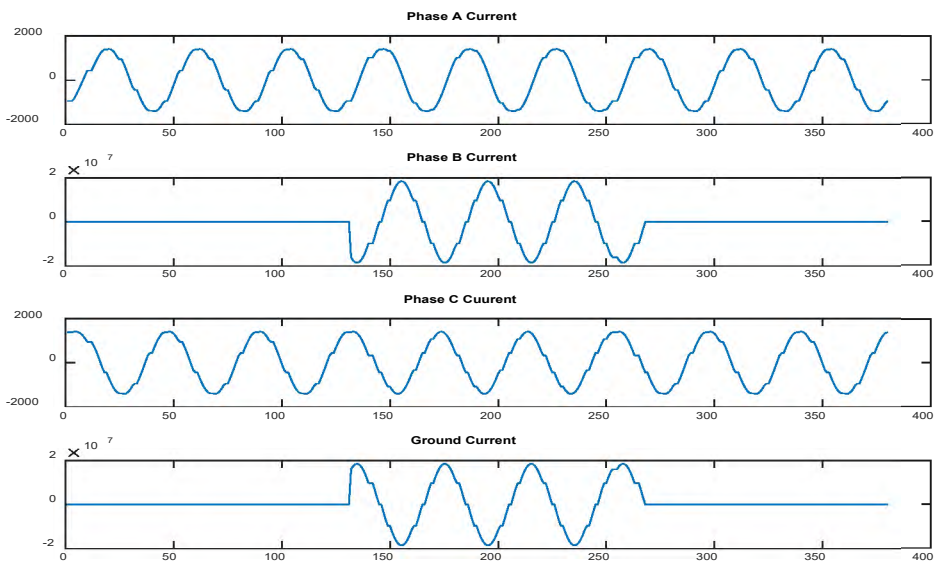


Fig. 6.87 Algorithm single-line-to-ground B-G fault currents DAM.

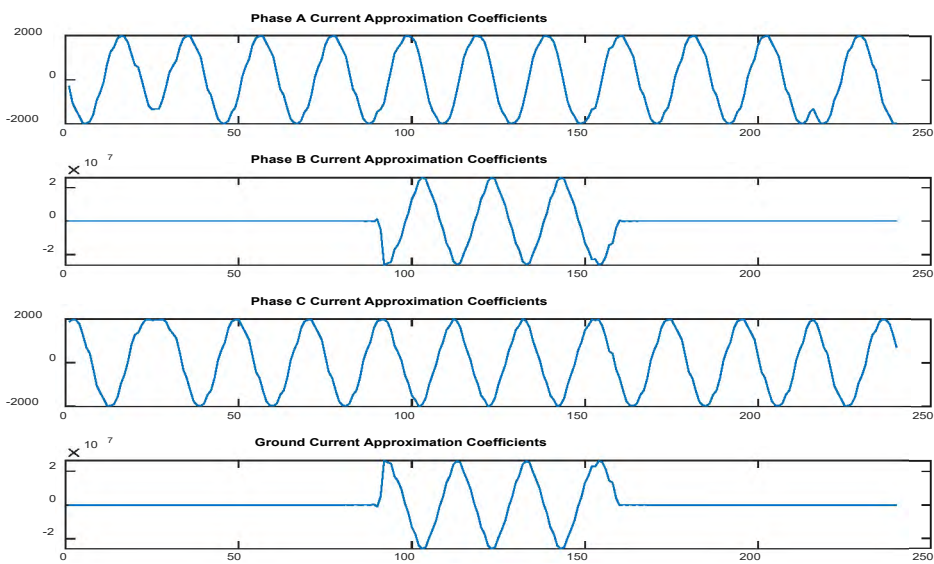


Fig. 6.88 Single-line-to-ground B-G fault currents approximation coefficients DAM.

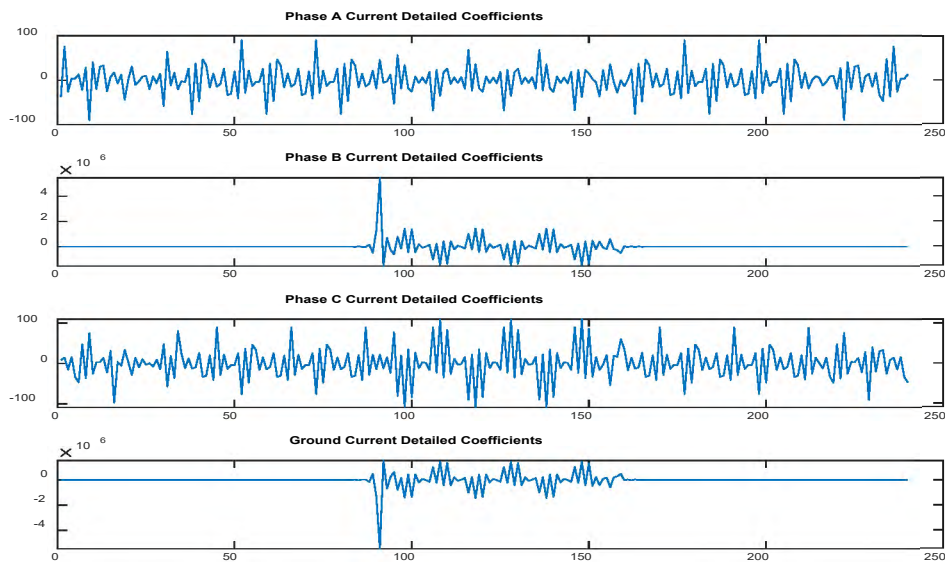


Fig. 6.89 Single-line-to-ground B-G fault currents detailed coefficients DAM.

Fig. 6.86 and Fig. 6.89 revealed the abnormal behavior of the phase B signal and the ground current when the fault introduced. During a fault event, the current in the affected phase experienced an increase, and the maximum value of the detailed coefficients for phase B and ground currents had a very high value. In contrast, phases A and C had a minimal coefficient value.

Fig. 6.90 Simulink double-line-to-ground AB-G fault currents DAM.

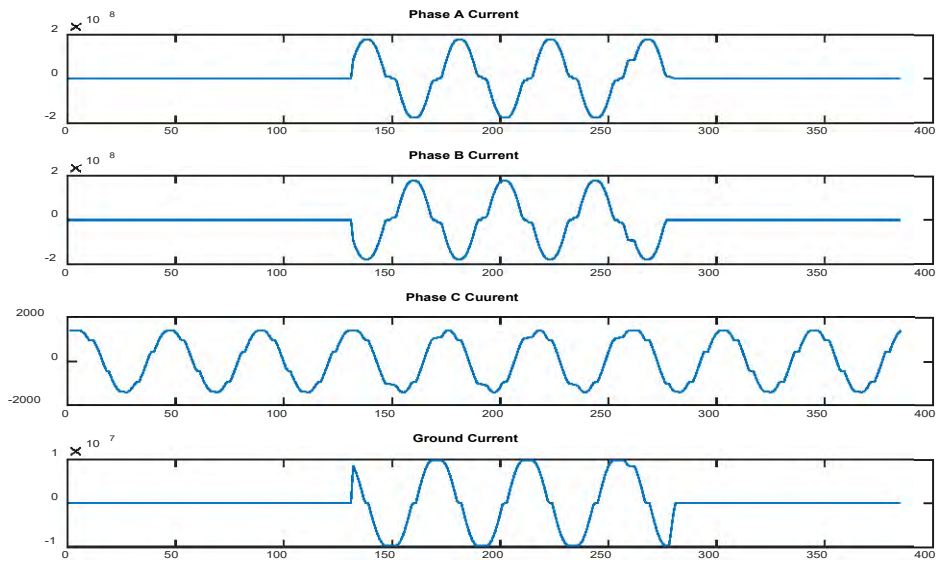


Fig. 6.91 Algorithm double-line-to-ground AB-G fault currents DAM.

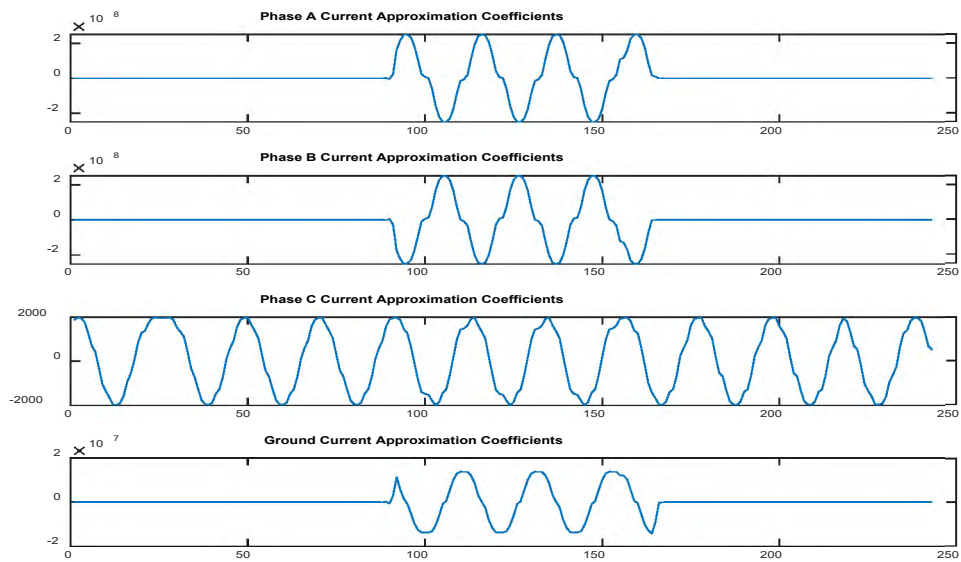


Fig. 6.92 Double-line-to-ground AB-G currents approximation coefficients DAM.

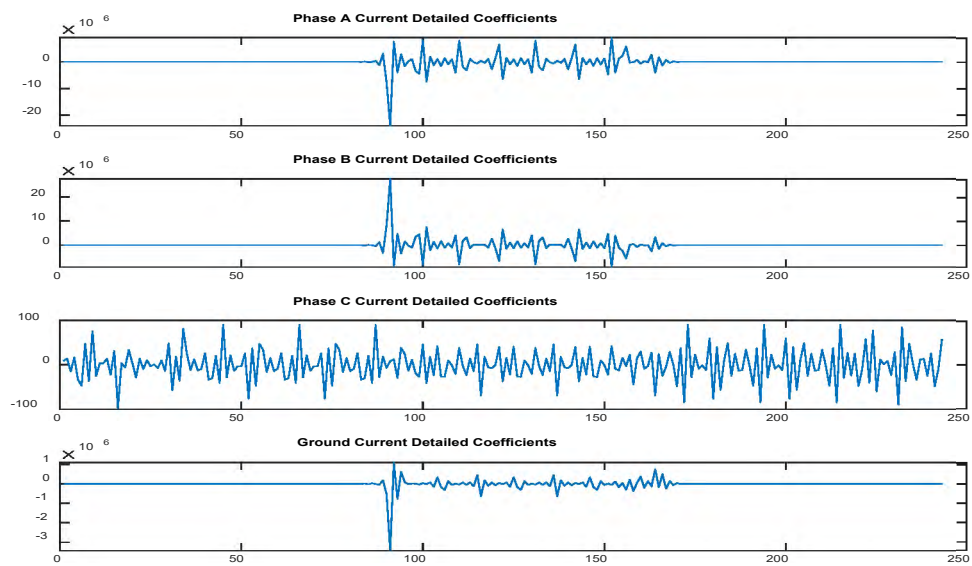


Fig. 6.93 Double-line-to-ground AB-G fault currents detailed coefficients DAM.

Fig. 6.90 and Fig. 6.93 revealed the abnormal behavior of phase A, phase B, and the ground current signals when the fault was introduced. During a fault event, the current

in the affected phase experienced an increase, and the maximum value of the detailed coefficients for phase A, phase B, and ground currents had a very high value. In contrast, phase C had a very small coefficient value.

Fig. 6.94 Simulink double-line B-C fault currents DAM.

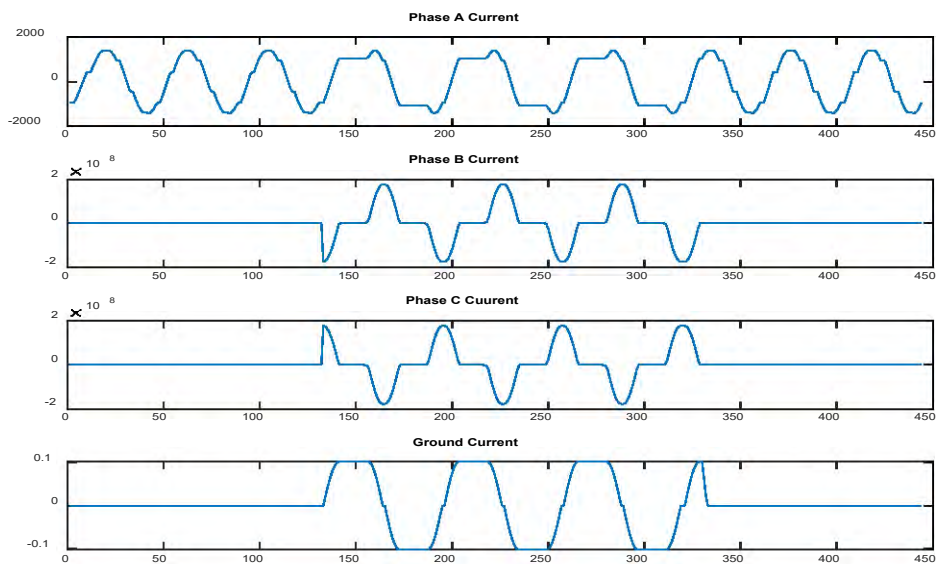


Fig. 6.95 Algorithm double-line-B-C fault currents DAM.

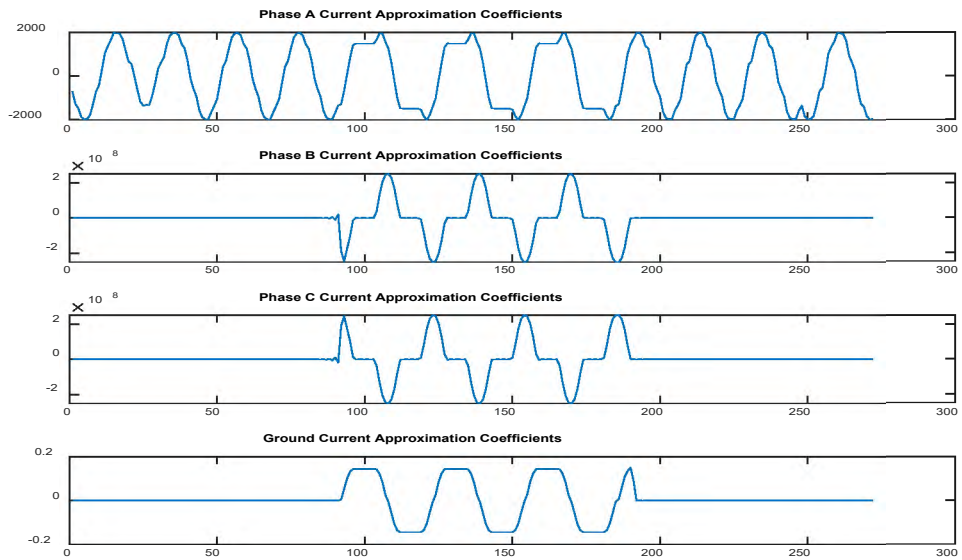


Fig. 6.96 Double-line B-C fault currents approximation coefficients DAM.

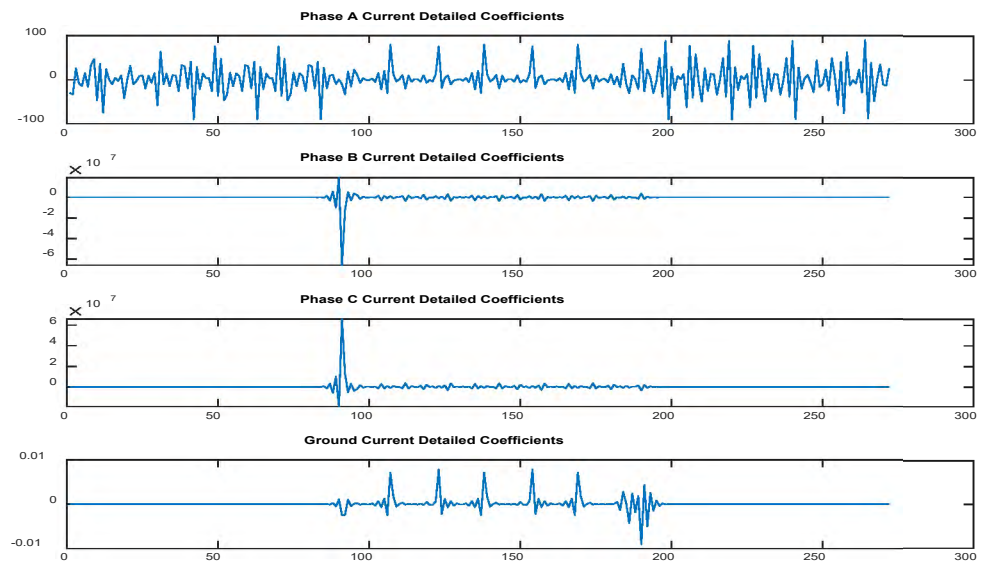


Fig. 6.97 Double-line B-C fault currents detailed coefficients DAM.

Fig. 6.94 and Fig. 6.97 revealed the abnormal behavior of the phase Band phase C current signals when the fault was introduced. During a fault event, the current in the

affected phase experienced an increase, and the maximum value of the detailed coefficients for phase B and phase C were very high. In contrast, phase A and G currents had very small coefficient values.

Fig. 6.98 Simulink three-Phase ABC fault currents DAM.

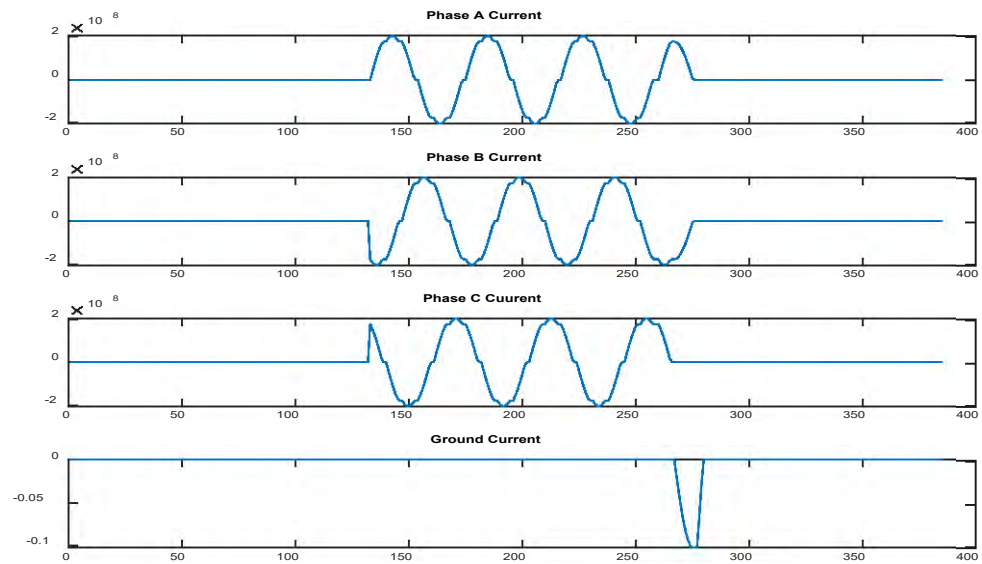


Fig. 6.99 Algorithm three-phase ABC fault currents DAM.

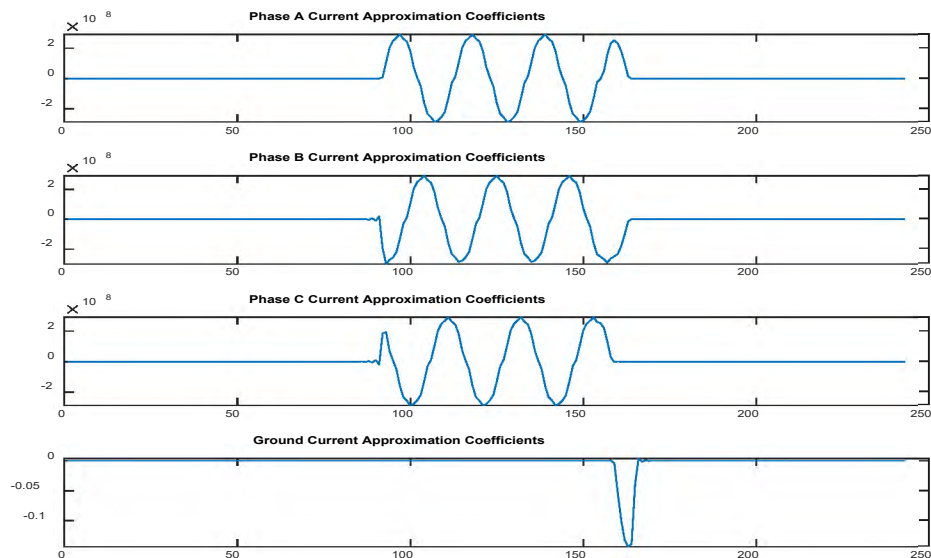


Fig. 6.100 Three-phase ABC fault currents approximation coefficients DAM.

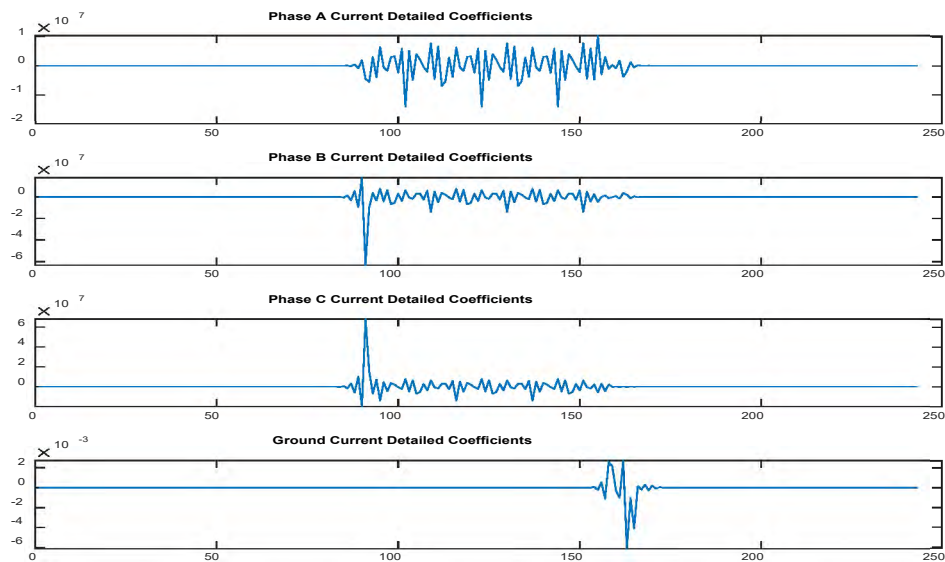


Fig. 6.101 Three-phase ABC fault currents detailed coefficients DAM.

Fig. 6.98 and Fig. 6.101 revealed the abnormal behavior of phase A, B, and C current signals when the fault introduced. During a fault event, the current in the affected

phase experienced an increase, and the maximum value of the detailed coefficients for phase A, phase B, and phase C were very high. In contrast, the ground current had a very small coefficient value.

Fig. 6.102 Simulink three-phase to ground ABC-G fault currents DAM.

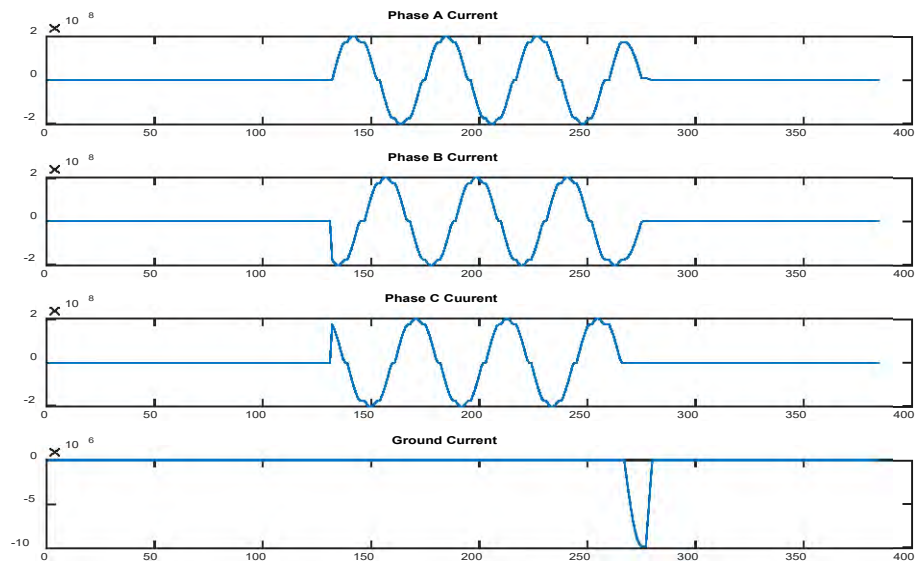


Fig. 6.103 Algorithm three-phase to ground ABC-G fault currents DAM.

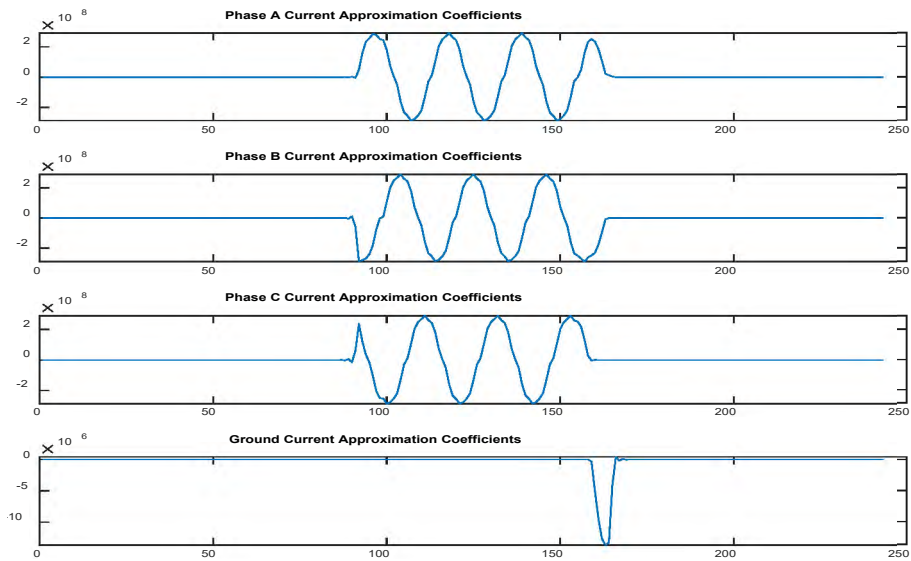


Fig. 6.104 Three-phase-to-ground ABC-G currents approximation coefficients DAM.

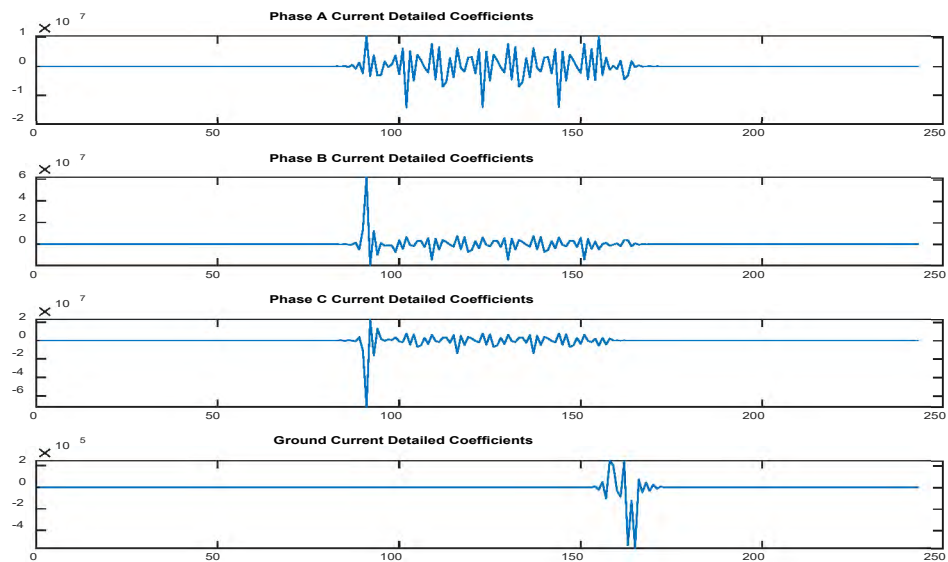


Fig. 6.105 Three-phase-ground ABC-G fault currents detailed coefficients DAM.

Fig. 6.102 and Fig. 6.105 revealed the abnormal behavior of phase A, phase B, phase C, and the ground current signals when the fault was introduced. During a fault event, the current in the affected phase experienced an increase, and the maximum value of the detailed coefficients for all phases and the current signals had a very high value.

The Wavelet decomposition and coefficient calculation process for the selected Wavelets (db4, Haar, sym5, DAM) in the study analysis followed the MATLAB's same steps and commands. It was vital for the study to achieve consistent and comparable results using the same systematic methodology. Several factors helped follow the same process for the MATLAB Wavelet decomposition and coefficient calculation. These Wavelet decomposition and coefficient calculation processes for the selected Wavelets, db4, Haar, sym5, DAM, shared similarities, such as the concepts of Wavelet decomposition, regardless of which Wavelet used, remain consistent. Each Wavelet followed the same process to break down the signal into approximation (CA) and detailed (CD) coefficients. In addition, these coefficients had information about the signal's frequency, making these coefficients essential for capturing transient features regardless of which Wavelet is used.

Another factor that allowed the same Wavelet decomposition and coefficient calculation process is that MATLAB's Wavelet Toolbox. The toolbox designed to work on various Wavelet families using the same commands and functions, such as 'wavedec' for decomposition and 'detcoef' for coefficient extraction. These factors allowed the application of the same fundamental principles to different Wavelets, making the process simple and efficient, enabling precise fault detection and classification.

6.6 Presentation of Data and Results of the Analysis

All fault scenarios and no-fault conditions simulated on the MATLAB/Simulink by introducing a three-phase fault at 0.05 seconds and clearing the fault at 0.1 seconds. By configuring the parameters of the Three-Phase Fault Block, the Simulink can extract the three-phase current from the system as well as the ground current, which observed through Scope1 as shown in Fig.6.1. The Discrete Wavelet Transform (DWT) employed to analyze the resulting current signals because of its efficacy in signal analysis.

The current signals obtained from the simulation were subjected to decomposition using different Wavelet families, including db4, Haar, sym4, and DAM, to extract the approximate and detailed coefficients at the first decomposition level. The detailed coefficients for the decomposed current signals further studied for fault detection and identification. Faults in power systems cause transient signals and high-frequency components in the faulty signal. We can detect these transient patterns associated with each fault by analyzing the detailed coefficients, which represent the high-frequency components in the signal.

Detailed coefficients obtained by Wavelet transforms can effectively capture the localized frequency information in a signal, which means they can highlight specific frequencies associated with faults. When a fault occurs in the power system, it causes a change in the frequency components in the faulty phase. By identifying the maximum detailed coefficient, we can highlight the frequency where the change occurred, which helped to detect faulty signals.

In this methodology for fault detecting and distinguishing between all different short circuit fault types, the knowledge that the detailed coefficients carry the signal

information that can provide information about transient faulty signals is applied. Using the MATLAB command $\max(\text{detcoef})$, the maximum value of the detailed coefficients is calculated for each of the three phases current, phase A, phase B, phase C, and the ground current obtained from the MATLAB/Simulink. Then the maximum detailed coefficients compared across all phases, Phase A, Phase B, Phase C, and the ground currents to detect fault and no-fault conditions, which allowed us to identify any transient changes among all current signals in the three-phase power system. A substantial difference in the maximum detailed coefficients between phases indicated the presence of a fault condition in that phase.

This methodology achieved that by comparing the maximum detailed coefficient against a predefined threshold value, which was set to 350 in our study based on the results we received for the maximum detailed coefficient value for all the 12 cases of the short circuit fault types, including the no-fault condition, using the various choose Wavelet families separately. If the maximum coefficient exceeded the threshold ($T_d=350$), it indicated the presence of a fault. Then the maximum coefficients pattern across all currents used for fault classification. Each fault type caused different coefficient patterns, which helped identify each case's fault type.

For illustration, the case of two-phase to ground fault considered here, as an example (Phase A and Phase B) to ground (AB-G) fault introduced into the power system using the three-phase fault block in the Simulink. After measuring the maximum detailed coefficient values for all signals, phase A, B, and the ground currents observed having significantly high coefficient values. In contrast, Phase C detailed coefficients were very small values.

This pattern of coefficient values, indicative of fault conditions, was observed across the various fault types in the power system using the different Wavelet families, including db4, Haar, sym5, and DAM. The results of these fault simulations for all cases of short circuit fault type and no-fault condition, along with the corresponding maximum coefficient values for Phase A, Phase B, Phase C, and the ground current, are presented in Table 6.1, Table 6.2, Table 6.3, and Table 6.4. This achieved detecting and identifying faults in the power system using the different selected wavelet families.

TABLE 6.1
MAXIMUM VALUES OF DETAILED COEFFICIENTS USING DB4 WAVELET

Case No.	Fault Type	Max. Coefficient Phase A Current	Max. Coefficient Phase B Current	Max. Coefficient Phase C Current	Max. Coefficient Ground G Current
1	No-Fault	103.9844	103.9844	103.9844	7.8793e-10
2	Line-to-Ground (A-G)	1.3523e+06	103.9844	119.5264	1.6087e+06
3	Line-to-Ground (B-G)	103.9857	3.7024e+06	134.4171	1.1253e+06
4	Line-to-Ground (C-G)	103.9857	103.9844	1.4099e+06	1.4099e+06
5	Line-to-Line (A-B)	3.6468e+07	1.2349e+07	104.6234	0.0454
6	Line-to-Line (A-C)	2.1185e+07	111.4911	4.9922e+07	0.0146
7	Line-to-Line (B-C)	104.6286	3.1411e+07	8.6390e+07	0.0101
8	Double-Line-to-Ground (AB-G)	1.0667e+07	2.1332e+07	119.5264	7.7120e+05
9	Double-Line-to-Ground (AC-G)	1.9807e+07	103.9844	8.6994e+06	1.9393e+06
10	Double-Line-to-Ground (BC-G)	103.9857	4.0725e+07	8.4664e+06	9.7973e+05
11	Three-Phase (ABC)	1.2506e+07	2.9173e+07	9.0875e+07	0.0065
12	Three-Phase-to-Ground (ABC-G)	1.2506e+07	4.0725e+07	1.6097e+07	4.6714e+05

Table 6.1 shows that the detailed coefficients for db4 associated with all types of faults had exceptionally high values. In contrast, when no fault applied in any of the phases

or the ground, the coefficient value remains significantly low, ranging from very small to a maximum of 134.4171.

TABLE 6.2
MAXIMUM VALUE OF DETAILED COEFFICIENTS USING HAAR WAVELET

Case No.	Fault Type	Max. Coefficient Phase A Current	Max. Coefficient Phase B Current	Max. Coefficient Phase C Current	Max. Coefficient Ground Current
1	No-Fault	191.1401	191.1401	191.1401	1.2520e-09
2	Line-to-Ground (A-G)	2.4279e+06	191.2134	191.4239	2.5028e+06
3	Line-to-Ground (B-G)	191.1437	1.1364e+07	191.2150	2.4278e+06
4	Line-to-Ground (C-G)	191.2136	191.1401	2.4279e+06	1.1364e+07
5	Line-to-Line (A-B)	2.5236e+07	2.5106e+07	206.8291	0.0149
6	Line-to-Line (A-C)	2.5237e+07	206.8411	2.5294e+07	0.0143
7	Line-to-Line (B-C)	202.5898	2.5236e+07	2.5236e+07	0.0292
8	Double-Line-to-Ground (AB-G)	2.4880e+07	6.5476e+07	205.6027	1.4069e+06
9	Double-Line-to-Ground (AC-G)	5.9524e+07	217.1758	2.5413e+07	5.9524e+06
10	Double-Line-to-Ground (BC-G)	205.6027	1.2500e+08	2.5203e+07	2.4338e+06
11	Three-Phase (ABC)	2.7193e+07	2.7193e+07	2.7193e+07	0.0138
12	Three-Phase-to-Ground (ABC-G)	2.7193e+07	1.2500e+08	2.7531e+07	1.3110e+06

Table 6.2 shows that the detailed coefficients for Haar associated with all types of faults had exceptionally high values. In contrast, when no fault applied, the coefficient value remained significantly low, ranging from very small to a maximum of 217.1758.

TABLE 6.3
MAXIMUM VALUE OF DETAILED COEFFICIENTS USING DAM WAVELET

Case No.	Fault Type	Max. Coefficient Phase A Current	Max. Coefficient Phase B Current	Max. Coefficient Phase C Current	Max. Coefficient Ground G Current
1	No-Fault	91.9586	91.6938	90.0662	5.8025e-10
2	Line-to-Ground (A-G)	1.4466e+06	108.8984	90.0644	1.4471e+06
3	Line-to-Ground (B-G)	90.0643	5.4678e+06	109.8145	1.5394e+06
4	Line-to-Ground (C-G)	112.0931	90.0645	2.0668e+06	6.4856e+06
5	Line-to-Line (A-B)	2.9493e+07	7.9945e+06	90.3129	0.0340
6	Line-to-Line (A-C)	1.1921e+07	91.6938	3.8000e+07	0.0090
7	Line-to-Line (B-C)	90.1153	1.9078e+07	6.5953e+07	0.0078
8	Double-Line-to-Ground (AB-G)	9.0798e+06	2.7385e+07	90.5198	1.0941e+06
9	Double-Line-to-Ground (AC-G)	3.9075e+07	90.0645	1.4048e+07	2.8930e+06
10	Double-Line-to-Ground (BC-G)	90.1127	6.5055e+07	1.8441e+07	6.3712e+05
11	Three-Phase (ABC)	1.0273e+07	1.7874e+07	6.7915e+07	0.0027
12	Three Phase to Ground (ABC-G)	1.0395e+07	6.1590e+07	2.2870e+07	2.4570e+05

Table 6.3 shows that the detailed coefficients for DAM associated with all types of faults had exceptionally high values. In contrast, when no fault applied the coefficient value remained very low, ranging from very small to a maximum of 112.0931.

TABLE 6.4
MAXIMUM VALUE OF DETAILED COEFFICIENTS USING SYM5 WAVELET

Case No.	Fault Type	Max. Coefficient Phase A Current	Max. Coefficient Phase B Current	Max. Coefficient Phase C Current	Max. Coefficient Ground G Current
1	No-Fault	90.1428	90.1428	90.1428	6.6284e-10
2	Line-to-Ground (A-G)	1.7748e+06	127.7881	90.1428	1.7747e+06
3	Line-to-Ground (B-G)	90.1428	7.4182e+06	127.7876	2.0883e+06
4	Line-to-Ground (C-G)	127.7876	90.1492	2.2988e+06	8.3474e+06
5	Line-to-Line (A-B)	1.5783e+07	9.5575e+06	102.8334	0.0235
6	Line-to-Line (A-C)	8.5584e+06	81.2203	2.7855e+07	0.0102
7	Line-to-Line (B-C)	102.8219	7.1210e+06	4.1919e+07	0.0098
8	Double-Line-to-Ground (AB-G)	9.7263e+06	3.8489e+07	90.1428	1.2041e+06
9	Double-Line-to-Ground (AC-G)	4.9015e+07	96.3743	1.4348e+07	3.8915e+06
10	Double-Line-to-Ground(BC-G)	90.1428	8.5854e+07	2.4185e+07	7.3568e+05
11	Three-Phase (ABC)	8.7610e+06	8.6119e+06	4.7012e+07	0.0051
12	Three-Phase-to-Ground (ABC-G)	8.9335e+06	8.1600e+07	2.5287e+07	4.8508e+05

Table 6.4 shows that the detailed coefficients for sym5 associated with all types of faults had exceptionally high values. In contrast, when no fault applied in any of the phases or the ground, the coefficient value remained significantly low, ranging from very small to a maximum of 127.7881. We gained valuable information about the signal's amplitude, frequency localization, and transient behavior by analyzing the maximum detailed coefficients. This information is essential in detecting and classifying faults in the power system.

6.7 Wavelet Coefficients Energy

While our study could have concluded successfully upon the detection and identification of all short-circuit fault types using the various chosen Wavelets, including db4, Haar, sym5, DAM, in combination with the threshold technique, we decided to push our study further. We took an additional step by finding the energy of Wavelet coefficients to provide an assessment of the performance of each selected Wavelet to provide a technique to enable us to determine the best Wavelet for power systems fault detection and identification based on the energy of the Wavelet coefficients for each of the chosen Wavelet in our methodology. Our decision to include this approach in our study was from the realization that the threshold technique alone did not offer sufficient criteria to identify which was the most suitable Wavelet from the selected Wavelets (db4, Haar, sym5, DAM) for fault detection for the power system simulated in this study.

6.7.1 What is Wavelet Coefficients Energy

Wavelet coefficients energy refers to each coefficient's energy, power, or information after applying the Wavelet transform on the signal or image. The Wavelet coefficients with higher energy carry more information and represent significant signal or

image features. In Wavelet analysis, Wavelets transform decomposed signals into different frequency components or scales. This decomposition results in a set of coefficients representing the signal's behavior at different scales and frequencies. By summing the squared values of these coefficients, we can calculate the energy associated with each level of decomposition. The Wavelet coefficients energy analysis is valuable for signal denoising, compression, and transient detection applications. That is because Wavelet coefficient energy provides important information about the signal's frequency content and helps identify significant components within the signal.

In general, the energy of Wavelet coefficients calculated as the sum of the squared absolute values of the coefficients. For a discrete set of coefficients, this expressed using the following equation:

$$E = \sum_{i=1}^N |c_i|^2 \quad (6.1)$$

Where

E is the energy of the Wavelet coefficients,

C_i represents an individual coefficient,

N is the total number of coefficients,

Note that squaring each coefficient ensures that the negative values of the Wavelet coefficients do not cancel out the positive values of the Wavelet coefficients when calculating the energy.

6.7.2 Selecting the Optimal Wavelet Function for Power System Fault Detection

We detected and identified faults using the selected Wavelet transforms (db4, Haar, sym5, DAM) combined with threshold techniques. However, because we realized that this technique did not identify the most appropriate Wavelet for fault detection, we decided to take our study a step further by applying the Wavelet coefficients energy analysis, which is a method that enabled systematically compare the performance of these Wavelets for power system short circuit fault detection and identification. We used this technique because the Wavelet coefficients energy analysis provides more information about the energy distribution across different signal frequency components.

This study applied the Wavelet coefficients analysis to the detailed coefficients extracted from the Wavelet transform performed on the current signals generated in the MATLAB/Simulink power system simulation. The decision to apply Wavelet coefficients energy analysis on detailed coefficients, not the approximation coefficients, came from our understanding that the detailed coefficients captured high-frequency signal components. Since power system faults usually cause high-frequency occurrences in the signal, such as transient signals, applying the Wavelet coefficients energy analysis on the detailed coefficients in our methodology was a strategically accurate approach to capture these high-frequency occurrences in the faulty signals accurately.

In our methodology, we studied the Wavelet detailed coefficients energy for all the short circuit fault cases and the no-fault condition in the three-phase power system. To accomplish this, after applying the Wavelet transform using the selected Wavelet families (db4, Haar, sym5, and the DAM) individually, for each case of the 12 cases, short circuit

fault types and no fault condition, we calculated the total energy of the Wavelet detailed coefficients for the current and ground signals using the MATLAB commands.

First, we calculated the energy of the detailed coefficients for the current signal, denoted as 'EnergyCoefCurrent.' We used the 'detcoef' function, which, in this case, was applied to 'current,' representing the three-phase power system current signals, Phase A Current = CurrentA, Phase B Current=CurrentB, Phase C Current=CurrentC, and Ground Current=CurrentG. The detailed coefficients executed from the 'detcoef' command then squared using the '^2' operator: $\text{EnergyCoefCurrent} = \text{detcoef}(\text{current}).^2$.

Second, we calculated the total energy of the Wavelet detailed coefficients by deploying the MATLAB command $\text{TotalEnergyDetCoefCurrent} = \text{sum}(\text{EnergyCoefCurrent})$. This command summed up the squared detailed coefficients, which provided us with the total energy content represented by these coefficients:

$$\text{TotalEnergyDetCoefCurrent} = \text{sum}(\text{EnergyCoefCurrent})$$

Third, the values of the total energy for each of the 12 cases, short circuit faults and no-fault conditions, recorded in separate Tables, with one Table for each of the selected Wavelet families as illustrated in Table 6.5, Table 6.6, Table 6.7, and Table 6.8. These Tables allowed us to analyze the performance of each Wavelet in detecting and identifying faults, helping us determine which Wavelet family performed best in our study for fault detection and identification.

TABLE 6.5
WAVELET COEFFICIENTS ENERGY FOR DB4 WAVELET

Case No.	Fault Type	Total Energy Detailed Coefficient Phase A Current	Total Energy Detailed Coefficient Phase B Current	Total Energy Detailed Coefficient Phase C Current	Total Energy Detailed Coefficient Ground G Current
1	No-Fault	2.7204e+05	2.7951e+05	2.8005e+05	1.2599e-17
2	Line-to-Ground (A-G)	1.7227e+13	2.6602e+05	2.0698e+05	1.7225e+13
3	Line-to-Ground (B-G)	2.1157e+05	3.0091e+13	2.6470e+05	3.0090e+13
4	Line-to-Ground (C-G)	2.6250e+05	2.2058e+05	3.3924e+13	3.3922e+13
5	Line-to-Line (A-B)	2.1497e+15	2.1497e+15	2.7154e+05	0.0031
6	Line-to-Line (A-C)	3.6016e+15	3.2219e+05	3.6016e+15	0.0024
7	Line-to-Line (B-C)	2.7863e+05	8.8984e+15	8.8984e+15	5.9695e-04
8	Double-Line-to-Ground (AB-G)	1.2995e+15	1.3855e+15	3.0307e+05	1.1673e+13
9	Double-Line-to-Ground (AC-G)	1.6929e+15	3.0108e+05	1.8216e+15	1.0611e+13
10	Double-Line-to-Ground (BC-G)	2.9312e+05	3.1673e+15	3.1729e+15	5.9772e+12
11	Three-Phase (ABC)	2.7204e+05	2.7951e+05	2.8005e+05	1.2599e-17
12	Three-Phase-to-Ground (ABC-G)	2.0376e+15	4.0038e+15	4.7391e+15	2.0968e+12

TABLE 6.6
WAVELET COEFFICIENTS ENERGY FOR HAAR WAVELET

Case No.	Fault Type	Total Energy Detailed Coefficient Phase A Current	Total Energy Detailed Coefficient Phase B Current	Total Energy Detailed Coefficient Phase C Current	Total Energy Detailed Coefficient Ground G Current
1	No-Fault	2.5576e+06	2.5762e+06	2.5674e+06	1.1351e-16
2	Line-to-Ground (A-G)	1.4749e+14	2.4542e+06	2.5900e+06	1.4748e+14
3	Line-to-Ground (B-G)	2.5576e+06	2.6221e+14	2.4579e+06	2.6219e+14
4	Line-to-Ground (C-G)	2.4277e+06	2.5779e+06	2.6025e+14	2.6024e+14
5	Line-to-Line (A-B)	1.5745e+16	1.5745e+16	2.7229e+06	0.0066
6	Line-to-Line (A-C)	1.4625e+16	2.7266e+06	1.4625e+16	0.0059
7	Line-to-Line (B-C)	2.7453e+06	1.5082e+16	1.5082e+16	0.0064
8	Double-Line-to-Ground (AB-G)	1.8611e+16	1.9398e+16	2.7246e+06	9.3677e+13
9	Double-Line-to-Ground (AC-G)	1.7998e+16	2.7354e+06	1.8726e+16	8.9680e+13
10	Double-Line-to-Ground (BC-G)	2.6774e+06	3.0559e+16	3.0628e+16	5.6018e+13
11	Three-Phase (ABC)	2.0144e+16	1.9018e+16	1.9155e+16	0.0015
12	Three-Phase-to-Ground (ABC-G)	2.5576e+06	2.5762e+06	2.5674e+06	1.1351e-16

TABLE 6.7
WAVELET COEFFICIENTS ENERGY FOR DAM WAVELET

Case No.	Fault Type	Total Energy Detailed Coefficient Phase A Current	Total Energy Detailed Coefficient Phase B Current	Total Energy Detailed Coefficient Phase C Current	Total Energy Detailed Coefficient Ground G Current
1	No-Fault	2.9660e+05	3.0450e+05	3.1896e+05	1.4229e-17
2	Line-to-Ground Fault (A-G)	3.2716e+13	3.9096e+05	2.7675e+05	3.2712e+13
3	Line-to-Ground (B-G)	2.6147e+05	6.8352e+13	4.1139e+05	6.8349e+13
4	Line-to-Ground (C-G)	4.0569e+05	2.8219e+05	8.6280e+13	8.6276e+13
5	Line-to-Line (A-B)	1.2869e+15	1.2869e+15	3.2464e+05	0.0019
6	Line-to-Line (A-C)	1.9927e+15	3.4411e+05	1.9927e+15	0.0017
7	Line-to-Line (B-C)	3.0329e+05	5.2908e+15	5.2908e+15	5.1976e-04
8	Double-Line-to-Ground (AB-G)	1.4809e+15	1.6825e+15	3.2180e+05	1.7942e+13
9	Double-Line-to-Ground (AC-G)	2.4653e+15	3.3574e+05	2.7416e+15	1.3881e+13
10	Double-Line-to-Ground (BC-G)	3.0517e+05	5.4509e+15	5.5072e+15	3.8829e+12
11	Three-Phase (ABC)	2.9660e+05	3.0450e+05	3.1896e+05	1.4229e-17
12	Three-Phase-to-Ground (ABC-G)	1.9883e+15	6.3267e+15	7.8071e+15	8.2025e+11

TABLE 6.8
WAVELET COEFFICIENTS ENERGY FOR SMY5 WAVELET

Case No.	Fault Type	Total Energy Detailed Coefficient Phase A Current	Total Energy Detailed Coefficient Phase B Current	Total Energy Detailed Coefficient Phase C Current	Total Energy Detailed Coefficient Ground G Current
1	No-Fault	2.5547e+05	2.4881e+05	2.6059e+05	1.0719e-17
2	Line-to-Ground (A-G)	5.1148e+13	4.1571e+05	2.1576e+05	5.1142e+13
3	Line-to-Ground (B-G)	2.2455e+05	1.1233e+14	4.2960e+05	1.1232e+14
4	Line-to-Ground (C-G)	4.3566e+05	2.3584e+05	1.2925e+14	1.2925e+14
5	Line-to-Line (A-B)	1.0313e+15	1.0313e+15	2.7228e+05	0.0014
6	Line-to-Line (A-C)	1.4263e+15	2.7065e+05	1.4263e+15	0.0012
7	Line-to-Line (B-C)	2.6424e+05	2.9679e+15	2.9679e+15	6.4922e-04
8	Double-Line-to-Ground (AB-G)	2.1918e+15	2.5071e+15	2.5654e+05	2.6038e+13
9	Double-Line-to-Ground(AC-G)	3.4850e+15	2.9909e+05	3.9158e+15	2.0859e+13
10	Double-Line-to-Ground (BC-G)	2.5269e+05	8.6661e+15	8.7453e+15	4.1139e+12
11	Three-Phase (ABC)	2.5547e+05	2.4881e+05	2.6059e+05	1.0719e-17
12	Three-Phase-to-Ground (ABC-G)	1.9865e+15	9.1883e+15	1.0648e+16	9.3542e+11

Data analyses in Tables 6.5 to 6.8 led to a very interesting and important observation. We discovered no universally superior Wavelet for all short circuit fault

scenarios within the power system. Instead, our analysis revealed that one of the selected Wavelet families outperformed the others for each type of fault. This observation is consistent across the different fault types. Each fault type has its winner from the selected Wavelet families.

For instance, in cases of line-to-line faults, one particular Wavelet consistently had the highest energy values for Wavelet detailed coefficients, Daubechies 4 (db4). In contrast, Symlet 5 (sym5) had the highest Wavelet detailed coefficients energy for line-to-ground faults. This pattern extended to three-phase and three-phase-to-ground fault scenarios, where each fault type had its winner Wavelet for fault detection. Therefore, it was crucial to choose the Wavelet for power system fault detection based on the specific fault type to achieve the highest accuracy in fault detection, as illustrated in Table 6.9 for the specific power system simulated for this study.

From the study findings, it is important to acknowledge that different power systems with varying parameters may cause different outcomes when selecting the optimal Wavelet for each fault type. The performance of Wavelet families in fault detection and identification depends on the characteristics of the specific power system under consideration. Factors such as voltage levels, system configurations, and fault scenarios can influence the performance of a particular Wavelet for detecting and identifying fault types in a power system.

TABLE 6.9
OPTIMAL WAVELETS BASED ON WAVELET
COEFFICIENT ENERGY ANALYSIS

Fault Type	Optimal Wavelet
Line-to-Ground (A-G)	Symlet 5
Line-to-Ground (B-G)	Symlet 5
Line-to-Ground (C-G)	Symlet 5
Line-to-Line (A-B)	Daubechies 4
Line-to-Line (A-C)	Daubechies 4
Line-to-Line (B-C)	Daubechies 4
Double-Line-to-Ground (AB-G)	Haar
Double-Line-to-Ground (AC-G)	Haar
Double-Line-to-Ground (BC-G)	Haar
Three-Phase (ABC)	Discrete Approximation Meyer
Three-Phase-to-Ground (ABC-G)	Daubechies 4 and Symlet 5

6.8 Investigating the Factors Leading to Optimal Wavelet Selection

To understand the why and how of the results in Table 6.9, we analyzed the relationship between current signal characteristics in power systems and the optimal Wavelets for the specific fault types in detail. We aimed to find the patterns or features of

the faulty current signals and compare them with the characteristics of the optimal Wavelet for that specific fault type.

This investigation provided valuable insights into why particular Wavelets were ideal for distinct fault scenarios. To understand the results better, the complex dynamics between power system faults, current nature, and Wavelet characteristics studied. The outcome of this analysis was extremely impressive, as it became evident that the optimal Wavelets align logically with the characteristics of each fault type, providing more validation for our results.

i. Line to Ground Fault and Symlet 5 Wavelet: this fault occurred when one of the power lines contacted the ground or a conducting path to the ground. It caused a sudden current flow between one line and the ground. This current signal had high frequency components and rapid fluctuations due to the sparking involved. Sym5 found to have the highest detailed coefficients energy for the line-to-ground faults. The Symlet Wavelets, such as sym5, designed to capture details in non-smooth signals. In line-to-ground faults, there were rapid fluctuations in the current, and sym5 effectively captured and represented these high frequency components, leading to higher detailed coefficients energy.

ii. Line-to-Line Fault and Daubechies 4: this fault occurred when two lines contacted each other. It led to a short circuit between two phases, causing the current to have smoother variations compared to line-to-ground faults. The current signal still had some high-frequency components but was generally more regular. Db4 found to have the highest detailed coefficient energy for line-to-line faults. Daubechies Wavelets, like db4, designed to capture signals that had smooth and regular components. In line-to-line fault,

the current signal had smoother variations, and db4 effectively captured and represented these variations, leading to higher detailed coefficients energy.

iii. Double Line to Ground Fault: this fault occurred when two lines simultaneously contracted with the ground. This fault combined aspects of line-to-ground and line-to-line faults. A mix of rapid fluctuations and smoother transitions characterized the current signal. The Haar Wavelet found to have the highest detailed coefficients energy for the double-line-to-ground faults. The Haar Wavelet designed to capture sudden transitions in signals. In double line to ground fault, there were sharp changes in current, and the Haar Wavelet effectively captured and represented these transitions, resulting in the highest detailed coefficients energy.

iv. Three-Phase Fault: this fault occurred when all the three-phase power system lines short-circuited together. This fault type produced a complex and highly unbalanced current signal with varying frequencies and amplitudes. The current signal had a combination of high frequency and low frequency components. The Discrete Approximation Meyer Wavelet found to have the highest detailed coefficients energy for three fault types. This Wavelet has good localization properties and adaptability to various signal features. For three fault types with complex current characteristics, the Discrete Approximation Meyer Wavelet effectively captured and represented the signal details, resulting in higher detailed coefficients.

v. Three-Phase to Ground Fault: this fault is similar to the three-phase fault, but with one or more phases short-circuited to the ground. It combines the characteristics of line-to-ground and line-to-line faults, resulting in complex and unbalanced current signals. Daubechies 4 and Symlet 5 had the highest detailed energy coefficients for three-phase to-

ground faults. This fault type combines characteristics of line-to-ground and line-to-line faults. Daubechies 4 and Symlet 5, with their flexibility in representing smooth and non-smooth signal components, were suitable for capturing the diverse characteristics of the three phase-to-ground faults, leading to higher detailed energy coefficients. These results reflect the adaptability of specific Wavelets to different fault types and signal characteristics, making them valuable tools for fault detection and analysis in power systems.

6.9 Summary

The simulation and algorithm chapter presented a detailed exploration of the study methodology. It outlined the process of simulating a three-phase power system using the MATLAB/Simulink, which is the foundation for the fault detection analysis. The chapter represented the Figs. for capturing and plotting current signals for various fault and no-fault scenarios within the simulated system.

This chapter focused on applying the selected Wavelets using the MATLAB commands in the algorithm to extract the detailed coefficients from the current signals. The methodology explained the Wavelet transformations implementation and the specific Wavelets chosen for analysis. The chapter emphasized the significance of visualizing the extracted detailed coefficients. The detailed coefficients for all current phases under different fault types plotted and displayed, providing a clear and insightful representation of the signal behavior during fault and no-fault conditions. These visualizations offered a practical and intuitive understanding of the distinct patterns and variations in the coefficients, which were essential in this fault detection and identification methodology.

In summary, the study's simulation and algorithm outline the methodology employed to simulate the three-phase power system, captured current signals, and applied Wavelet analysis. It presented the importance of visualizing the detailed coefficients as a powerful tool for comprehending the power system's behavior under various fault conditions.

The Results chapter of this study project uncovered significant insights into the fault detection and identification process in three-phase power systems using various Wavelet transforms, the threshold technique, and Wavelet coefficients energy analysis. This summary chapter offered a concise overview of the findings for the study questions and sub-questions:

Various Wavelet transforms tested, including db4, Haar, sym5, and DAM for short circuit faults in a three-phase power system. They successfully detected and classified different fault types combined with the threshold technique. The threshold technique proved effective in isolating fault-induced transients within the signals, enhancing the overall detection accuracy.

The study showed that analyzing the energy of Wavelet coefficients was a valuable approach for identifying the most suitable Wavelet (optimal Wavelet) for fault detection under specific fault conditions. Integrating quantitative and qualitative study methods provided a comprehensive understanding of power system behavior during fault conditions, bridging the gap between numerical data and real-world insights.

Summary of the Findings and Conclusion

Using the various selected Wavelets, the results used Tables to list the maximum detailed coefficients' values and the Wavelet detailed coefficients energy for each current signal in all fault and no-fault conditions. These findings helped find the optimal Wavelet.

The analysis of these Tables showed that there was no universal "best" Wavelet across all fault types. Instead, the optimal Wavelet depended on the fault type. This illustrated the importance of choosing the most appropriate Wavelet family for each fault type. The Wavelet detailed coefficient Tables showed that different Wavelets had the highest energy values for line-to-line and line-to-ground faults, making them the optimal Wavelet for that specific fault type. Meanwhile, for three-phase and three-phase-to-ground faults, other Wavelets were the optimal choices. Integrating quantitative and qualitative methods was challenging but successful, where expert insights helped understand the data findings. In conclusion, this chapter advanced understanding of fault detection in power systems. It emphasized the importance of choosing the suitable Wavelet for each type of fault. These findings will be discussed and interpreted further in the next chapter.

7. DISCUSSION, CONCLUSIONS AND FUTURE WORK

This chapter evaluates the thesis work and the significance of the results. In addition, offers a personal insight into how the results interpreted and make recommendations for future work. Furthermore, it discusses potential areas for improvement or expansion in the study to contribute to the broader field of knowledge.

7.1 Introduction

The discussion chapter explores the work and methodology approach and analysis performed in the previous chapters to highlight the study findings' significance and offer recommendations for future studies. This chapter summarizes the study findings, their interpretation, and how this work is significant to the knowledge of power systems fault detection and Wavelet applications. In addition, the chapter presents the limitations that could have influenced the results. The chapter concludes by providing recommendations for future studies to enhance this study. These sections in the discussion chapter provide a clear picture of how the conclusion chapter fits into the overall thesis by bringing together the study objective, the methodologies used, and the findings presented in the previous chapters.

7.2 Summary of the Results

This section summarizes the critical elements of the study, restating the study problems, the significance of the study, the methodology used, and a concise review of the findings. The study's main objective is to enhance power systems' fault detection with a focus on short-circuit fault detection in three-phase power systems using Wavelet analysis to increase the reliability and stability of the power system. The study's design methodology approach is based on quantitative and qualitative techniques, providing a

holistic understanding of fault detection. The approach also combined methodology instruments, including the MATLAB, Wavelet analysis, threshold techniques, and Wavelet coefficients energy, and the study's objectives achieved.

Here is a concise review of the study's findings, starting with the MATLAB/Simulink to simulate various fault and no-fault scenarios, extracting detailed coefficients by different Wavelet families, including db4, Haar, sym5, and DAM. These coefficients were crucial for identifying transient events. Then, the maximum detailed coefficients obtained to compare against the threshold value for fault detection and identification. This method offered an accurate and reliable method for fault detection and identification.

One of the significant findings was that while the threshold technique worked well for fault detection, it needed more information or patterns to determine the optimal Wavelet for fault detection and identification. The Wavelet coefficients energy analysis technique introduced to overcome this limitation in the threshold technique to highlight the optimal Wavelet for short circuit fault detection in three-phase power systems. This technique applied to the detailed coefficients for the current signals for all fault and no-fault conditions for the selected Wavelets. Our finding revealed that the optimal Wavelet for fault detection was not uniform across all fault types. Instead, the winner Wavelet varied depending on the fault type.

7.3 Discussion of the Results

Discussing the results obtained from the study on short-circuit fault detection and identification in three-phase power systems using various Wavelets provides an interpretation of the study findings, relates them to the initial hypotheses and study

questions, and explores their practical and theoretical implications. In addition, the discussion review of the study's limitations, acknowledging potential constraints and areas for refinement in future research.

The study's primary objective was to detect and identify faults in the power system using a variety of Wavelets. The Wavelet transform analysis combined with the threshold technique performed. From the results obtained from this analysis, this objective achieved. This achievement aligns with the initial hypotheses about using Wavelet transform for short circuit fault detection and identification for the three-phase power system.

The threshold technique is a well-established signal processing method, but in this study, the threshold did not reveal the optimal Wavelet for fault detection. This limitation for the threshold technique was an important finding. It prompted another technique analysis to answer the second study's question about the optimal Wavelet for fault detection: the Wavelet coefficients energy analysis technique. This approach overcame the threshold technique's limitation for the optimal Wavelet.

This analysis provided a crucial realization that there was no optimal Wavelet for all fault detection and identification, and the choice of the optimal Wavelet depended on the specific fault type. Whether it was a single-line to-ground, double-line fault, double-line-to-ground, three-phase fault, or three-phase to-ground fault, the results indicated that the optimal Wavelet selection was based on which fault type existed in the power system, even though all the selected Wavelets achieved successfully fault detection for all fault types. This discovery enhanced the understanding of fault detection methodologies.

The practical implications of the findings are significant. The study identified the optimal Wavelet solution for different fault types within the three-phase power systems.

By selecting Wavelets based on the specific fault conditions, power system engineers can enhance their fault detection methodologies, improving the power system's reliability and stability. For the theoretical implication, this study increases the understanding of Wavelet analysis and fault detection methodologies, contributing to the knowledge of the signal processing and the power system fields to consider the power system behavior during faults to apply more analysis before concluding.

7.4 Limitations

While this study provided valuable insights for short circuit fault detection and identification in three-phase power systems using various Wavelets, several limitations exist. First, the fault types investigated were limited to the short-circuit scenarios only, which means the results achieved may not apply to more complex fault scenarios. Second, the study used a controlled environment and a simple power system model, which may not represent the real world's complex power system. Differences between the simulation environment and actual power systems can affect the results since this study did not consider external factors, such as environmental conditions or system changes.

Another limitation was that the threshold value for fault detection manually set to a fixed number since the behavior of a power system can vary with different conditions, which requires a dynamic threshold value to detect faults accurately. Another observation is that there was a delay in the ground current to show the transient signal until after clearing the fault, in the case of the three-phase to-ground current only. This is very critical because it could affect identifying this fault type correctly.

7.5 Conclusions

This study investigated methodology for enhancing short circuit fault detection and identification in three-phase power systems by applying various Wavelets and a threshold-based technique. The study's overarching objective was to contribute to the knowledge concerning power systems fault detection, and the following conclusions drawn from the study findings in response to the two fundamental study questions:

i. Effectiveness of Wavelet Transform in Fault Detection: The first study objective focused on utilizing Wavelet transform to detect short circuit faults in three-phase power systems, employing a variety of selected Wavelets individually. The study successfully demonstrated the practicality of this approach. By comparing the maximum values of the detailed coefficients with predefined threshold values, researchers effectively detected and classified faults in the power system. This achievement highlights the significance of Wavelet-based methodologies in enhancing fault detection accuracy.

ii. Optimal Wavelet Selection for Fault Detection: The second study objective delved into identifying the optimal Wavelet for fault detection. The investigation led to the realization that the choice of the optimal Wavelet was more than just a one-size-fits-all solution. Instead, it depended on and should customize to the specific fault type. By comparing Wavelet detailed coefficients energy for various fault types across selected Wavelets, we revealed the dynamic nature of optimal Wavelet selection. This insight is very significant for engineers and researchers working in the field of power systems fault detection.

In conclusion, this study significantly contributes to short-circuit fault detection in three-phase power systems. The successful applications of Wavelet transform and

determining optimal Wavelets for different fault scenarios provide enhanced fault detection and identification tools. As the power system industry continues to evolve, the findings will be of great insight to improve the reliability and the accuracy of fault detection mechanisms. This thesis represents a significant step forward for more effective fault detection methodologies in power systems.

Therefore, as this chapter closes, the study is not just ending. This study represents starting a new chapter in the world of power system engineering. The study is a small step toward something more significant, and cannot wait to see where it leads next.

7.6 Future Work

By exploring the limitations faced in the study, there are exciting opportunities for future study. One limitation was using a fixed threshold value for fault detection. To overcome this, researchers could explore the application of neural networks and deep learning techniques. These advanced methods can adaptively learn from the data, so there is a need for manually set threshold values. Combining artificial intelligence with fault detection techniques could lead to more adaptable solutions.

Another limitation was the need to consider the impact of environmental factors and the power system's complexity in the real world. Future work may involve collecting diverse data, studying the influence of external conditions on fault behavior, and developing techniques considering the dynamics of three-phase power systems. These approaches can refine fault detection methods and enhance the resilience of power systems.

One alarming observation was the delay in the appearance of transient signals in the ground current in the case of three-phase to-ground faults. This could affect the accurate identification of this specific fault type. This observation is particularly concerning

because, as evidenced by the Figs. captured from the Scope in Simulink and the detailed coefficients, the fault was only immediately detected once cleared. Even though the study successfully identified this fault type, future studies must investigate this delay to ensure fault detection and identification reliability.

7.7 Summary

This chapter discussed the findings and their implications. It began with an introduction and a summary of the results. The chapter analyzed the results of the study questions. It also acknowledged the study's limitations and proposed directions for future study. The findings summarized, their practical significance discussed, and potential areas for future study mentioned. The discussion chapter connected the results to their broader meaning and impact on future power systems fault detection studies.

REFERENCES

- [1] W. D. Stevenson Jr., "Elements of Power System Analysis," 4th ed. International ed. New York, NY: McGraw-Hill, 1982, pp. 1-36, ISBN 0-07-061278-1.
- [2] J. W. Chang, "A Wires Report on the Benefits of Electric Transmission: Identifying and Analyzing the value of investments," WIRES Group, July 2013, pp. 4-63, [Online]. Available: www.WIRESgroup.com. [Accessed: January 11, 2023].

- [3] "Electric power transmission," Wikipedia, [Online]. Available: https://en.wikipedia.org/wiki/Electric_power_transmission. [Accessed: January 11, 2023].
- [4] C. M. Akujuobi, "Wavelets and Wavelet Transform Systems and their Applications: A Digital Signal Processing Approach," Springer, 2022, pp. 1-79, DOI: 10.1007/978-3-030-87528-2.
- [5] R. C. Gonzalez and R. E. Woods, "Digital Image Processing," 2nd ed., Prentice-Hall, Inc., 2002, pp. 349-408, ISBN 0-201-18075-8.
- [6] Mengistu, E., Verma, A., Khan, B., Mahela, O. P., & Saket, R. K. (2023). Fault Detection on Distribution Network Planning Using Fast Fourier Transform-Based Steady State and Transient Response. In 2023 IEEE IAS Global Conference on Renewable Energy and Hydrogen Technologies (GlobConHT) (pp. 1-6). Male, Maldives. doi: 10.1109/GlobConHT56829.2023.10087853.
- [7] J. -p. Zhou, Y. -p. Zheng and Z. -p. Wang, "Detection of the transmission line short-circuited fault based on lifting Wavelet," in 2008 Third International Conference on Electric Utility Deregulation and Restructuring and Power Technologies, Nanjing, China, 2008, pp. 1663-1666, doi: 10.1109/DRPT.2008.4523672.
- [8] P. J. Broniera, W. S. Gongora, A. Goedel and W. F. Godoy, "Diagnosis of the stator winding inter-turn short circuit in three-phase induction motors by using artificial neural networks," 2013 9th IEEE International Symposium on Diagnostics for Electric Machines, Power Electronics and Drives (SDEMPED), Valencia, Spain, 2013, pp. 281-287, doi: 10.1109/DEMPED.2013.6645729.
- [9] Huang, S.-J. and Hsieh, C.-T., "High-Impedance Fault Detection Utilizing AMorlet Wavelet Transform Approach," in IEEE, Oct. 1999.
- [10] S. Koley, S. Chattopadhyay, S. A. Hamim and S. Debnath, "High Impedance Single Line to Ground Fault Detection and Wavelet-alienation Based Faulty Phase Identification," 2022 IEEE 6th International Conference on Condition Assessment Techniques in Electrical Systems (CATCON), Durgapur, India, 2022, pp. 182-186, doi: 10.1109/CATCON56237.2022.10077667.
- [11] S-J. Huang and C-T. Hsieh, "Computation of continuous Wavelet transform via a new Wavelet function for visualization of power system disturbances," in 2000 Power Engineering Society Summer Meeting (Cat. No.00CH37134), 2000, pp. 951-955. DOI: 10.1109/PESS.2000.867500.

- [12] B. R. Reddy, M. V. Kumar, M. Suryakalavathi, and C. P. Babu, "Fault detection, classification and location on transmission lines using Wavelet transform," in 2009 IEEE Conference on Electrical Insulation and Dielectric Phenomena, 2009, pp. 409-411. DOI: 10.1109/CEIDP.2009.5377788.
- [13] A. Contreras-Valdes, J. P. Amezcuita-Sanchez, D. Granados-Lieberman and M. Valtierra-Rodriguez, "Data compression based on discrete Wavelet transform and fault detection of short-circuit faults in transformers," *2019 IEEE International Autumn Meeting on Power, Electronics and Computing (ROPEC)*, Ixtapa, Mexico, 2019, pp. 1-6, doi: 10.1109/ROPEC48299.2019.9057136.
- [14] P. Chiradeja and C. Pothisarn, "Identification of the fault location for three-terminal transmission lines using discrete Wavelet transforms," 2009 Transmission & Distribution Conference & Exposition: Asia and Pacific, Seoul, Korea (South), 2009, pp. 1-4, doi: 10.1109/TD-ASIA.2009.5356924.
- [15] S. I. Abood, "Digital Signal Processing: A Primer with MATLAB," 1st ed., CRC Press, June 13, 2022. ISBN-13: 978-1032337166.
- [16] A. Taspinar, "A guide for using the Wavelet Transform in Machine Learning," 2018. [Online]. Available: <https://ataspinar.com/2018/12/21/a-guide-for-using-the-Wavelet-transform-in-machine-learning/>. [Accessed: Month Day, Year].
- [17] E. Awada, "Numerical voltage relay enhancement by integrated discrete Wavelet transform," *Journal of Southwest Jiaotong University*, vol. 56, no. 6, 2021, pp. 843-854. DOI: 10.35741/issn.0258-2724.56.6.74.
- [18] E. Awada, E. Radwan, M. Nour, A. Al-Qaisi, and A. Y. Al-Rawashdeh, "Modeling of power numerical relay digitizer harmonic testing in Wavelet transform," *Bulletin of Electrical Engineering and Informatics*, vol. 12, no. 2, 2023, pp. 659-667. DOI: 10.11591/eei.v12i2.4553.
- [19] Website: "PyWavelets Documentation." PyWavelets, <https://Wavelets.pybytes.com/>. [Accessed: 13 October 2023].
- [20] "Understanding Wavelet Properties and Their Applications," Section.io Engineering Education. [Online]. Available: <https://www.section.io/engineering-education/understanding-Wavelet-properties>. [Accessed: February 22, 2023].

- [21] J. Fuller, P. Obiomon, and S. I. Abood, "Power System Operation, Utilization, and Control," 1st ed., CRC Press, July 21, 2022. ISBN-13: 978-1032277455.
- [22] M. H. Fayyadh and S. I. Abood, "Philosophy of Power System Protection and Security: Computer-Aided Design and Analysis," Nova Science Pub Inc, February 10, 2021. ISBN-13: 978-1536190991.
- [23] S. I. Abood, "Power System Generation, Stability, and Control," Central West Publishing, Australia, 2021. ISBN 978-1-922617-00-2.
- [24] S. I. Abood and J. Fuller, "Power System Protection and Relaying: Computer-Aided Design Using SCADA Technology," 1st ed., CRC Press, September 29, 2023. ISBN-13: 978-1032495507.
- [25] S. I. Abood and M. H. Fayyadh (Eds.), "Advanced Power Systems and Security: Computer Aided Design," Nova Science Pub Inc, January 1, 2021. ISBN-13: 978-1536187854.
- [26] S. I. Abood, Ed., Fundamentals of Electrical Power Systems: A Primer With Matlab. ISBN-13: 978-1536186376.
- [27] S.H. Asman, N.F. Ab Aziz, U.A. UngkuAmirulddin, and M.Z. Ab Kadir, "Transient fault detection and location in the power distribution network: A review of current practices and challenges in Malaysia," *Energies*, vol. 14, no. 11, 2021, Art. no. 2988.
- [28] A. Abdelmoumene and H. Bentarzi, "Reliability enhancement of power transformer protection system," *Journal of Basic and Applied Scientific Study*, 2012, pp. 10534-10539.
- [29] Z. Zbunjak and I. Kuzle, "System integrity protection scheme (SIPS) development and an optimal bus-splitting scheme supported by phasor measurement units (PMUs)," *Energies*, vol. 12, no. 17. DOI: 10.3390/en12173404.
- [30] I. G. Akhmetova et al., "An optimized adaptive protection scheme for numerical and directional overcurrent relay coordination using Harris hawk optimization," *Energies*, vol. 14, no. 18. DOI: 10.3390/en14185603.
- [31] M. R. Harwell, "Study Design in Qualitative/Quantitative/Mixed Methods," University of Minnesota, [Online].
- [32] L. Hong, M. Rizwan, S. Rasool, and Y. Gu, "Optimal relay coordination with hybrid timecurrent–voltage characteristics for an active distribution

- network using alpha Harris hawks optimization," *Engineering Proceedings*, vol. 12, no. 1. DOI: 10.3390/engproc2021012026.
- [33] S. Abood, N. Khatir, and M. Fayyadh, "Numerical and Engineering Analysis: Computer-Aided Design by Python," Central West Publishing, May 31, 2023. ISBN-13: 978-1922617408.
- [34] S. P. Ramli, H. Mokhlis, W. R. Wong, M. A. Muhammad, N. N. Mansor, and M. H. Hussain, "Optimal coordination of directional overcurrent relay based on a combination of improved particle swarm optimization and linear programming considering multiple characteristics curve," *Turkish Journal of Electrical Engineering and Computer Sciences*, vol. 29, no. 3, 2021, pp. 1765-1780. DOI: 10.3906/elk-2008-23.
- [35] A. G. Phadke, P. Wall, L. Ding, and V. Terzija, "Improving the performance of power system protection using wide area monitoring systems," *Journal of Modern Power Systems and Clean Energy*, vol. 4, no. 3, 2016, pp. 319-331. DOI: 10.1007/s40565-016-0211-x.
- [36] H. K. V. Gadiraju, V. R. Barry, and R. K. Jain, "Improved performance of PV water pumping system using dynamic Reconfiguration algorithm under partial shading conditions," *CPSS Transactions on Power Electronics and Applications*, vol. 7, no. 2, 2022, pp. 206-215. DOI: 10.24295/CPSS TPEA.2022.00019.
- [37] A. Kalas, M. Fauzy, M. E. Dessouki, A. M. El-refay, and M. El-zefery, "High performance direct torque control for induction motor drive fed from a photovoltaic system," *Int. J. Electr. Comput. Energ. Electron. communication Eng.*, 2015, p. 9:11.
- [38] A. A. Alawady, A. Alkhayyat, M. A. Jubair, M. H. Hassan, and S. A. Mostafa, "Analyzing bit error rate of relay sensors selection in wireless cooperative communication systems," *Bulletin of Electrical Engineering and Informatics*, vol. 10, no. 1, 2020, pp. 216-223. DOI: 10.11591/eei.v10i1.2492.
- [39] E. S. M. T. Eldin, "Fault location for a series compensated transmission line based on Wavelet transform and an adaptive neuro-fuzzy inference system," in *Proceedings of the 2010 Electric Power Quality and Supply Reliability Conference*, 2010, pp. 229-236. DOI: 10.1109/PQ.2010.5549994.
- [40] [22] C. Marven and G. Ewers, "A Simple Approach to Digital Signal Processing," John Wiley & Sons, Inc., 1996, pp. 4-187, ISBN 0-471-15243-9.

- [41] Y. Nievergelt, "Wavelets Made Easy," Birkhauser, 2001, pp. 3-281, ISBN 3-7643-4061-4.

CURRICULUM VITAE

Maysoun Alshrouf
malshroouf@pvamu.edu

EDUCATION

- M.S. Electrical Engineering, Prairie View A&M University, Prairie View, Texas, 2023
- M.S Information System Management, Keller Graduate School of Management of DeVry University, Houston, Texas, 2008
- B.A. Electrical and Communications Engineering, Amman University, Amman, Jordan, 1997

WORK EXPERIENCE

- **Company: Houston International Wellness Center**
 Position: General Manager, 2012-Present
 Job: Oversees strategic healthcare management, operational, financial, compliance, technology integration and ensure the success and growth of the clinic
- **Company: Ki-Essentials**
 Position: General Manager 2011-Present
 Job: Leading strategic vision, operations, online customer experiences, clinic integration, marketing, and development
- **Company: Devry University and Keller Management School of Management**
 Position: Visiting Professor, 2008-2016
 Job: Thought Electronics w/Lab, Electronics Product Development, Foundations of Managerial Mathematics and Matlab courses. Responsibilities include designing curriculum and syllabus, conducting hands-on lab, mentoring students, staying abreast of industry trends, and contributing to the academic and research.
- **Company: General Electric GE/ NBC Universal (KTMA Channel 47)**
 Position: Engineer/ IT Manager, 1999-2011
 Job: Maintaining broadcast operations and IT infrastructure, ensuring seamless transmission, and collaborating with cross-functional teams to optimize technology solutions for efficient broadcasting operations
- **Company: Al-Alhliyya Amman University**
- Position: Supervisor, Electronics & Communications Laboratory. 1997-1998
- Job: Supervise electronics and communications labs and tutoring sessions

Honors and Awards

- TopMISM Capstone project Award among all national Keller Graduate School of Management programs of DeVry University in the USA.
- Class valedictorian for Bachelor's degree in Electronics and Communications Engineering.
- "Above and Beyond Effort "Ovation Award from Telemundo/NBC-Universal-GE Company
- Completed GE Leadership Program at the John F. Welch Leadership Development Center
- Lead the Hispanic Forum for GE in Houston
- Achieved a certification in Holistic Health Care.

Publications

M. Alshrouf, C. M. Akujuobi, and E. Awada, 'Discrete Wavelet Transform Application to Three Phase Power System Short Circuit Fault Detection,' Wavelet Theory and Modern Applications [Working Title]. IntechOpen, Oct. 08, 2023. doi: 10.5772/intechopen.1002958.